UNIVERSITY OF CALIFORNIA

SANTA BARBARA

Aptamer targeted delivery of synergistic drug combinations for effective cancer therapy

A dissertation submitted in partial satisfaction of the requirements for the degree

Doctor of Philosophy in Chemical Engineering

by

Anusha Pusuluri

Committee in charge:

Professor Samir Mitragotri, Co-chair

Professor H. Tom Soh, Co-chair

Professor Michelle A. O'Malley

Professor Craig J. Hawker

Daniel Greenwald, MD, Sansum Clinic

September 2018

The dissertation of Anusha Pusuluri is approved.

_____

Professor Michelle A. O'Malley

_____

Professor Craig J. Hawker

_____

Dr. Daniel Greenwald

_____

Professor H. Tom Soh, Committee Co-chair

_____

Professor Samir Mitragotri, Committee Co-chair

August 2018

Aptamer targeted delivery of synergistic drug combinations for effective cancer therapy

Acknowledgements

I am extremely fortunate to have had the guidance and support of several incredible mentors, colleagues and friends during the completion of my dissertation. I take this opportunity to express my deep gratitude and appreciation to everyone who have encouraged me and played a crucial role in my trajectory thus far.

First to Samir Mitragotri, my graduate school advisor, I'm deeply indebted to you for your unrelenting patience and support throughout my time in your lab. Your valuable advice in research and professional matters, the tremendous freedom that you allowed and your profound belief in my abilities was instrumental in nurturing the research acumen and confidence that I needed for exploring bold ideas. At the same time, you also helped me stay on track and taught me how to recognize the big picture and conduct research efficiently towards an overarching goal. Your infectious positivity and passion for research have been invaluable in shaping my personality and I could not have asked for a better role model and mentor during my Ph.D.

To Tom Soh, I am extremely grateful to you for overseeing my research as a co-advisor at UCSB. You have lent a helping hand in all matters during my Ph.D. and this dissertation would not have been possible without your support. Your unceasing enthusiasm and discipline in conducting research always inspires me to keep furthering myself and to never yield.

To my committee members, Michelle O'Malley, Craig Hawker and Daniel Greenwald, I am particularly grateful for your constructive criticisms, feedback on my thesis project and your deep insight into areas that I was unfamiliar with. Your encouragement and support helped me greatly in navigating my way through graduate school.

To Kat Camacho, thank you so much for welcoming me into the Mitragotri lab. I benefited greatly from your extensive combination chemotherapy knowledge while I was commencing my dissertation project to extend your foundational work. You generosity in mentoring and assisting me has simplified and continues to simplify so many things at every step in my career to this day. To Andrew Csordas, thank you for spending an enormous amount of time and energy in training me on performing aptamer selections and all the basic techniques and skills that one needs to pursue lab work. I've been a great admirer of your

patience and dedication towards research and forever strive to emulate these qualities in my work. To Jia Niu, I am indebted to all the practical chemistry suggestions and advice you gave me while I was navigating several roadblocks in my thesis project. No matter what, you were willing to help and I greatly appreciate all of your assistance.

To my colleagues in the Mitragotri and Soh labs, thank you for making our lab's atmosphere an interesting and lively space to work in. It was an honor to work amongst such brilliant minds and I am grateful for all the helpful conversations and support during long and arduous lab hours. I must especially thank Vinu Krishnan and Apoorva Sarode, for providing unwavering assistance during animal and other research experiments. You helped me stay calm and lent me a shoulder to rest on during stressful times both in lab and outside and I am particularly grateful to you for that. To Doug Vogus, thank you for being a great mentor and constantly motivating me during the hectic final phases of graduate school. Your critical approach towards tackling research problems have made collaborating and working with you very enjoyable. To Michael Evans, thank you for helping me with the tumor spheroid studies and for capably taking on the chemical safety officer duty. To Debra Wu, thank you for providing me with liposomes and collaborating with me on new undertakings. I am sure that with your hard work you will progress these projects enormously. To Izzy Jarvis, thank you for all the fun and heartwarming conversations in lab and outside and for making Mitragotri lab the most fun lab to work in. To Dave Smith, Mengwen Zhang, Sandy Chen, Kevin Peng and Diana Wu, thank you for being around to help with homework or research issues. I had a great time working with all of you.

To Valerie Lensch and Elaine Bunyan, you have both played a vital role while assisting me in laying the groundwork for my dissertation. I cannot thank you both enough for spending long grueling hours to help me conduct experiments that failed more often than not! You both are incredibly fast learners and helped me troubleshoot very difficult issues in my research with great enthusiasm. To Erica Diaz, Renwei Chen and Ruby Holder, thank you for your immense administrative and logistical help during my time at UCSB and in ensuring my smooth transition to Harvard.

To Juili Shelke and Chinmay Save, thank you for making me a home away from home in Boston. Your constant love and generosity ensured my well being and helped me get through the final stretch at Harvard much more easily. To Eva Padilla, Ekta Prashnani, Rucha

Thakar, Anirudha Banarjee, Anchal Agarwal, Samhita Banavar and many other friends at UCSB, I could not have asked for a more incredible set of people to unwind and do fun things with! Thank you for making my graduate school experience exceptionally memorable and fun. I thoroughly enjoyed each and every moment here and I have learnt a great deal from all of you both personally and professionally.

To Pratik Soni, thank you for being my constant pillar of support this past year. No matter what, you have helped me keep calm, motivated me when I was on the verge of giving up, and have constantly tried to keep my spirits high. There are no words to describe how helpful and reassuring your presence in my life has been and I am forever grateful to the almighty for that. To my brother Abhinand Pusuluri, you have been a tremendous friend and confidante growing up, thank you for always lending your ear during challenging times and for supporting and believing in every decision that I have made. Without your encouragement and counsel, I could not have even dreamt of pursuing the things that I am doing today.

Finally, I would like to thank my parents, to whom this thesis is dedicated. To Amma and Daddy, there are no words to describe how incredibly lucky I consider myself to be your daughter. You have strived to provide the best of things for me and never once hesitated in prioritizing my interests over yours. Thank you for being my biggest critic and my biggest advocate and for never holding me back as I chased my dreams!

Curriculum Vitae

Anusha Pusuluri

Education

2013-2018	**Doctor of Philosophy in Chemical Engineering with Emphasis in Bioengineering (Expected)** University of California, Santa Barbara
2009-2013	**Bachelor of Technology in Pharmaceutical Sciences and Technology** Institute of Chemical Technology, Mumbai

Professional Experience

2017-2018	**Visiting Research Fellow** Harvard University, Cambridge
2013-2017	**Graduate Researcher and Teaching Assistant** University of California, Santa Barbara
2013	**Undergraduate Researcher** Institute of Chemical Technology, Mumbai
2012	**Manufacturing Intern** Sun Pharmaceuticals Ltd., Silvassa

Publications

- **Pusuluri, A.,** Lensch, V., Krishnan, V. K., Bunyan, E., Sarode, A., Menegatti, S., Soh, H.T., & Mitragotri, S. Treating tumors at ultra-low drug doses using an aptamer-peptide synergistic drug conjugate, *Manuscript submitted*.

- Niu, J., Lunn, D. J., **Pusuluri, A.,** Yoo, J. I., O'Malley, M. A., Mitragotri, S., Soh, H. T. & Hawker, C. J. (2017). Engineering live cell surfaces with functional polymers via cytocompatible controlled radical polymerization, *Nature Chemistry.*

- Vogus, D. R., **Pusuluri, A.,** Chen, R., & Mitragotri, S. Schedule dependent synergy of Gemcitabine and Doxorubicin: Improvements of in vitro efficacy and lack of in vitro□in vivo correlations (2018), *Bioengineering & Translational Medicine.*

- Vogus, D. R., Evans, M. A., **Pusuluri, A.,** Barajas, A., Zhang, M., Krishnan, V., Nowak, M., Menegatti, S., Helgeson, M.E., Squires, T.M., & Mitragotri, S. (2017). A hyaluronic acid conjugate engineered to synergistically and sequentially deliver gemcitabine and doxorubicin to treat triple negative breast cancer, *Journal of Controlled Release.*

- Camacho, K. M., Menegatti, S., Vogus, D. R., **Pusuluri, A.,** Fuchs, Z., Jarvis, M., Zakrewsky, M., Evans, M.A., Chen, R., & Mitragotri, S. (2016). DAFODIL: A novel

liposome-encapsulated synergistic combination of doxorubicin and 5FU for low dose chemotherapy, *Journal of Controlled Release.*

Presentations

- **Pusuluri, A.,** Lensch, V., Krishnan, V. K., Bunyan, E., Sarode, A., Menegatti, S., Soh, H.T., & Mitragotri, S. Enhanced cancer efficacy and selectivity via aptamer targeted dual drug delivery, *Gordon Research Conference and Symposium: Drug Carriers in Medicine and Biology*, Aug 2018: West Dover, VT, USA (Poster).

- **Pusuluri, A.,** Menegatti, S., Soh, H.T., & Mitragotri, S. Aptamer-peptide-drug conjugates: Delivery of precise synergistic drug ratios for enhanced cancer selectivity, *American Institute of Chemical Engineers (AIChE) 17th Annual Meeting*, Nov 2017: Minneapolis, MN, USA (Oral).

- **Pusuluri, A.,** Menegatti, S., Soh, H.T., & Mitragotri, S. Aptamer-peptide-drug conjugates: targeted delivery of synergistic drug combinations with ratiometric precision, *American Chemical Society (ACS) 253rd National Meeting*, Apr 2017: San Francisco, CA, USA (Oral).

- **Pusuluri, A.,** Mitragotri, S., Aptamer-Peptide Conjugates: Targeting Metastatic Cancer with Synergistic Precision, *6th Chemical Sciences Student Seminar*, Oct 2016: Santa Barbara, CA, USA (Oral).

- **Pusuluri, A.,** Menegatti, S., Soh, H.T., & Mitragotri, S. Aptamer-peptide conjugates: delivering synergistic drug combinations with precision, *UCSB Chemical Engineering Clorox-Amgen Graduate Student Symposium*, Oct 2015: Santa Barbara, CA, USA (Poster).

Outreach

2014 - 2017	Center for Science and Engineering (CSEP) research mentor. Designed 8-week undergraduate research projects and mentor a sophomore (2016) and trained four freshmen (2015)

Awards and recognitions

2017	AIChE Division 15 Best Oral Presentation Award - Top 3 from 109 Entries
2013	Gold Medal from Indian Pharmaceutical Association – highest GPA across all undergraduate institutions
2012-2013	Sir Ratan Tata Scholarship for meritorious engineering undergraduates (pan India participants) and Mrs. Usha M. Joshi/S.M. Joshi Scholarship - highest GPA (out of 115 students),

Abstract

Aptamer targeted delivery of synergistic drug combinations for effective cancer therapy

by

Anusha Pusuluri

Potent chemotherapy combinations identified and optimized *in vitro* often fail in clinic because the current paradigm aims to deliver drugs at or near their maximum tolerated doses (MTD), elevating the risk of treatment related toxicity in patients. Further, it does not achieve optimum relative drug concentrations, required to maximize the therapeutic impact of a combination, at the tumor site. Thus, combination chemotherapy regimens must be designed to adequately strike the difficult balance between safety and efficacy. In the first part of this dissertation, two chemotherapeutic drugs, doxorubicin (DOX) and camptothecin (CPT), whose potency can be tuned by combining them in different molar ratios, are investigated as a treatment option against triple negative breast cancer (TNBC). Albeit causing toxicity to control breast epithelial cells *in vitro,* the optimized combination inhibited the disease progression in an aggressive orthotopic human TNBC mouse tumor model at very low drug doses of DOX (2mg/kg/dose) and CPT (1.4 mg/kg/dose). Targeted delivery of these non-specific yet potent compounds was envisaged to further enhance clinical outcomes by improving cancer specificity. Since aptamers offer excellent advantages over other molecular targeting agents, an aptamer capable of specifically recognizing an overexpressed TNBC marker was explored and found to be suitable for this application. To amalgamate anti-cancer potency with cancer specificity, a modular framework for the aptamer-targeted delivery of drug combinations at synergistic molar ratios is described in the next part. Specifically, a nucleolin targeting aptamer was coupled to peptide scaffolds laden with DOX and CPT at precisely defined molar ratios. Ap-DOCTOR (Aptamer-targeted DOX and CPT

in Therapeutically Optimal Ratios) exhibited an extremely low IC_{50} value of 31.9 nM specifically against TNBC cells *in vitro*. This value is 15-fold lower than the IC_{50} of DOX alone, and 7-fold lower than the IC_{50} of CPT alone. *In vivo*, Ap-DOCTOR outperformed cocktails comprising equivalent doses of unconjugated DOX and CPT, exhibiting efficacy at micro-dose injections (500 μg/kg/dose) of DOX and (350 μg/kg/dose) CPT. These doses are respectively 8-fold and 21-fold lower than those required with DOX or CPT individually to induce measurable anti-tumor effects, and a further, 20–30-fold lower than the reported MTD values of these drugs. The approach outlined in this dissertation represents a generalizable strategy for the safe and consistent delivery of empirically defined optimal molar ratios for a diverse set of combination drugs in oncology. Ultimately, this could enable treatment at doses much lower than MTDs and facilitate effective translation of anticancer chemotherapeutic combinations into the clinic.

List of Figures

List of Tables

Table of Contents

Chapter 1

Overview of Dissertation

A 19th century surgeon once described cancer as "the emperor of all maladies, a king of terror". Indeed it continues to be as deadly even in the 21st century. 4 out of 10 people are likely to develop cancer in their lifetime and it is one of the leading causes for disease related mortality. About 16 billion dollars are spent annually towards cancer research, which have resulted in the emergence of several novel cancer treatment modalities. Recent discoveries such as check point blockade inhibitors and cell therapy have revolutionized the current treatment landscape [1]. While the overall survival rates are slowly improving, the survival rates for cancers detected in late stages are still quite stark. A reported 8.2 million of the 14.1 million new worldwide registered cases in 2012 resulted in death and most of these are a consequence of the cancer advancing [2]. Although limited in success, combination chemotherapy is the gold standard therapy option for several advanced stage cancers [3]. In addition to tumor resistance, toxicity limits the effectiveness of chemotherapy. The reason for their failure in the clinic is predominantly because of the administration of each drug component at its maximum tolerated dose (MTD). Patients are exposed to toxic doses of several agents simultaneously, causing severe adverse effects and undermining their intended therapeutic benefit. My Ph.D. broadly focused on improving outcomes of combination dosing by simultaneously optimizing drug ratios of chemotherapeutic agents and imparting cancer recognizing properties to them. This dissertation describes in detail the steps I

undertook to identify and validate an approach to generate enhanced cancer-specific therapeutic effects using chemotherapy combinations at highly reduced drug doses.

In Chapter 2, I first review the prevalence of combination chemotherapeutic regimens in cancer and how current regimens are effective yet toxic. Next, I summarize the latest research endeavors being pursued to minimize toxicity and improve the potency of a combination.

Triple negative breast cancer (TNBC) is currently the most lethal and difficult subtype of breast cancer to treat. There is a great requirement for identifying efficacious treatment options against TNBC [4]. In Chapter 3, I identify a drug combination against metastatic TNBC after screening a panel of commonly used chemotherapeutic drugs against breast cancer. Camptothecin (CPT) and Doxorubicin (DOX), topoisomerase I and II inhibitors respectively, when combined show extreme potency and also molar ratio dependent synergy. Although the most potent molar ratio does not provide cancer exclusive toxicity *in vitro*, it displayed efficacy at very low doses *in vivo*. This provided a good motivation to employ this combination against TNBC after further optimization. Improvements needed for effective translation of this drug pair are discussed in the last section of this chapter.

Chapter 4 outlines a targeting approach to reduce the non-specific and off-target accumulation of small-molecule drugs in healthy tissues and simultaneously unify different pharmacokinetic, bio distribution and transport properties of distinct drugs. Three specific considerations for designing an effective targeted delivery vehicle are defined and aptamers, a novel class of targeting agents, are evaluated for their suitability based on these guidelines. The limitations of previous aptamer delivery vehicles are also reviewed.

A combination therapy vehicle that targets tumor cells via aptamers and delivers multiple therapeutic agents at pre-defined ratios selected for maximum effectiveness is described in Chapter 5. A novel strategy to conjugate multiple drug molecules to a single aptamer molecule using peptides is first described. Then the development of aptamer-peptide drug conjugates loaded with different DOX and CPT molar ratios is shown. Next, the optimal molar ratio is identified and the construct's performance is validated both in cultured cells and in a relevant TNBC animal model. Critical pharmacological aspects of the formulation like construct solubility and drug release rates are also studied. Finally, a discussion on parameters crucial for successful aptamer-mediated dual drug delivery is provided. In Chapter 6, experimental methods like *in vitro* and *in vivo* assays, chemical synthesis, and material characterization techniques used in all the experiments described in this dissertation are summarized.

Finally, in this dissertation, I intended to answer three main questions: "Are two drugs better than one?" "What is the benefit of targeting?" and "How can drug combinations be translated more effectively to the clinic?" In Chapter 7, I attempt to answer them with a summary of the main findings and a comprehensive conclusion of the work done so far. I also lay down suggestions for future research pathways that build upon the knowledge presented here.

Permissions and attributions

Some of the content presented in this thesis has been used to prepare a research manuscript for submission to Angewandte Chemie.

Chapter 2

Dosage Concerns in Chemotherapy

2.1 Chemotherapy against cancer

Current methods of clinical treatments against cancer include surgery, radiation therapy, chemotherapy, immunotherapy, targeted therapy and hormone therapy [5]. Depending on the type and stage of the cancer, one or more of the above strategies are prescribed to the patient. Despite the advent of several new cancer treatment modalities, clinicians continue to rely on cytotoxic chemotherapy (using highly toxic drugs to kill cancer cells) for treating late stage cancer patients. In at least seven out of the ten most commonly occurring cancers, chemotherapeutic drugs are used as the main treatment, either alone or in combination with other treatment modes (Table 1). In addition to the wide panel of relatively inexpensive options available for most types of cancer, chemotherapeutics possess the ability to reach all three heterogeneous late stage cancer components - primary tumor sites, remote metastases and circulating tumor cells - via systemic circulation. This makes them a popular remedy choice compared to other localized therapeutic options like surgery or radiation and relatively newer and more expensive drugs like biologics or immune-mediated therapies [3,6].

However, the five-year survival rates of late stage cancers treated with chemotherapy are rather disheartening and indicate severe limitations in current regimens. Propelled by the principle of dose-dependent tumor inhibition, introduced first by Schabel and Skipper,

clinicians deliver high drug doses to achieve high efficacies. The advent of bone marrow transplants and other supportive care options like hematological growth factors, blood cell transfusions etc. made delivering high drug doses possible. High-dose chemotherapy, therefore, became the mainstay of cancer treatment for over 50 years [6,7].

Table 1. Primary late stage treatment strategies for the ten most prevalent cancers types.

Cancer	*Primary treatment in late stages*	*5-year survival rate (%)*	
Breast	Chemotherapy and/or radiation	27	[9]
Lung	Chemotherapy +/- radiation	1-5	[10]
Prostate	Surgery +/- radiation	30	[11]
Colorectal	Chemotherapy +/- surgery/radiation	12.5	[12]
Melanoma	Surgery and immunotherapy	21	[13]
Bladder	Chemotherapy	8.1	[14]
Non-Hodgkins Lymphoma	Chemotherapy +/- radiation	71	[15]
Leukemia	Chemotherapy *	24 -83	[3]
Kidney	Surgery and targeted therapy	7 -23	[16]
Pancreatic	Chemotherapy †	6	[17]

Since, chemotherapeutic agents are designed to affect any rapidly dividing cell, they can launch an indiscriminate attack on both healthy and tumor tissues. Unsurprisingly, exposing a patient to excessive concentrations of such narrow therapeutic index drugs is shown to cause acute toxicity and results in poor patient compliance, treatment delay and

* Chemotherapy is used in patients resistant to Tyrosine Kinase Inhibitors.
† Sometimes combined with targeted therapy.

ultimately forced treatment withdrawal. Tumors relapse from drug resistant sub-clones due to unsuccessful therapy, contributing towards increased failure rates [8].

2.2 Popularity and confines of combination chemotherapy in the clinic

Development of multi-drug resistance and tumor relapse post chemotherapy is commonly observed in many cancers [18]. Combination chemotherapies are routinely employed in the clinic to improve treatment efficacies against such cancers. First demonstrated by Frei, Freireich and Holland in 1965 against childhood acute lymphoblastic leukemia (ALL), combination drugs displayed an increased anticancer effect compared their single counterparts, especially in patients whose cancer had metastasized or had a high risk of relapse after surgery [6]. Soon after its success in the clinic, several other combination therapies were developed empirically based on various postulates that still form the basis for current clinical trials design. For example, drugs that operate by different mechanisms are co-administered to affect separate pathways necessary for cell proliferation and potentially manifest in biochemical synergy. Similarly, drugs that possess non-overlapping toxicities are hypothesized to elicit an improved tumor response without enhancing the cumulative side effects and finally, cross-sensitive drugs are combined to overcome resistance to the partner drug [8,19,20].

As mentioned previously, drugs are administered at the highest possible dose to maximize their therapeutic effect and this rule was immediately extended to combination chemotherapy. Currently, most treatments co-administer combination drugs at their individual maximum tolerated dose (MTD) to reduce the risk of sub-therapeutic exposure of either drug constituent. Typically, the dose of one drug is kept constant and the relative dose

of the other drug is varied or the relative dose is kept constant and the cumulative drug dose is escalated until dose-limiting side effects are observed [21].

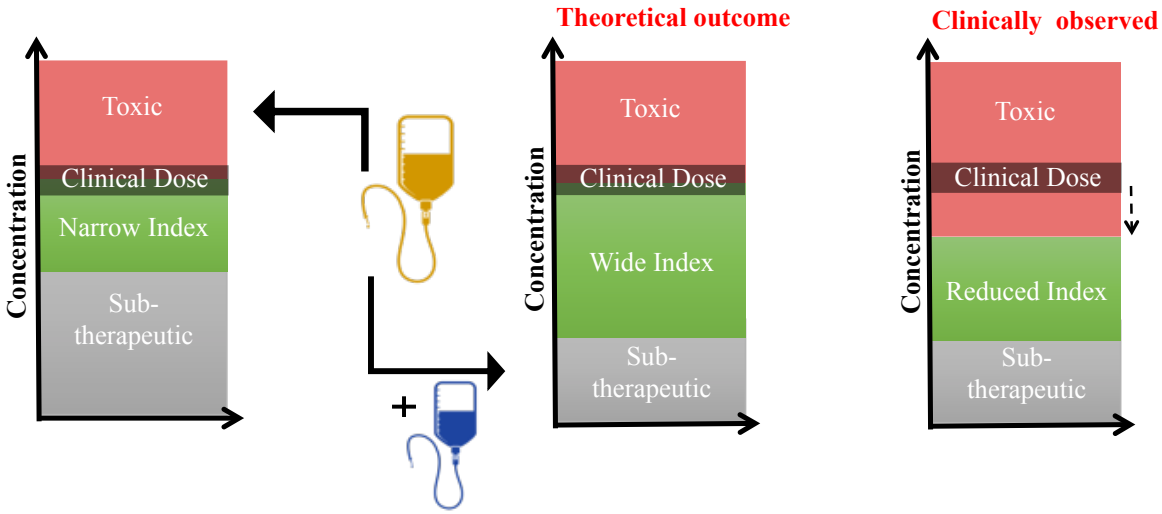

Figure 1. Cartoon depicting the expected theoretical benefit and the diminished clinical outcome observed after combination chemotherapy.

While in theory drug combinations appear superior, recent probes into the clinical outcomes suggest otherwise. Combination regimens have been linked to more severe side effects and greatly diminished overall therapeutic benefit compared to single drugs especially in advanced solid cancers (Figure 1) [21,22]. Analysis of data from 65 randomized trials (13601 patients cumulatively recruited) for advanced non-small-cell lung cancer (NSCLC) revealed that addition of a second drug to the chemotherapy regimen resulted in a modest 5% improvement in the 1-year survival rates. Further, adding a third drug did not provide any survival advantage and significant enhancement in toxicity was observed in patients

receiving combination chemotherapy [23]. Similar trends are seen in other solid cancers, where the benefits of combining chemotherapeutic agents remain debated (Table 2).

Table 2. Modest benefits of combination chemotherapy in advanced solid cancers.[*]

Cancer	*Therapeutic improvement*	*Toxicity effect*	
Breast	12% improvement in overall survival and 22% in time to progression	Overall grade 3/4 toxicity increased by 1.5-fold	[22]
Lung	5% improvement in 1-year survival and 2.4-fold in tumor response	Thrombopenia increased by 6.8-fold and neutropenia by 3.2-fold	[23]
Colorectal	Insignificant 6% improvement in 3-year survival	Overall grade 3/4 toxicity increased by 2.07-fold	[24]
Bladder	2.25-fold improvement in overall survival	Leukopenia increased by 2.54-fold	[25]
Pancreatic	No benefit of combination	Not studied	[26]

On a more fundamental level, synergy between a drug pair is of crucial importance. Synergy can be best described as the generation of a greater therapeutic effect by a drug combination compared to the expected sum of their individual therapeutic effects. When the combinatorial effect is equal to the sum of individual drug effects, the drug pair is said to be

[*] All comparisons are made at overall population-level patient responses between the combination and control arms.

additive and when the combinatorial effect is lesser than the effect of one or more constituent agents, the pair is deemed antagonistic. After interpreting data from 230 pre-clinical and 8 human clinical trials, Palmer and Sorger argued that, at a population level, combination drugs act independently and provide an improvement only because of their ability to treat a larger fraction of patients and not necessarily because of synergy. This idea is depicted schematically in Figure 2. Further, they suggest that translation of in vitro synergy into the clinic remains unsuccessful and greater improvements in the response rates should be observed if the drugs were truly synergistic [27]. Similarly, when synergistic drug pairs identified in 132 preclinical studies were compared to 86 corresponding clinical trials, no additional improvements were observed in the clinical response rates of the combination groups [28].

The reasons for poor translation of synergistic combinations will be discussed in more detail later; however, these studies highlight a critical shortcoming with the MTD strategy. If the addition of a second drug to a treatment regimen elevates the side effects without any commensurate improvement in the therapeutic response, then risking a patient's exposure to toxic concentrations of this added drug becomes unnecessary. In summary, the exposure to near toxic doses of multiple drugs elevates the risk in overall safety and outweighs any therapeutic advantage provided by a drug combination. This makes the current MTD method a poor dosing strategy. To fully realize the benefit of drug combinations, there is an immediate need to design therapies that are effective at lower drug doses.

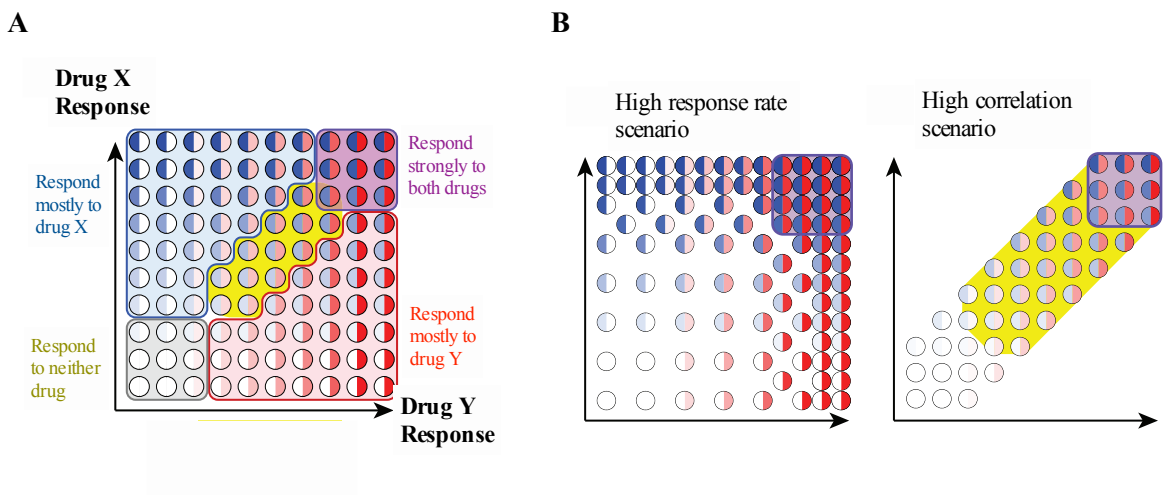

Figure 2. Understanding the benefit of combination chemotherapy at a population level. (A) Possible outcomes after a drug combination administration to a diverse population having different responses to the individual components. (B) Higher response can either be due to a high number of patients cumulatively responding to high doses of either individual drug component (high response rate scenario) or due to patients responding to both drug components at low doses (yellow portion in high correlation scenario). True drug synergy is manifested in the latter case where patients respond to both drugs. Figure reprinted with permission from [27].

2.3 Advances towards designing effective combination chemotherapies

Several strategies have been developed to reduce the adverse effects of combination chemotherapy and improve the overall response. The two most common ones being (i) the variation of drug administration sequence and (ii) optimization of the relative molar ratios in which drugs are given. Sequential drug administration has been historically employed to improve tolerability by preventing the concurrent exposure to toxic side effects of multiple

drugs. However, achieving synergy or additional potency by varying the drug administration sequence or relative drug molar ratios is relatively fresh and increasingly being recognized as a strategy to improve treatment efficacy. These concepts are discussed in detail below.

Dependency on drug sequence

Studies have demonstrated that the sequence in which drugs are administered dictates the synergy of a combination [29–31]. For example, tumors pre-treated with methotrexate before administering 5-fluorouracil had a significant improvement in response as compared to tumors treated in the reverse sequence [32]. Similarly, staggered administrations of erlotinib, an EGFR inhibitor, prior to doxorubicin, a DNA damaging agent, conferred synergy over simultaneous administrations in a few breast cancer cell lines. Several time-dependent intracellular pathways, cell-cycle kinetics and interdependent regulatory networks are responsible for such schedule-dependent synergies [33]. Moreover, appropriately sequencing drugs has been shown to overcome cell-cycle mediated drug resistance across four commonly employed classes of chemotherapeutic agents [34]. In clinical trials, multiple factors were affected based on the sequence in which drug combinations were administered. While efficacy improvement is observed with some combinations [35,36], other trials show sequence dependent improvements on the pharmacological behavior like clearance rates [37] and toxicity levels [38]. However, there is a lack of one to one mapping between observed *in vitro* synergies and *in vivo* effects due to complex physiology and transport effects encountered by drugs in circulation [39]. Efforts are underway by drug delivery scientists to translate such sequence dependent synergies observed *in vitro* to superior dose reductions *in vivo* by engineering novel delivery vectors [31,40].

Dependency on drug ratios

The recent FDA approval of Vyxeos (CPX-351) heralds a new era in combination chemotherapy. [41] Vyxeos is a liposomal formulation that delivers a synergistic molar ratio of two chemotherapeutic drugs, daunorubicin and cytarabine, to leukemic cells. During its pre-clinical development, several different molar ratios of the combination liposomally encapsulated were tested *in vivo* in a leukemic mouse model. Improved survival was observed in the group that received daunorubicin and cytarabine in a molar ratio of 1:5 daunorubicin:cytarabine. To further probe the dependence of synergy on molar ratios, the dose of cytarabine was kept constant and the dose of daunorubicin was increased to result in a molar ratio of 1:3 daunorubicin:cytarabine. Impressively, despite an increase in the dose of daunorubicin, the group receiving the 1:3 molar ratio had only a 55% 55-day survival rate whereas the group receiving the 1:5 molar ratio had a 100% 55-day survival rate [42]. This observation clearly contradicts the "more is better" intuition. Along with CPX-351, several emerging studies show that different molar ratios of the same drug combination have different cell-killing effects and there is a growing consensus on combining chemotherapy drugs at specific molar ratios to afford higher potency [43]. Hence, delivering drugs at these specific ratios can greatly diminish doses required for an effective clinical response [Table 3,6,43].

Thus, along with schedule dependency, relative drug concentrations play a critical role in determining the potency of a drug combination. Drugs interact with each other and affect a cell through several complex intracellular pathways. Moreover, apoptosis and other cell-death pathways are inter-dependent and one drug could affect another drug's cell-death

pathway either upstream or downstream [50,51]. Due to the non-linear interactions between a drug and its target, it would be hard to predict the relative concentration of a sister drug that could influence any drug's dose-effect curve [52]. Hence, it would be hasty to assume that toxicity profiles of a drug in the presence and absence of other drugs would remain similar. The MTD approach relies on the assumption that two drugs act independently and wrongly disregards the interdependent effects of drug combinations on its potency.

As a case study, let us consider a co-therapy of irinotecan and floxuridine. At high concentrations of irinotecan, an agent that causes DNA damage, a greater fraction of cells are arrested in the S phase. Floxuridine on the other hand, causes cell death by prematurely progressing S phase cells to M phase. Hence, if a larger number of cells were already arrested in the M phase, the presence of irinotecan would not induce any further cell death since S phase precedes the M phase. In the opposite scenario, cells that have already undergone DNA damage by irinotecan can undergo a further premature progression to the M phase resulting in enhanced cytotoxicity and biochemical synergy. This was indeed observed in HT-29 human colorectal cancer cells and Capan-1 human pancreatic cancer cells where a 1:1 molar ratio of irinotecan and floxuridine was synergistic and the higher 1:5 and 1:10 molar ratios were antagonistic [53].

More recently, cancer specific cell death was achieved by fine-tuning the ratios in which the two drugs were exposed. Camacho et.al. were able to identify drug ratios that were extremely synergistic against a breast cancer cell line and simultaneously antagonistic to an endothelial cell line. They speculated that the vast difference in cytotoxicity was due to the inherent differences in the mechanisms by which the drugs induce cell death in the cancer

and healthy cell lines [47]. Although this preliminary result needs further testing, it nevertheless opens a new dimension to be considered while optimizing drug combinations.

Table 3. Manifestation of ratio dependent synergy in combination chemotherapy vehicles.

Formulation name	*Drugs (Most effective molar ratio)*	*Delivery vehicle*	*Development Stage*	*Disease*	
Vyxeos	Daunorubicin:cytarbine (1:5)	Liposome	Clinically Approved	Acute Myeloid Leukemia	[42]
CPX 1	Irinotecan:Floxuridine (1:1)	Liposome	Phase II	Colorectal Cancer	[45]
DAFODIL	Doxorubicin:5-fluorouracil (0.15:1)	Liposome	*In vivo*	Breast Cancer	[46]
HA-DOX-CPT	Camptothecin:Doxorubicin (3.2:1)	Hyaluronic acid polymer	*In vivo*	Breast Cancer	[47]
PLGA NP	Gemcitabine:Cisplatin (5:1)	PLGA-PEG nanoparticle	*In vivo*	Bladder Cancer	[48]
PTX/GEM LB-MSNP	Gemcitabine:Paclitaxel (10:1)	Lipid coated mesoporous silica nano particle	*In vivo*	Pancreatic Cancer	[49]

Chapter 3

Optimizing drug combinations for triple negative breast cancer

25% of all female cancer patients worldwide suffer from cancer in the breast. In 2012, it was identified as the second most common cancer in the world after lung cancer and the most prevalent cancer in women. Being the second leading cause for cancer related deaths, it contributes enormously to the global burden of cancer [54]. This year, a further worsening in the situation was witnessed with the expected number of new breast cancer cases (approximately 268,670) in the United States surpassing all other cancer types. Early detection of breast cancer results in a remarkable 99% five-year survival rate. However, advanced breast cancers comprising both locally advanced and metastatic breast cancers have a rather poor five-year survival rate of ~ 25%. Moreover, metastatic breast cancer still remains an incurable disease with a median overall survival between 2 and 3 years [3,55].

Thus, current methods of managing advanced breast cancers are insufficient. Accelerated research efforts in pursuit of understanding the disease biology better, overcoming resistance mechanisms and developing novel therapies are needed to improve the dire outcomes in late stage breast cancers.

Typically, international consensus guidelines recommend preferred treatment options and drugs for advanced breast cancers. However, for treating advanced triple negative breast cancers no such drug recommendations are available [55]. In this chapter, after screening a panel of chemotherapeutic drugs on a human triple negative breast cancer (TNBC) cell line, a novel drug pair is identified to mitigate this aggressive subtype. *In vitro* and *in vivo* tests are performed on the drug pair to evaluate its potential as an efficacious treatment option. Further, studies on a control cell line are performed to identify areas that need to be addressed for developing the drug pair into a viable late stage breast cancer therapy.

3.1 Role of chemotherapy in managing advanced breast cancer

Lumpectomy, tumor and surrounding tissue removal via surgery, or mastectomy i.e. complete removal of the breast surgicaly, are performed for treating relatively localized tumors. Radiation is also sometimes recommended in addition to surgery for large sized tumors in place of mastectomy or if axillary lymph nodes are involved with tumor. In advanced stage cancers, chemotherapy (primary or adjuvant therapy), hormone therapy or targeted therapy is recommended based on the subtype and extent of cancer spreading. Breast cancers are classified into subtypes by profiling the expression levels of immunomarkers such as the estrogen receptor (ER), the progesterone receptor (PR) and the human epidermal growth factor 2 (HER2). Currently, there are five groups: Luminal A (ER^+, $PR^{+/-}$, $HER2^-$), Luminal B (ER^+, $PR^{+/-}$, $HER2^+$), Basal (ER^-, PR^-, $HER2^-$), Claudin-low (ER^-, PR^-, $HER2^-$), and HER2 (ER^-, PR^-, $HER2^+$) [3,56].

To effectively treat advanced breast cancers, international guidelines were developed based on the joint consensus of several international and regional breast cancer organizations.

ER^+ and PR^+ breast cancers depend on estrogen and progesterone hormones for proliferation; the first line of treatment recommended for such cancers is endocrine therapy, which inhibits or removes these proliferation aiding hormones, thereby slowing or stopping the growth of the tumors. The benefits of concomitant chemotherapy and other combinations with endocrine therapy are currently being investigated in clinical trails. The largest progress has been achieved in treating $HER2^+$ breast cancers. Anti-HER2 agents are the standard first line of treatment for such cancers and a single chemotherapeutic agent is combined in the later lines of therapy. Again, the toxicity profile influences the selection of combinations of two or more therapeutic modalities. TNBC cells, however, do not express any of the immunomarkers (ER^-, PR^-, $HER2^-$) and are the most difficult cancers to treat. There is a large unmet need to develop effective treatments against them. In the clinic, they respond modestly only to chemotherapy. Hence, experts are unable to make any specific recommendations for treating advanced triple negative breast cancer other than chemotherapy [55]. Since they can greatly benefit from advances made with chemotherapy compared to other subtypes, chemotherapy drug combinations in this framework were studied and optimized for TNBC.

3.2 A look at chemotherapy combinations against breast cancer

In 1970's chemotherapeutic agents, cyclophosphamide, methotrexate and 5-fluorouracil were combined to improve the short tumor responses observed with single agents in breast cancers. A review evaluating the efficacy of combination agents over single agents on 7147 randomized women suffering from metastatic breast cancer revealed that a heterogeneous yet statistically significant benefit was obtained for combination regimens over single regimens in terms of tumor progression and overall survival. Notwithstanding these improvements, the

median survival times were still very low and between 1-2 years, plus the survival benefit was counterbalanced with a proportional increase in the toxicity contributing to severe morbidity and poor quality of life in patients [22]. While the modest benefits observed support the effort to employ chemotherapy combinations in the clinic they also motivate the need for identifying additional ways to improve the treatment outcomes. Several combination regimens have since been approved in the clinic to treat breast cancers (Table 4).

Table 4. Approved chemotherapy combinations against breast cancer

(Adapted from NIH National Cancer Institute website - www.cancer.gov)

Combination	*Drugs in the combination*
AC	Doxorubicin and Cyclophosphamide
AC-T	Doxorubicin, Cyclophosphamide and Paclitaxel
CAF	Cyclophosphamide, Doxorubicin and Fluorouracil
CMF	Cyclophosphamide, Methotrxate and Fluorouracil
FEC	Fluorouracil, Epirubicin and Cyclophosphamide
TAC	Docetaxel, Doxorubicin and Cyclophosphamide

TNBC patients had an improved response to these commonly employed combinations as compared to non-TNBC patients. Further, TNBC patients who had completely responded to neoadjuvant chemotherapy without any residual disease had excellent survival rates and patients with residual disease had significantly worse survival rates than non-TNBC patients [57]. This foreshadows a sense of optimism in using chemotherapy drug combinations specifically against TNBC and developing therapies that can completely eradicate the

disease. As outlined earlier in section 2.3, optimizing schedules and ratios of a polychemotherapy regimen could improve its potency and lead to better clinical responses.

3.3 Identifying a potent drug pair against TNBC

The basis to form a potent drug combination was to combine drugs that independently exhibited high anti-cancer efficacies. Additionally, it was necessary to understand the efficacy of each drug so that they could later be compared to their individual efficacy contributions in a combination. Therefore we began by assessing several drugs for their *in vitro* toxicities on a TNBC cell line. MDA-MB-231 is an extremely aggressive TNBC cell line belonging to the claudin-low subtype with an intermediate response to chemotherapy [56]. We screened a panel of drugs spanning the most commonly used classes of chemotherapeutic agents (Table 5) against this cell line.

Specifically, we chose doxorubicin (DOX) from the anthracycline family, paclitaxel (PTX) from the taxane family and gemcitabine (GEM) from the antimetabolite family (Figure 3). We did not evaluate any platinum drug because of excess toxicity and minimal survival benefit reported in a review, evaluating 24 separate studies and a total of 4418 women with metastatic breast cancer, comparing platinum-based regimens and non-platinum based regimens (anthracyclines and taxanes) [62]. Additionally, topoisomerase I inhibitors have gained widespread attention as well tolerated drugs in managing refractory metastatic breast cancers that progressed after treatment with anthracyclines and taxanes [63,64]. Their synergistic interactions with other drug classes described in several *in vitro* and *in vivo* studies warranted an evaluation of this class. Camptothecin (CPT), an extremely potent

topoisomerase I inhibitor, was chosen as the fourth drug to be tested on MDA-MB-231 in addition to the above drugs [65].

Table 5. Commonly used chemotherapy drug classes in breast cancer

Drug Class	*Mechanism of Action*	*Main Adverse Effect*	*Examples*
Anthracyclines [58]	Topoisomerase II inhibition due to intercalation between adjacent DNA base pairs	Cardiotoxicity from hydroxyl free radicals and myelosuppression	Doxorubicin Daunorubicin Epirubicin
Taxanes [59]	Bind to β subunit of tubulin and stabilize microtubules	Myelosuppression and neuropathy	Paclitaxel Docetaxel
Antimetabolites [60]	Folic acid or nucleotide analogs that inhibit DNA synthesis enzymes	Myelosuppression, Mucositis and Thrombocytopenia	5-fluorouracil Gemcitabine Methotrexate
Platinum-based [61]	Bind covalently to purine DNA bases	Nephrotoxicity and gastrointestinal toxicity	Cisplatin Carboplatin

To assess potency, the cell inhibitory effects of each drug were determined by fitting experimental data from the MTT cytotoxicity assay to the median-effect model (Box 1) to obtain the half maximal inhibitory concentration (IC_{50}) i.e. the drug dose where 50% of the cell population's growth is inhibited. The efficacies of single agents were later used to rationally determine the range of drug concentrations to be used in the combination studies.

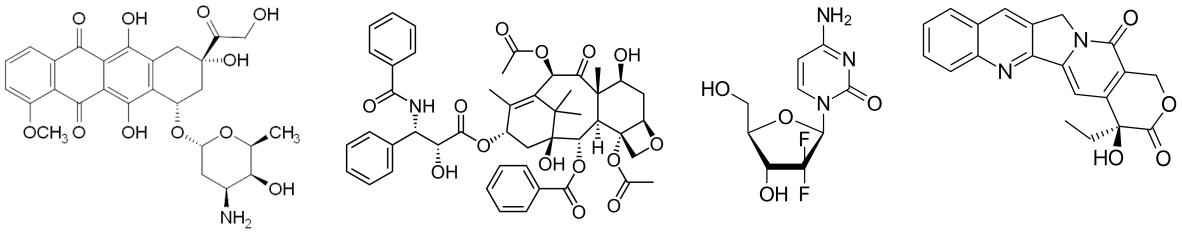

Figure 3 Chemical structures of drugs tested on cancer and control cells.

Box 1 Median effect model equations

Experimental f_a	$f_a = 1 - \frac{A_i - A_{Blank}}{A_0 - A_{Blank}}$ *A_i - Absorbance of well i* *A_{Blank} - Absorbance of well with no cells* *A_0 - Absorbance of well with cells but no drug*
Median effect analysis	$log\left(\frac{f_a}{f_u}\right) = m\ log(D) - m \log(D_m)$ *f_a - fraction affected and f_u - fraction unaffected* *m - shape coefficient* *D - Dose* *D_m - Dose corresponding to 50% f_a*
Dose-effect model	$\frac{f_a}{f_u} = \left(\frac{D}{D_m}\right)^m$

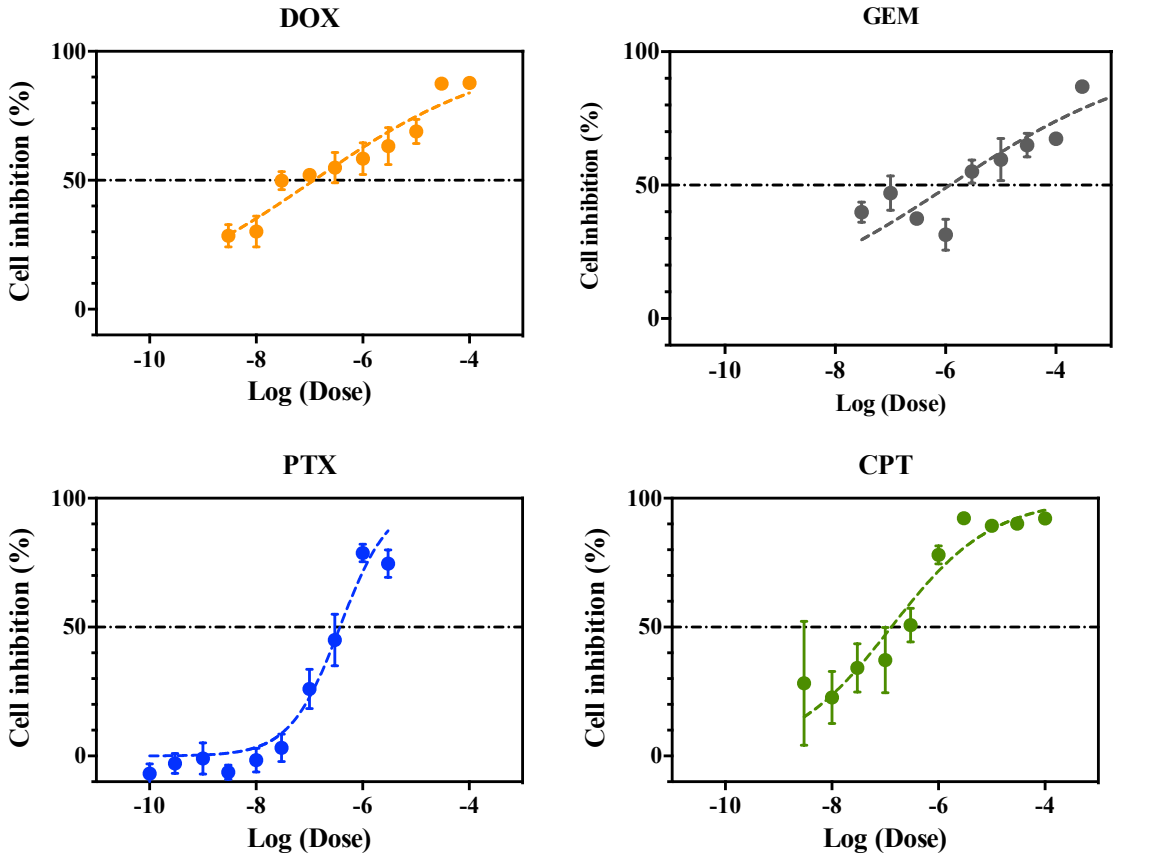

Drug	IC_{50} (µM)
DOX	0.120 ± 0.025
PTX	0.374 ± 0.034

Drug	IC_{50} (µM)
GEM	1.19 ± 0.030
CPT	0.130 ± 0.030

Figure 4. In vitro assays to assess single drug toxicity.

Cell inhibition on MDA-MB-231 in the presence of DOX (orange circles), PTX (blue circles), GEM (grey circles), CPT (green circles) for 72h. Cell viability data were fitted to the median-effect model to obtain IC_{50} values. Data are expressed as mean ± standard error of individual drug model fits ($n \geq 4$).

This model is based on the principles of an enzyme kinetic system comprising of mass action law, Michaelis Menten and Hill equations. Most drugs follow similar kinetics in exhibiting their cell killing effects and thus this model can be extended for multiple drug combinations. Since, the median effect analysis is a simple quantitative method to assess drug potency by performing a linear regression without using complex fitting parameters to account for different shapes (hyperbolic or sigmoidal) of the corresponding dose-effect curves, it is by far the most prevalent method for evaluating single drugs and their combination effects [8].

Amongst the four drugs, GEM was the least potent; PTX, DOX and CPT exhibited intermediate toxicities (Figure 4). In addition to the low IC_{50} values, previously, certain molar ratios of DOX and CPT were shown to exhibit cancer selective toxicity in a mouse TNBC cell line *in vitro* [47]. While researchers have shown molar ratios to alter the efficacy of many drug pairs, the distinctive cancer selectivity exhibited by combining DOX and CPT motivated us to pick this drug pair for our studies against human TNBC.

3.4 Optimizing DOX and CPT molar ratios for TNBC selective synergy

Cytotoxicity in MDA-MB-231 cells at various molar ratios of DOX and CPT were measured. Ratios were chosen such that both partner drugs most likely contributed to the combination cytotoxicity. Since DOX and CPT exhibited similar potencies, we chose molar ratios such that, in any given ratio, either drug is not more than 4-fold higher in concentration compared to the partner drug. Combination cell toxicity data show that as the molar ratio of DOX decreases, the IC_{50} value of DOX in the combination decreases. However, as the molar ratio of CPT increases, the CPT IC_{50} does not increase or decrease monotonically and rather varies

significantly across ratios and has a valley-like IC_{50} profile (Figure 5). This suggests that the DOX's individual contribution towards the cumulative cell-killing effect is lower at a DOX lower concentration, which is within intuitive grasp, but that of CPT is not so straightforward. The individual contribution of CPT in the cumulative cell-killing effect is variable across the ratios tested.

Besides, if the drugs had a purely additive effect, the dose reductions would be inversely proportional to the ratios in which they were combined. For example, for a 1:3 molar ratio of DOX:CPT, the dose reduction in DOX should be 75% (4 fold) and that for CPT should be 25% (1.33-fold) for an additive effect. Similarly, at a 1:1 molar ratio of DOX:CPT, there should be a 50% (2-fold) reduction in doses for each drug.

Remarkably, when DOX and CPT are combined at a 1:1 ratio, the dose reduction observed for DOX was 86% (7-fold) and for CPT was 68% (3-fold). This perplexing phenomenon of additional dose reduction, more than the expected level, is referred to as "synergy" and quantitatively measured by calculating the combination index (CI). Chou and Talalay introduced the method for calculating synergy via CI. Synergism, additivism, and antagonism are indicated by CI values less than 1, equal to 1, and greater than 1, respectively (Box 2). Drug doses for calculating CI are obtained by median effect analysis. Using this method interactions at different drug ratios and at different effect levels can be evaluated for up to three agents simultaneously combined [44]. CI can be expressed for any effect level, but since the median effect represents a linear approximation of a non-linear function, the plot may be unreliable at the extremes. Hence, the most accurate determination is when 50% of cells are affected; the corresponding drug dose is. IC_{50} [8]. This concept is schematically described in Figure 6.

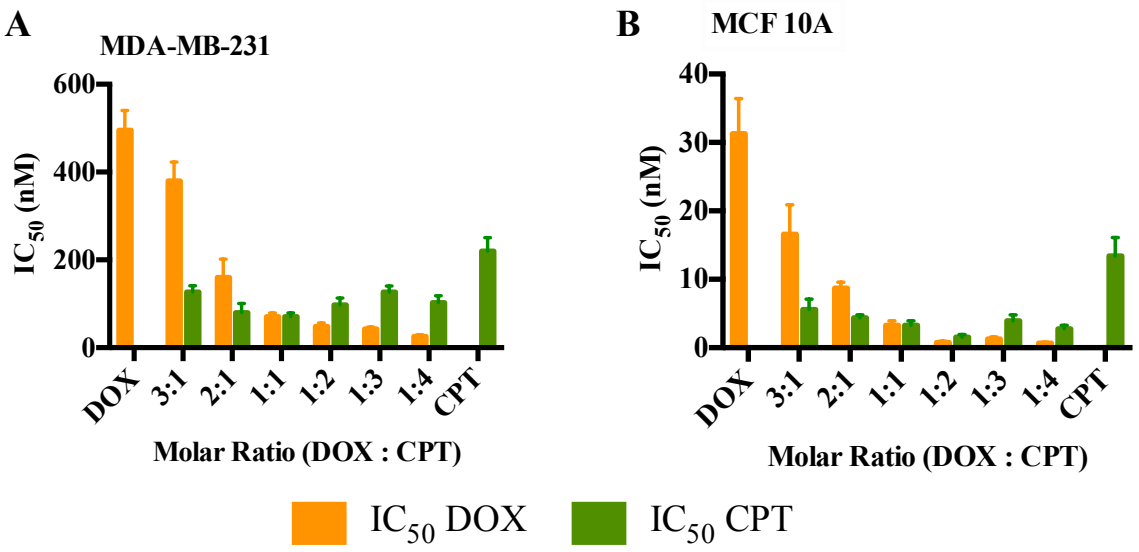

Drug ratio [DOX:CPT]	IC_{50} DOX (nM)	IC_{50} CPT (nM)
DOX	495.4 ± 44	
3:1	380.2 ± 42	126 ± 14
2:1	160 ± 41.5	80.2 ± 20
1:1	70 ± 8.8	70 ± 8
1:2	48 ± 7.8	97.3 ± 15
1:3	42 ± 4.6	127.1 ± 13.6
1:4	25 ± 3.9	102.6 ± 15.8
CPT		220.3 ± 30.2

Drug ratio [DOX:CPT]	IC_{50} DOX (nM)	IC_{50} CPT (nM)
DOX	31.3 ± 5.1	
3:1	16.6 ± 4.3	5.6 ± 1.5
2:1	8.7 ± 0.9	4.4 ± 0.4
1:1	3.3 ± 0.7	3.3 ± 0.7
1:2	0.7 ± 0.2	1.6 ± 0.4
1:3	1.3 ± 0.3	3.92 ± 0.9
1:4	0.68 ± 0.1	2.7 ± 0.5
CPT		13.4 ± 2.7

Figure 5. Effects of varying molar ratio in DOX and CPT combination treatments on MDA-MB-231 and MCF 10A cell growth.

The MTT assay was used to measure fractional cell inhibition of MDA-MB-231 and MCF 10A cells due to the combination treatment after 72 h incubations. Cell viability data were fitted to the median-effect model to obtain IC50 values corresponding to DOX (orange) and CPT (green). Data are expressed as mean ± standard error of individual drug model fits (n ≥ 5).

Box 2 Calculation of combination index

Combination Index, CI :	$CI = \frac{(D)_1}{(D_x)_1} + \frac{(D)_2}{(D_x)_2}$ *$(D_x)_1$ and $(D_x)_2$: Drug doses required to achieve a certain f_a* *$(D)_1$ and $(D)_2$: Individual dose of each drug in a given mixture that results in the same f_a*

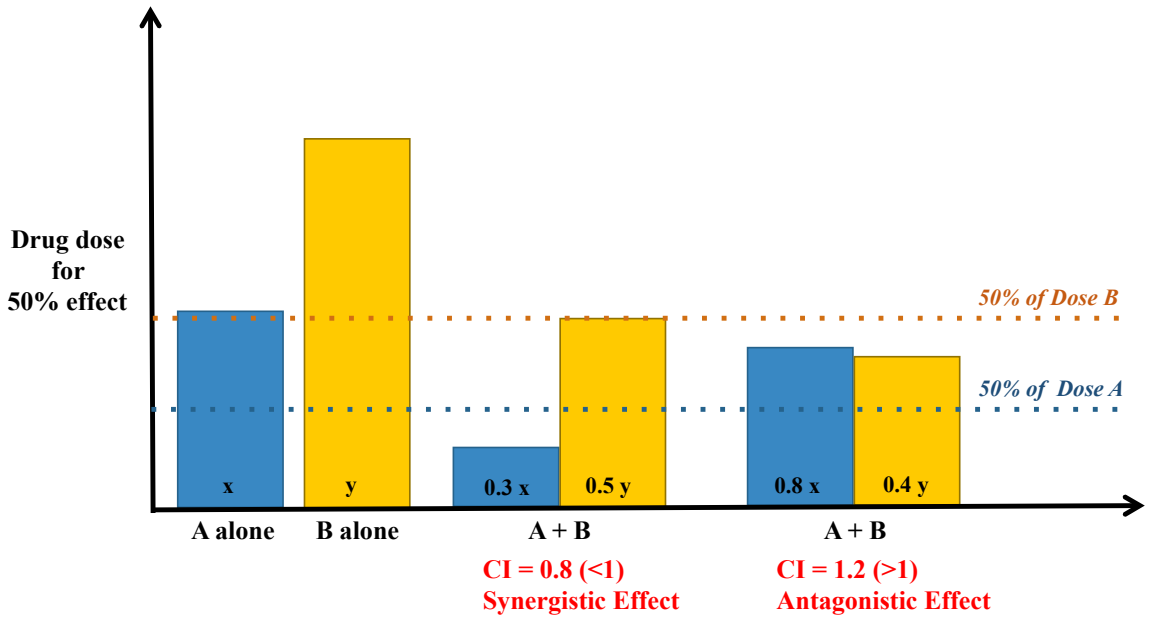

Figure 6 Cartoon showing how changes in drug dose correspond to a synergistic or an antagonistic effect.

To examine if any molar ratio of DOX and CPT exhibited cancer selective toxicity, we studied their effect on a control human breast epithelial cell line, MCF 10A. DOX and CPT displayed an approximate 20-fold reduction in the individual drug IC_{50} values on MCF 10A compared to MDA-MB-231 cells. In addition to being individually more toxic to control cells, cell proliferation in MCF 10A cells was muted more effectively at all ratios compared to MDA-MB-231 cells making it difficult to identify ratios of the drug pair that are relatively more toxic to the cancer cell and less toxic to the control cell line.

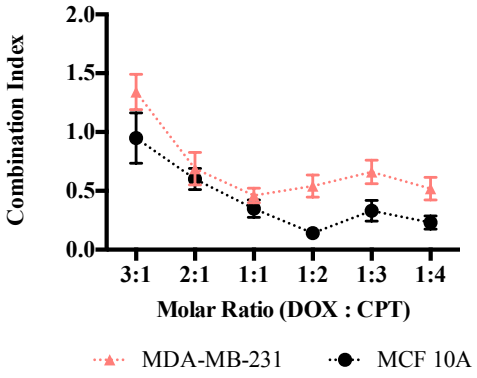

Drug ratio [DOX:CPT]	Combination Index		Significance
	MDA-MB-231	MCF 10A	
3:1	1.34 ± 0.15	0.95 ± 0.21	n.s.
2:1	0.69 ± 0.14	0.60 ± 0.09	n.s.
1:1	0.46 ± 0.06	0.35 ± 0.07	n.s.
1:2	0.54 ± 0.09	0.14 ± 0.04	$p < 0.01$
1:3	0.66 ± 0.10	1.02 ± 0.21	$p < 0.05$
1:4	0.52 ± 0.09	0.23 ± 0.06	$p < 0.05$

Figure 7. In vitro CI assessment to identify optimal molar ratios for DOX and CPT synergy. CI was calculated by the Chou-Talalay method for each drug ratio tested on MDA-MB-231 and MCF-10A cells. Errors were propagated from corresponding errors in cell viability data and standard errors of the drug model fits ($n \geq 5$). Statistical significance was performed using the Student's t test.

To identify a drug molar ratio that could be selectively toxic to the cancer cell line, we calculated the CI values of the drugs at all molar ratios on both the cell lines. Since lower CIs correspond to higher potencies, the highest difference in CI (MCF 10A CI > MDA-MB-

231 CI) would indicate highest cancer selectivity, with the best-case scenario being synergy (CI < 1) in breast cancer cells and antagonism in control cells (CI > 1). Contrary to previous experience where good synergy towards mouse TNBC cells and extreme antagonism to mouse control epithelial cells was observed, in this case the drug pair had comparable or lower CIs for all ratios and therefore exhibits more synergistic or equivalent killing in the control human epithelial cells compared to human TNBC cells (Figure 7). Also, enhanced killing in MCF 10A cells was observed when higher molar amounts of CPT were present in the combination suggesting that of the two drugs, CPT is an extremely potent drug with a narrow therapeutic index.

3.5 *In vivo* performance of DOX and CPT free drug cocktails

Despite the lack of cancer selective potency, the low CI values encouraged us to pursue this drug pair for further *in vivo* studies. At a molar ratio of 1:1 (DOX:CPT) we observed the highest synergy towards MDA-MB-231 breast cancer cells without a significant increase in synergy towards MCF 10A control epithelial cells. *In vitro* this synergy corresponded to a combination treatment that can achieve similar efficacies with a 7-fold reduced DOX dose and a 3-fold reduced CPT dose compared to the single drug counterparts (Figure 5). It was hypothesized that due to the high *in vitro* synergy; considerably lower drug doses would be needed *in vivo* for effective tumor reductions, Subsequently five different drug doses of DOX and CPT at a molar ratio of 1:1 were tested in an *in vivo* TNBC mouse tumor model.

MDA-MB-231 cells were injected subcutaneously into the mammary fat pad of athymic nude mice to generate robust orthotopic tumors in the breast and then these animals were treated with the formulations. A total of four injections of either saline or different

doses of DOX + CPT drug cocktail were administered intravenously every other day, starting 11 days post-tumor inoculation. At the end of 44 days, tumor volumes for the groups treated with 1.5 mg/kg DOX and 0.9 mg/kg CPT exhibited a statistically significant 82% size reduction relative to the saline-treated group (Figure 8). Slightly increasing the dose to 2 mg/kg DOX and 1.2 mg/kg CPT achieved over 90% reduction in tumor volumes relative to the saline-treated group. More remarkably, of one of the five mice in this group two mice had their tumor completely cured by day 31. Also, no significant body weight changes were observed in any of the mice, indicating that the drug dose levels used in the treatments did not cause any acute toxicity.

At the highest dose level, a 2-fold reduction in cumulative dosing of DOX (8 mg/kg) was achieved compared to a previous study that reported similar tumor regression on MDA-MB-231 tumors after treatment with 16 mg/kg free DOX (cumulative dose) [66]. The reduction in cumulative dose for CPT is even larger. A previous *in vivo* study reported only 49% tumor suppression after administering 30 mg/kg of free CPT [67]. In contrast, a superior tumor volume reduction at a 6-fold lower CPT dose was obtained. These dose reduction levels are also comparable in magnitude to the *in vitro* dose reduction levels.

Additionally, a potent therapeutic response was observed even though the dosage was roughly 4-fold lower than the Maximum Tolerated Doses (MTD) of DOX (between 8-12 mg/kg/dose [68,69]) and CPT (3 mg/kg/dose [70]). This is particularly exciting since one can now envision administering drugs at lower doses to achieve meaningful therapeutic effects while simultaneously producing lesser toxicity.

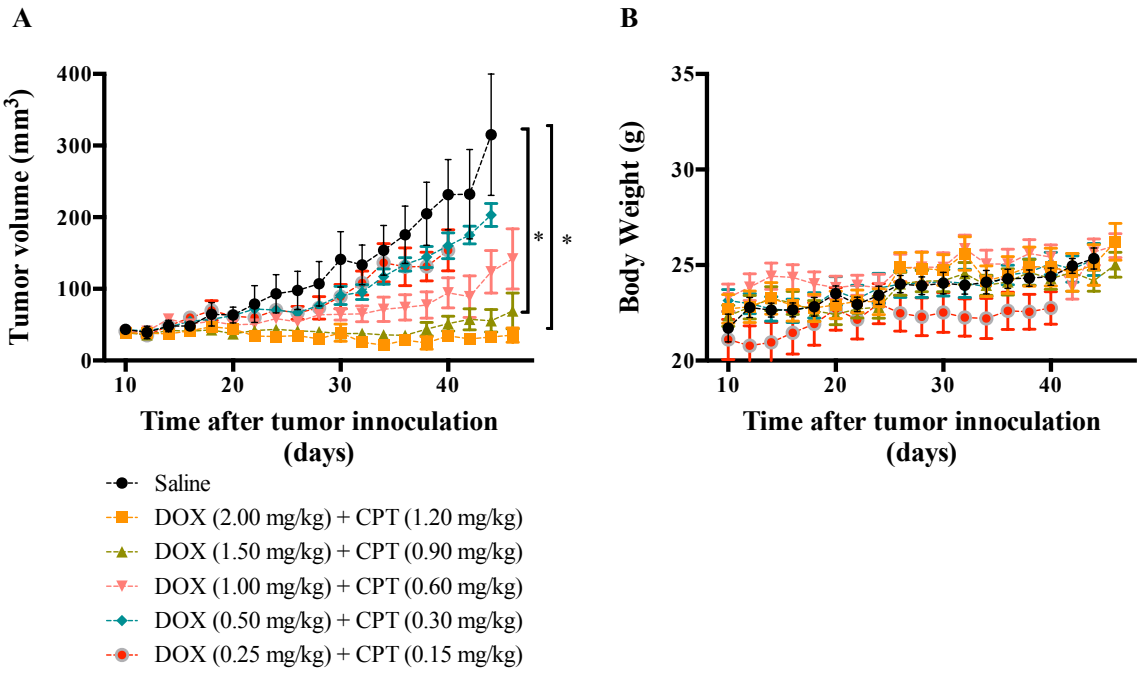

Figure 8. In vivo efficacy of different dose levels of DOX and CPT cocktail treatments in athymic nude mice.

*(A) Tumor growth curves in an orthotopic MDA-MB-231 mouse breast cancer model treated with a cocktail of DOX and CPT. Four injections were administered i.v. every other day starting on day 11 post-tumor inoculation. Statistical significance determined with the Holm-Sidak method (α = 5%) is provided for the last day on the curve (day 44). * = $p < 0.05$. (B) Body weight changes for all treatment groups. Data are expressed as mean ± SEM (n = 5).*

To verify if the low-dose tumor responses observed were a result of ratio-mediated synergy and if the drugs were still operating in the synergistic ratio regime *in vivo*, pharmacokinetic studies were performed. Drug concentrations in the plasma at different times were tested. The drug ratios were improperly maintained *in vivo*, which is unsurprising since different drugs have different pharmacokinetic properties. In humans the half-life for

CPT is about 71 -90 min and that for DOX is approximately 4 min [47]. A similar pattern is seen in mice, where DOX is cleared much faster than CPT (Figure 9). It is thus apparent that at the tumor sites, drugs are no longer present in the desirable ratio regime. The longer elimination time for CPT is also unfavorable since at molar ratios where CPT is available in excess to DOX, the drug combination is extremely synergistic to the control epithelial cells and could potentially cause toxicity at higher drug doses (Figure 7).

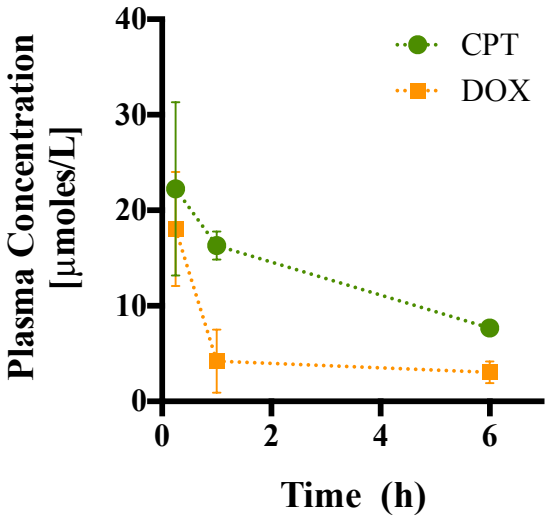

Figure 9. In vivo plasma pharmacokinetics of DOX and CPT in athymic nude mice.

Plasma concentration of DOX (orange squares) and CPT (green circles) after i.v. administration of DOX and CPT as a cocktail at 2 mg/kg DOX and 1.4 mg/kg CPT. Data are expressed as mean ± SEM (n = 5).

Nevertheless, the low dose tumor response suggests that with additional optimization, this drug pair can be translated into the clinic for testing as a potential therapy against TNBC.

3.6 Discussion on synergy and translational considerations for DOX and CPT

Identifying clinically successful synergistic combinations, albeit non trivial, is attributed to selecting drugs that are not cross-resistant and exhibit highly uncorrelated responses [27]. DOX and CPT are a suitable combination since these two drugs exhibit ratio-dependent synergy via cross-sensitive drug interactions [47,71,72]. CPT and DOX are topoisomerase I and II inhibitors respectively, and in combination exhibit collateral drug sensitivity or in other words sensitize cancer cells to one-another and synergistically inhibit tumor growth [73].

It has been previously shown that treating cells with DOX prior to CPT leads to antagonism in contrast to a concomitant or the reverse schedule [74]. Increased levels of topoisomerase II in response to CPT induced topoisomerase I down regulation are seen, sensitizing the cell to anthracyclines. Others have shown that the reverse case, increase in topoisomerase I levels in the presence of topoisomerase II inhibitors also occur. Hence, collateral drug sensitivity does not explain the occurrence of schedule or ratio dependent synergy. Interestingly, the authors also report an increase in the expression levels of p-glycoprotein proportional to the increase in topoisomerase II expression levels. P-glycoprotein is an efflux pump, overexpressed in drug resistant cancer cells, and is responsible for rapid and active removal of drugs from within the cells [75]. DOX is a known substrate for this pump and is rapidly expelled from a cell whereas CPT is a poor substrate and its intracellular accumulation is not hindered in the presence of this efflux pump [74,76].

Table 6. Topoisomerase I and Topoisomerase II inhibitor combinations in clinical trials

Topoisomerase Inhibitor		*Indication, Phase*	*Response*	*Main Adverse Effect*
I	*II*			*(Grade 3/4 toxicity)*
Topotecan	DOX or Pegylated DOX	Advanced solid tumors, Phase I [80]	27% PR *	Myelosuppression (25%)
		Ovarian Cancer, Phase I [81]	6% PR and 43% SD	Thrombocytopenia, neutropenia (40%)
Irinotecan	DOX or Pegylated DOX	Solid tumors, Phase I [82]	41% SD	Neutropenia (8%)
		Ovarian Cancer, Phase II [83]	30% OR	Leukopenia, neutropenia (48%)
		Refractory SCLC, Phase II [84]	12.9% PR	Neutropenia (6.5%)
Irinotecan	Epirubicin	Metastatic solid tumors, Phase 1 [85]	No OR	Neutropenia (~33%)
		Advanced solid tumors, Phase I [86]	12.5% PR	Neutropenia (51%)
Irinotecan	Amrubicin	SCLC, Phase I/II [87]	70% PR	Neutropenia (30%)
		Advanced NSCLC, Phase I [88]	11% PR	Neutropenia (23%)
		Relapsed NSCLC, Phase II [89]	29% OR	Neutropenia (77%)

* All in ovarian cancer

PR – Partial Response, OR – Objective Response, SD – Stable Disease

This differential response of the drugs to the efflux pump hints at the possibility of observing ratio dependent synergy. At higher molar ratios of DOX:CPT, since the absolute amount of DOX is higher, a larger amount of drug could undergo expulsion resulting in a lower cumulative drug dose o within the cell. This difference in intracellular drug accumulation levels could explain the trend of observing lower toxicity and therefore lower synergy at higher molar ratios of DOX:CPT; in turn giving rise to molar ratio dependent synergy.

Other combinations of topoisomerase I and II inhibitors are also of significant interest in the clinic due to extensive pre-clinical evidence of synergy via collateral drug sensitivity (Table 6). Several topoisomerase II inhibitors like, DOX, daunorubicin and epirubicin are clinically approved for treating cancers like breast, lung, ovarian and hematological cancers [58,77]. On the other hand, only two topoisomerase I inhibitors, irinotecan and topotecan, are clinically approved [78]. Irinotecan is approved for use in ovarian and SCLC and topotecan is approved for gastrointestinal malignancies, SCLC and NSCLC [65]. Hence, most topoisomerase I and II inhibitor combinations are currently being clinically tested either in ovarian or lung cancers. However, there is an increase in the use of topoisomerase I inhibitors to treat breast cancer in pre-clinical and clinical settings. Perez et.al. and Hayashi et. al. have shown that irinotecan could be used as a salvage therapy in patients with anthracycline or taxane-based refractory metastatic breast cancer [63,64]. Topotecan has shown promise for treating breast cancer brain metastases [79]. Furthermore, two other topoisomerase I inhibitors diflomotenac and lurtotecan are in phase II clinical trials against several indications including breast cancer [76,78].

Despite being the first topoisomerase I inhibitor discovered, CPT on its own has not been successfully translated to the clinic due to its poor water solubility. Initial efforts to increase its solubility at neutral pH were mostly focused on opening of its lactone ring, which resulted in a dramatic reduction of its cytotoxicity. As a countermeasure, very high drug doses of CPT were administered to achieve meaningful efficacies but it resulted in severe myelosuppression. Secondly, the active drug form, favored in urine due to spontaneous ring closure at acidic pH, caused severe bladder toxicity. In addition to the unpredictable toxicity in patients, variable and limited objective responses in phase II clinical trials led to its failure [65]. Nevertheless, ever since the mechanism of action of CPT was elucidated, there has been an enhanced interest in using topoisomerase I inhibitors against cancer. To overcome problems associated with CPT, water soluble derivatives like irinotecan and topotecan were discovered and used along with DOX (Table 6, 80, 81). Their success is however limited due to significant worsening in toxicity and minimal therapeutic benefit after combining them. Further, the water soluble counterparts have been demonstrated to possess decreased anti-tumor activity compared to their water insoluble counterparts [65,92], instigating a wide effort to find alternative ways to translate them.

Parallel efforts to revive CPT have shown that covalent conjugation at the 20-OH position to water soluble polymers can stabilize the labile lactone ring and improve solubility [93,94]. Several vectors for delivering CPT have been developed and are actively undergoing clinical investigation (Table 7). These technologies were developed with a focus on improving the solubility, pharmacokinetic properties and reducing the adverse reactions of CPT to enhance its therapeutic window and tumor accumulation levels. Although moderate antitumor activities were observed for several of these drug conjugates, clinical advancement

is stunted due to the bladder toxicity from high levels of camptothecin excreted via urine [95]. Recently, it was shown that imparting targeting capabilities to CPT using antibodies significantly decreased off target binding without compromising its potency [96,97].

Hence, targeted delivery of CPT in a drug conjugate format could resolve the traditional problems of toxicity and poor pharmacokinetics faced by the free drug detrimental to its translation. Extrapolating this concept to a synergistic drug pair could lead to even greater benefits. Specifically, lack of cancer selectivity of DOX and CPT can be tackled by conjugating them to a TNBC specific carrier and the specificity can be leveraged to reduce the dose even further.

Significant tumor reductions observed at extremely low drug doses bolsters the potential of DOX and CPT to be a potent drug combination against TNBC. An obvious molar ratio dependence of DOX and CPT on the TNBC cells was seen but the difference in the CIs between TNBC and control cells were not satisfactory since the combination is not selectively toxic to the cancer cells in the range of molar ratios tested. Moreover, the ratios in circulation were poorly maintained. Thus, achieving additional dose reduction by a two-step approach is envisaged. First step would be to effectively control the drug ratios in circulation so that they accumulate at the tumor site in a desirable window and the second step would be to improve the drug pair's selectivity towards cancer. The next chapter describes targeting strategies for delivering a chemotherapeutic drug pair specifically to TNBC cells.

Table 7. Camptothecin drug carriers undergoing clinical trials.

Name (drug)	*Description*	*Cancer, Phase*	*Trial Identifier*
CRLX101	CPT conjugated to cyclodextrin-poly(ethyleneglycol) copolymer [93]	Several, Phase II	NCT02769962 NCT01380769
CT-2106	CPT conjugated to polyglutamic acid backbone [94]	Colorectal and Ovarian, Phase I/II	NCT00291785
XMT-1001	CPT conjugated to polyacetal poly(1-hydroxymethylethylene hydroxymethylformal) [95]	SCLC and NSCLC, Phase I	NCT00455052
MAG-CPT	CPT conjugated to methacryloylglycinamide [98]	Malignant solid tumors, Phase I	NCT00004076
PEG-CPT	Pegylated-CPT [99]	Sarcoma and stomach cancers, terminated	NCT00079950 NCT00080002

Chapter 4

Targeting cancer with aptamers

Different pharmacokinetics, biodistribution and transport properties of small molecules makes it extremely difficult to develop an optimized dosing and scheduling regimen to deliver combination drugs to the tumor in a synergistic window [100]. Unsurprisingly, it is one of the root causes for not witnessing synergy in clinical settings despite obtaining synergistic effects in vitro or in preliminary rodent tumor models [27]. The other major concern of small-molecule drugs, causing toxicity to healthy tissues by non-specific and off-target accumulation has been comprehensively discussed in Chapter 2.

Nanomaterials have proven their competence in improving the therapeutic window of toxic drugs for safer delivery, minimizing issues with degradation and poor circulation half-lives of commonly employed small molecule drugs [75,101]. Most importantly, nanoparticles are predominantly used to unify pharmacokinetics and biodistribution of different drugs. Drugs with distinct chemical properties can be co-encapsulated in nanoparticles for synchronous and uniform delivery of multiple agents that would otherwise undergo non-uniform distribution when injected as a drug cocktail due to their separate biological and physiological fates. This concept is schematically depicted in Figure 10 along with the commonly employed types of nanoparticles used in combinatorial drug delivery. Further, it has been shown that appropriately sized nanoparticles can evade rapid renal and biliary clearance and passively accumulate in tumor sites via the enhanced permeation and retention (EPR) effect [8,102,103]. In conjunction with this ‘passive’ mode of targeting, ‘active’

targeting to cancer specific ligands or receptors is also employed. It can serve as a crucial accumulation strategy for tumors without an apparent EPR effect such as small unvascularized metastases or a circulating tumor cell (either in transit or buried in between non-cancerous cells) that cannot be passively targeted [104,105]. In this chapter, current tumor targeting strategies are reviewed and a blueprint for effective tumor accumulation is proposed. A new class of targeting agents- aptamers- as an option for improved cancer targeting is explored and specifically a TNBC recognizing aptamer is identified and validated.

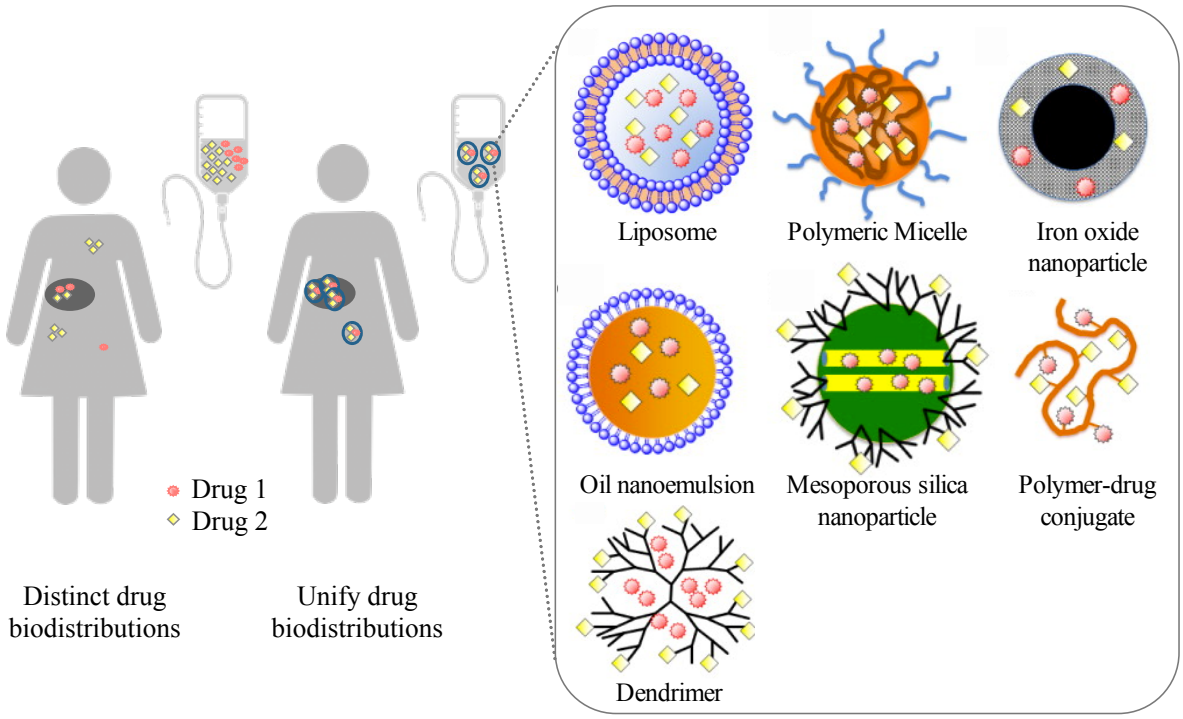

Figure 10. Pharmacokinetic advantages of delivering drug combinations via nanoparticles. Different types of nanoparticles used for dual drug delivery are depicted in the box. Nanoparticle diagrams have been reprinted with permission from [43].

4.1 Current tumor targeting strategies

Delivering lethal drugs specifically to cancer cells while avoiding healthy tissues is the Holy Grail of cancer therapy. Significant strides have been made in providing drug vectors with cancer homing properties by leveraging naturally occurring phenomena like EPR and recognition of cancer markers by antibodies or by incorporating engineered materials and drug linkers that can provide cancer-specific drug release.

Passive targeting by EPR

In 1986, Maeda and Matsumara first noted the phenomenon of preferential tumor accumulation of proteins and large molecules of various sizes. Their superior accumulation was attributed to the "leaky" feature of tumor blood vessels due to the rapid angiogenesis and lack of sufficient lymphatic drainage in solid tumors. Several nanoparticles were shown to have similar tumor tropic effects and have been tuned extensively to take advantage of the phenomenon. Some characteristics that affect EPR of nanoparticles include: molecular size, surface charge and blood circulation time. Particles that are over 40 kDa in molecular weight and smaller than a couple hundred nanometers in size with a neutral or weak negative surface charge and long circulation times are predicted to have favorable accumulation within tumors [106,107]. However of late, EPR is increasingly being considered as a heterogeneous occurrence in the clinic and even non-existent in some cancers. For example, the EPR offers less that 2-fold increase in nanoparticle tumor accumulation in comparison to other organs. In a comparison done with stealth liposomes across clinical tumors of breast, head and neck and bronchus, the accumulation levels fluctuate widely between 2.7 to 53% ID/kg. This effect is

also often over-predicted in preclinical models due to the abnormally high growth rates in tumor xenografts that are not truly representative of the real disease condition [108,109].

A drug carrier parameter that is becoming increasingly relevant due to heterogeneity in tumor vasculature and morphology is its molecular size. Several barriers exist in tumor microenvironments that hinder the transport of nanoparticles into the tumors. Tumors often have heterogeneous, tortuous vasculature and high blood viscosity resulting in slow diffusion rates. The interstitial matrix comprises of collagen and other proteins resulting in a characteristically dense environment and the lack of functional lymphatics can lead to increase in interstitial fluid pressure thereby limiting convection-mediated transport and forcing diffusion-mediated transport. Nonspecific uptake by tumor stromal cells further aggravate the already diffusion compromised tumor penetration problem [110,111]. Cancer therapeutics have to typically traverse intercapillary distances of 80-100 micrometers to reach tumor cells that are distant from the blood vessels. Since the rate of diffusion is inversely proportional to the cube root of molecular weight smaller particles would more readily diffuse within the tumor tissue [103,112]. However, there is a risk of rapid elimination of small particles by renal filtration and secondly, therapeutic agents that can easily diffuse into the tumor can also rapidly diffuse out of the tumor. Thus, finding alternative ways to enhance retention properties of such small therapeutics within a tumor becomes extremely important.

Active targeting approaches

Paul Ehrlich's vision of 'magic bullets' – agents that seek and destroy targets specifically without damaging the host organism's tissue - has long fascinated researchers in the field of

oncology [113]. The surfaces of several nanoparticle platforms, such as liposomes and micelles, are decorated with ligands that recognize and interact specifically with cancer receptors to deliver a drug combination by active targeting [114]. Other active approaches include stimuli-responsive and prodrug based strategies. Prodrugs are inactive derivatives of drugs that are metabolized at specific target sites in the body for generating the active for of the drug [115]. In cancer drug delivery approaches, drugs are loaded on either inert or tumor specific carriers and released under very specific conditions inside the tumor environment or a cancer cell. Drugs coupled to a backbone are usually inactive but once released they regain their activity. For example, drugs conjugated to certain engineered linkers do not elicit any cytotoxicity but when released in response to endogenous stimuli like reduced pH, different intracellular and extracellular redox conditions or by enzymatic action, they elicit their toxic effects. These types of systems are still very naïve and under investigation in the preclinical stages. The main challenge in advancing these systems is to work around the problem of widely varying tumor physiologies leading to non-uniform tumor responses. Drug delivery systems have also been developed to release drugs based on external stimuli like heat, light and ultrasound. Though these systems are more reliable, they require prior knowledge of the tumor lesion location [115,116].

4.2 Considerations for effective tumor drug accumulation and delivery

Although the tumor targeting strategies are conceptually sound, several emerging studies are questioning its advantage in real clinical settings. A folate receptor targeting liposome did not display an enhanced tumor accumulation compared to a control PEGylated liposome [117]. Similarly, a recent meta-analysis published by Chan and coworkers compared the delivery

efficiencies of 117 nanoparticle papers and found that the median delivery efficiency to tumors is only 0.7%. But more disappointingly, the tumor accumulation difference between active and passive targeting approaches is a mere 0.3%, a far cry from the concept of "magic bullets" [103].

Thus it is clear that targeting does not play a heavy role in enhancing the tumor accumulation levels. However, the improved tumor efficacies of targeted systems imply that they have rather important contributions in other aspects of the drug delivery process. The consequence of imparting targeting properties to formulations is their enhanced retention capacities in tumors and ability to enter cells via alternative cellular uptake mechanisms. In agreement to this concept, in a recently published study, when receptors overexpressed on tumor cells or tumor vasculatures were independently or jointly targeted they correlated to significantly improved tumor efficacies, which in turn was credited largely to the improved retention times and cellular uptake rates instead of differences in absolute drug uptake levels [118].

Apart from traversing the tumor interstitium, cell uptake and distribution of delivery systems to the appropriate subcellular compartment where the drugs can elicit their inhibitory effect presents another major transport barrier. This secondary barrier is often neglected and not considered while designing drug delivery systems. Targeted systems nonetheless have an advantage over non-targeted systems of being internalized via active mechanisms such as: clathrin-dependent endocytosis, clathrin-assisted receptor mediated endocytosis, cell adhesion molecule mediated endocytosis, fluid phase endocytosis and caveolin assisted receptor mediated endocytosis. Apart form offering a more rapid route for cellular internalization, these mechanisms also provide an alternative pathway for cell uptake that is

superior to conventional diffusion and non-specific endocytosis methods where drugs and non-targeted systems are prone to removal by efflux pumps and slow uptake rates, respectively. By decorating delivery systems with appropriate ligands, active targeting can be exploited to traffic the delivery system and in turn the drug being carried to the subcellular compartment of interest [119].

Taking all these facts into consideration, a revised approach to determine the ability of a delivery system to effectively accumulate and exhibit a cytotoxic effect in a tumor mass is proposed. For favorable clinical outcomes, instead of optimizing properties of drug delivery systems separately, three aspects have to be simultaneously optimized – tumor penetration or permeation, tumor site retention and the cell internalization mechanism (Figure 11).

The advantages of active targeting described above can have great implications in this revised format for optimizing small drug delivery vehicles for cancer therapy. First, smaller delivery systems can diffuse and penetrate heterogeneous tumor masses more effectively compared to larger sized nanoparticles. Secondly, they do not have to solely rely on EPR for extravasation and retention since they can be given tumor cell and tumor vasculature targeting properties for preferential cancer uptake and retention. Finally and most importantly, they can be designed to have improved cell internalization rates and a suitable intracellular trafficking property for efficient delivery of drugs to their final target site.

Another approach to circumvent the lack of substantial responses due to low tumor accumulation levels is to deliver an extremely potent payload to the tumor. To this end, some report the use of extremely toxic drugs such as monomethyl auristatin E (MMAE) and derivative of maytansine 1 (DM1) but these drugs are so lethal that even at extremely low

doses, or due to a small off target gathering, lead to the manifestation of severe adverse effects. Another alternative to these low therapeutic index drugs is to deliver a potent synergistic combination of commonly employed chemotherapeutics as discussed in Chapter 3. By carefully optimizing the molar ratios at which drugs are exposed, potency of a combination can be improved by several folds.

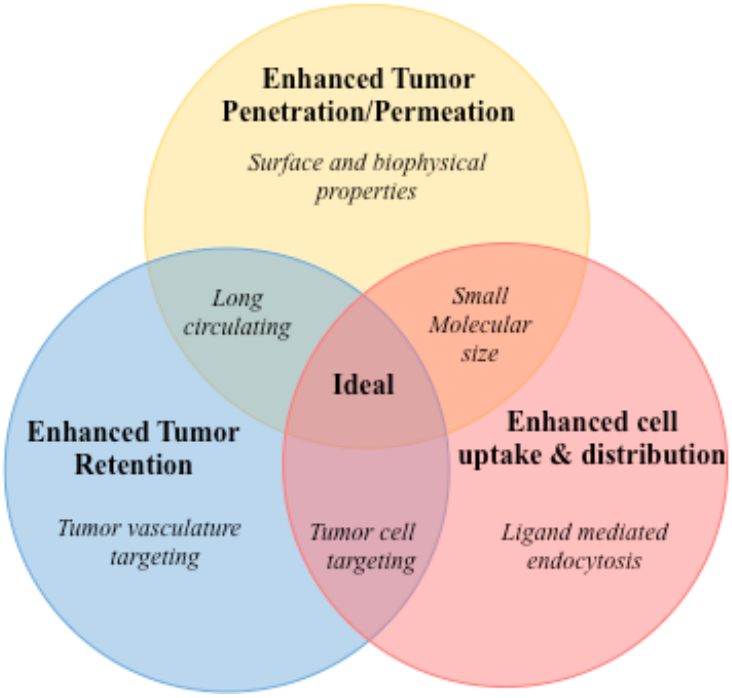

Figure 11. Favorable phenomena (bolded) and discrete properties of a delivery system affecting them (italicized) to be optimized simultaneously for successful treatment of solid tumors.

Antibodies have long been exploited as molecular targeting agents to enhance accumulation of non-specific toxic payloads to tumors. Antibody drug conjugates (ADC) are the current gold standard small-sized delivery systems that deliver potent drugs to tumors by

active targeting. Chemotherapeutic drugs are covalently conjugated to an antibody, which serves as a drug carrier and the targeting ligand simultaneously, to enhance tumor accumulation and also promote specific receptor-mediated cellular uptake. After the failure of first-generation ADCs, where drugs were conjugated to the antibody via weak and labile linkers, second-generation ADCs were designed to incorporate drugs by sophisticated linker technologies that allowed preferential drug release in target cells/cell organelles [103,120]. Several other breakthrough efforts in the field of antibody drug conjugates, such as the development of human or humanized antibodies along with improved drug linker technologies, overcame traditional issues of immunogenicity and non-specific drug release of ADCs [120–122]. Two ADC formulations (brentuximabvedotin and adotrastuzumab) are already approved by the FDA and over 30 more ADCs are in clinical trials [120].

Antibodies, even humanized ones, suffer from a few disadvantages. They have an Fc region which undesirably interacts with soluble Fc receptors and Fc receptors expressed on immune/other cells to result in non-specific immune stimulation or hypersensitivity (immune adverse effects). Furthermore, an antibody's molecular weight, though small enough to show improved circulation times, is high enough to impede its penetration into deep solid tumors. Diffusion is also affected by antibody affinity. 'Binding site barrier effect' decreases penetration of antibodies because high affinity antibodies bind tightly to the antigens expressed on tumor periphery and do not penetrate until all peripheral antigen molecules are saturated. Hence, antibodies with optimal affinities are required and engineering such optimal affinities to them is extremely challenging. Apart from limiting their tumor penetration, their large molecular weight impedes cellular uptake and access to many biological compartments leading to an additional compromise in their bioavailability.

In addition to low delivery efficiencies, due to poor tumor penetration and cellular uptake levels, another drawback that poses a significant hurdle in their translation is the low drug loading capacity. For ADCs, the optimal drug to antibody ratio (DAR) is around 4. Even though antibodies contain about 80 – 90 conjugation sites, higher drug loading affects them negatively. Antibodies with higher DARs (6 or 8) have been shown to have undesirable chemical and physical properties and also compromised targeting capabilities. Site-specific conjugation techniques were introduced to overcome the interference in affinity due to drug conjugation at random sites on the antibody; however, the maximum number of drug molecules that can be conjugated using these technologies are either 2 or 4. Other antibody shortcomings include, off-target cross reactivity, denaturation, limited shelf life due to poor chemical and thermal stability and batch-to-batch variability in their manufacturing process [122–127].

4.3 Aptamers – a new class of tumor targeting agents

Aptamers have garnered tremendous interest as antibody replacements due to their ability to penetrate deeper into tissues while still retaining specificity to cancer markers and flexibility to target a wide range of tumor ligands [126–128]. Aptamers are short, single-stranded, synthetic nucleic acid oligomers, DNA or RNA that can form complex three- dimensional structures with a capability to bind to proteins, enzymes, cell surface markers and small molecules with high affinity and specificity [123,129,130]. In contrast to antibodies, aptamers possess chemical and thermal stability, display minimal immunogenicity, can be chemically modified in a facile and controlled fashion without affecting its binding affinity, and can be rapidly discovered against both known and unknown cell-surface targets [131].

Table 8 Aptamers in clinic or clinical trials.

Name	*Disease*	*Target*	*Phase*	*[Ref]*
Macugen	Age related macular degeneration, Diabetic macular edema, Proliferative diabetic retinopathy	$VEGF_{165}$	Approved	[132,133]
AS1411	Metastatic renal-cell carcinoma, Advanced solid tumors	Nucleolin	Phase II	[134]
NOX-A12	Multiple Myeloma and non-Hodgkin lymphoma, chronic lymphocytic leukemia	CXCL12	Phase II	[135,136]
NOX-E36	Chronic inflammatory diseases, Type 2 diabetes mellitus, Systemic lupus erythematous, Albuminuria, Renal impairment	CCL2	Phase II	[137–139]
NOX-H94	Anemia, End-stage renal disease, Inflammation	Hepcidin peptide hormone	Phase II	[140–142]
NU172	Heart disease	Thrombin	Phase II	[143]

These advantages are extremely applicable for developing successful anti-cancer targeted delivery systems and hence we chose to explore aptamers as potential targeting

agents against TNBC. For our studies, we used an aptamer known as AS1411 that recognizes and binds specifically to nucleolin, a protein that is overexpressed on the cell surface of several cancer cells and tumor endothelial cells. In normal cells, nucleolin is detected only in the nucleus but in cancer cells nucleolin is detected in both the nucleus and the cytoplasm [118]. Since it is a guanine quadruplex aptamer, the structure makes it resistant to nuclease degradation in the serum and enhances the cell uptake rate.

AS1411 has been extensively studied and is currently in phase II clinical trials for acute myeloid leukemia and renal carcinoma [124]. Preclinically, AS1411 has been shown to inhibit more than 80 types of cancer cell lines in vitro and has shown efficacy in several xenograft models, including non-small cell lung, renal and breast cancers. Also, it has been proposed that AS1411 first binds to cell surface nucleolin and gets internalized via receptor-mediated endocytosis to the nucleus. This is particularly advantageous to deliver the drug pair of DOX and CPT, since they both inhibit enzymes that are present in the nucleus. MDA-MB-231 TNBC cells, used earlier in Chapter 3 to test the synergy of DOX and CPT, are also known to overexpress cell surface nucleolin. Thus the targeting ability of AS1411 against these cells was tested *in vitro* to verify if it would qualify as an agent that could provide effective tumor accumulation and retention (Figure 11).

Enhanced tumor penetration of aptamer drug delivery systems

One of the major advantages of aptamers over other molecular targeting agents is its small size. Aptamers range anywhere between 10 to 20 kDa in size, almost one-tenth the size of an antibody that is typically sized around 150 kDa. An EpCAM targeting aptamer and antibody were tested for their cell internalization ability *in vitro* and penetration capacity in an *in vitro*

tumor sphere model in an *in vivo* tumor xenograft model. Cells were able to uptake aptamers more efficiently than antibodies and aptamers penetrated better into both the tumor spheres and xenografts. Surprisingly, aptamers were also retained better in the tumor, 24 h after the injection [144].

To test if AS1411 is small enough to display enhanced tumor penetration, its performance was compared against two other drug carriers of different sizes – hyaluronic acid (HA) conjugates and liposomes. All drug carriers were loaded with DOX as the model drug since it is fluorescent and the extent of tumor penetration of the carrier can be read via DOX fluorescence. The final drug carriers were an aptamer-DOX conjugate (Aptamer-DOX) around 9.0 ± 2.1 nm in size, a 122 ± 43 nm HA-DOX conjugate and a 75.5 ± 2.3 nm DOX-Liposome (DOX-L).

Penetration capacities of differently sized drug systems were tested in an *in vitro* tumor-spheroid model. Tumor spheroids are 3 dimensional *in vitro* cultures of tumor cells that were originally developed to overcome the traditional limitations of a monolayer cell culture that does not capture vital *in vivo* characteristics of tumors such as gradients in oxygen, growth factors, nutrients or the presence of necrotic or hypoxic regions in the tumor core. Several different techniques are used to develop tumor spheroids such as rotary vessels, liquid overlay microplates, aqueous two phase system and hanging drop arrays [145]. The hanging drop array method was used since it is a high throughput technique that can form uniformly sized spheroids which is essential to accurately test the penetration capacities of different carriers. Specifically, a spheroid using a co-culture of 4T1 breast cancer cells and 3T3 fibroblast cells was established. To decouple the penetration capacity of the aptamer from its tumor cell binding property, 4T1 cells were chosen because they not over express

cell surface nucleolin. Further, 3T3 fibroblast cells were used in the spheroid architecture to provide a dense extracellular matrix, a characteristic responsible for impeding diffusion of drug molecules and carriers in tumors [146].

A clear trend between size and penetration efficiency is not immediately apparent. Free DOX penetrated the most at all time points followed closely by Aptamer-DOX system (Figure 12). At 12 hours, the aptamer system penetrated 29% and 75% more than the HA-DOX and DOX-L systems, respectively. After 48 hours, it reduced to 20% and 24% respectively. However, it is worth noting that in the HA-DOX system, the amount of uptake seemed to saturate after 24 h but the penetration of Aptamer-DOX system was still steadily increasing.

Superior binding of AS1411 aptamer to TNBC cells over control cells

Once it was established that AS1411 drug conjugates had superior penetration capabilities, an aptamer-binding assay was used as a surrogate to study how efficiently it would be retained in a tumor. A 50 to 100-fold enhancement in AS1411 binding to TNBC cells relative to the control epithelial cells was observed. Also, when a control aptamer was tested on MDA-MB-231 cells, it displayed a significantly lower binding capacity (Figure 13). Cumulatively, these results suggest that AS1411 aptamer molecules that penetrate a tumor mass would bind to the tumor cells that overexpress nucleolin on the cell surface and be retained better.

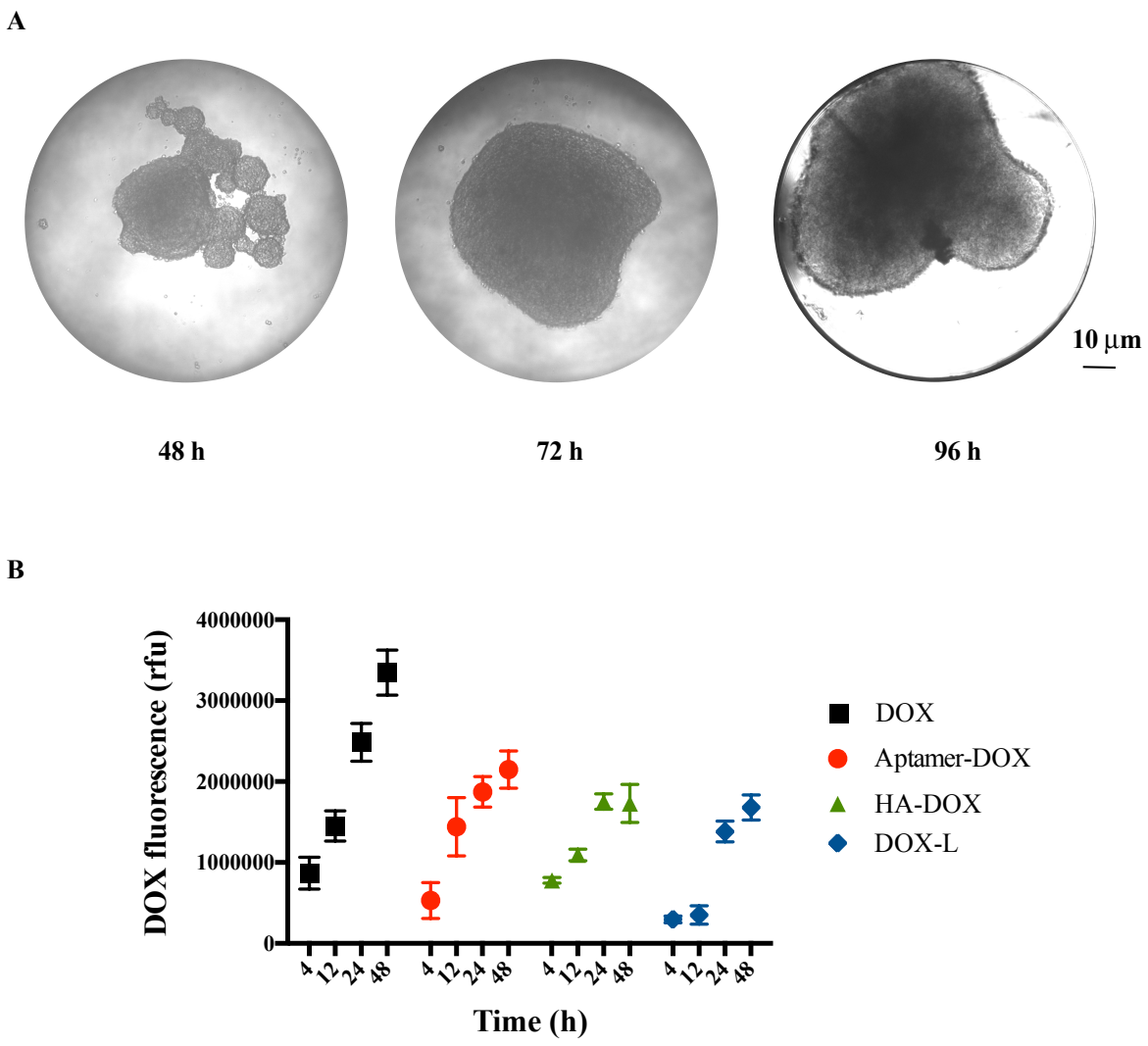

Figure 12. In vitro aptamer penetration in tumor spheroids.

(A) Representative images of 4T1/3T3 co-culture tumor spheroids at 48 h, 72 h and 96 h. Scale bar represents 10 microns. All images were taken under bright field at respective time points. (B) Drug carrier penetration measured at 4 h, 12 h, 24 h and 48 h measured by fluorescence of DOX at each time point. Data are represented as average DOX fluorescence and standard deviation (n=6).

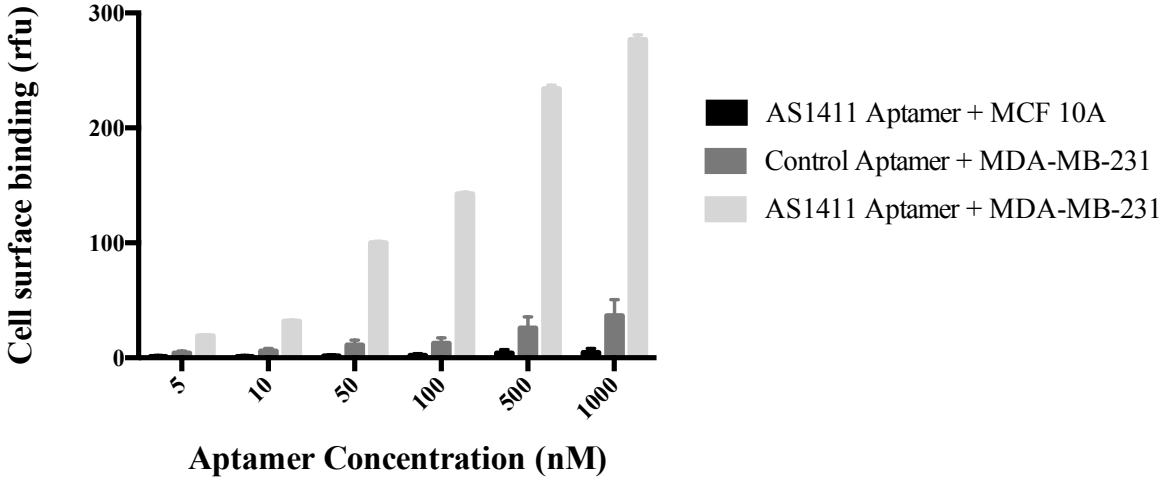

Figure 13. In vitro assays to evaluate aptamer binding to cells.

Specific binding of modified AS1411 aptamer to MDA-MB-231 cells was verified via flow cytometry. 3 × 10^5 cells were stained with Cy5-NucA (Table 11) or Cy5-CRO (Table 11) for 1 h at 4 °C in PBS buffer containing 5% FBS and 0.1% sodium azide. Post-incubation, cells were washed twice and analyzed via flow cytometry. Fold-increase in median Cy5 fluorescence compared to a control cell population is plotted on the y-axis against different aptamer concentrations. Data express mean± SD (n =3)

This can be extended to tumors expressing a heterogeneous mix of markers, which is a more realistic version of clinically observed cancers. Unlike antibodies, which can be generated only for antigens that can be well tolerated and can cause an immune response in animals, aptamers for virtually any target can be rapidly selected via SELEX (Systematic Evolution of Ligand by Exponential enrichment). The selection can be done either *in vitro* or *in vivo* based upon the final application [147,148]. This has huge implications for the field of

metastatic cancer since malignant neoplasms have a pronounced cellular heterogeneity and often develop resistances to various therapies by phenotypic or genome variation [149]. For example, in metastatic prostate cancer, a gold standard treatment is to block the androgen-androgen receptor pathway, but despite initial response to this type of therapy, patients develop resistance and proceed to highly resistant cancer stages that often have very poor prognosis [150].

Hence, as these disease stages evolve and progress, newer targeting strategies have to be employed to tackle tumor progression. In such situations, screening for an aptamer for these newly evolved phenotypes can be done much more rapidly and easily as compared to developing an antibody. Using methods like cell-SELEX, it is possible to generate highly specific aptamers without having to know anything about the protein, receptor or target of interest [109]. In contrast, it is virtually impossible to develop an antibodies against cell-surface markers that are not available in functional recombinant form due to limited ability in generating negative selection pressures for antibody selection [123]. Also, aptamers with wide ranges of affinities and specificities can be screened for in a single SELEX experiment. Hence, issues such as 'binding site barrier effect' can more effectively be tackled with aptamers.

Aptamer localizes to nucleus after cell uptake

It has been proposed that AS1411 bound to cell surface nucleolin is carried to the nucleus where it is released and the nucleolin receptor is recycled back to the cell surface (Figure 14). DOX and CPT inhibit enzymes that are present in the nucleus and hence this aptamer would be a perfect choice to deliver this drug pair. Specific binding of the aptamer to MDA-

MB-231 was already observed, hence if the aptamer localized efficiently to the nucleus was next investigated. To verify this, confocal microcopy was done where MDA-MB-231 cells and MCF 10A cells were incubated with a fluorophore labeled nucleolin aptamer and their nuclei were stained with the Hoecsht dye. Enhanced internalization and exclusive nuclear colocalization of AS1411 aptamer within 4 h in TNBC MDA-MB-231 cells was confirmed. In the control MCF 10A cells, the aptamer was mostly stuck non-specifically to the external cell membrane (Figure 15).

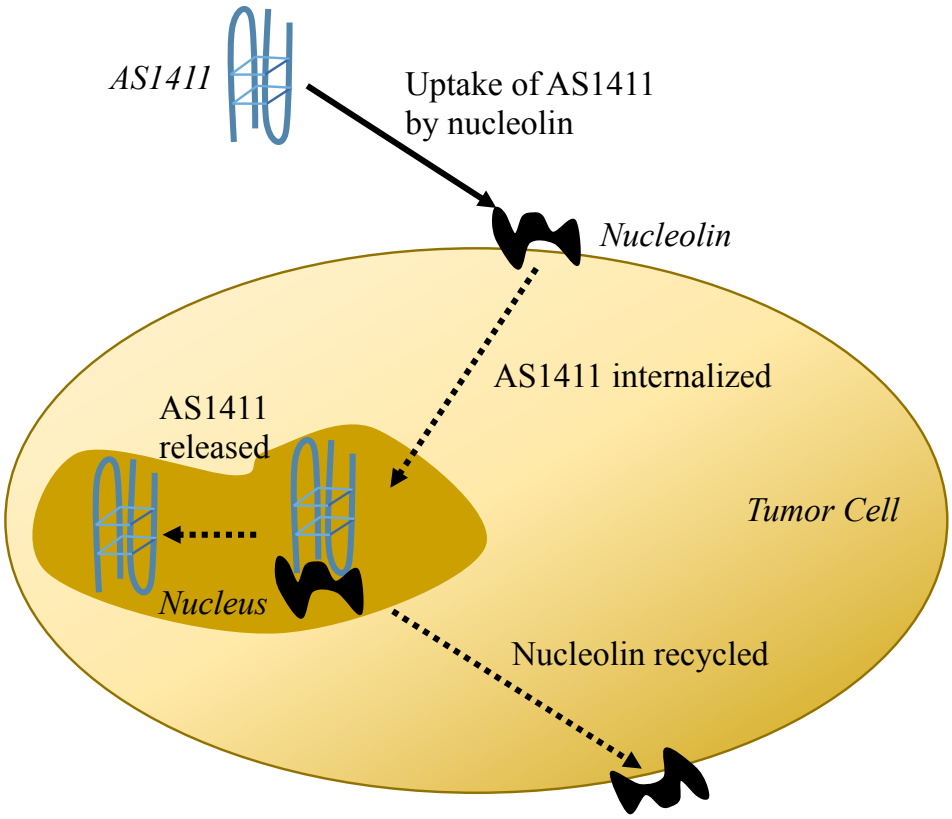

Figure 14. AS1411 cell uptake mechanism [151].

These results suggest that AS1411 aptamer a promising targeting agent to use against TNBC cells that overexpress nucleolin on their surface.

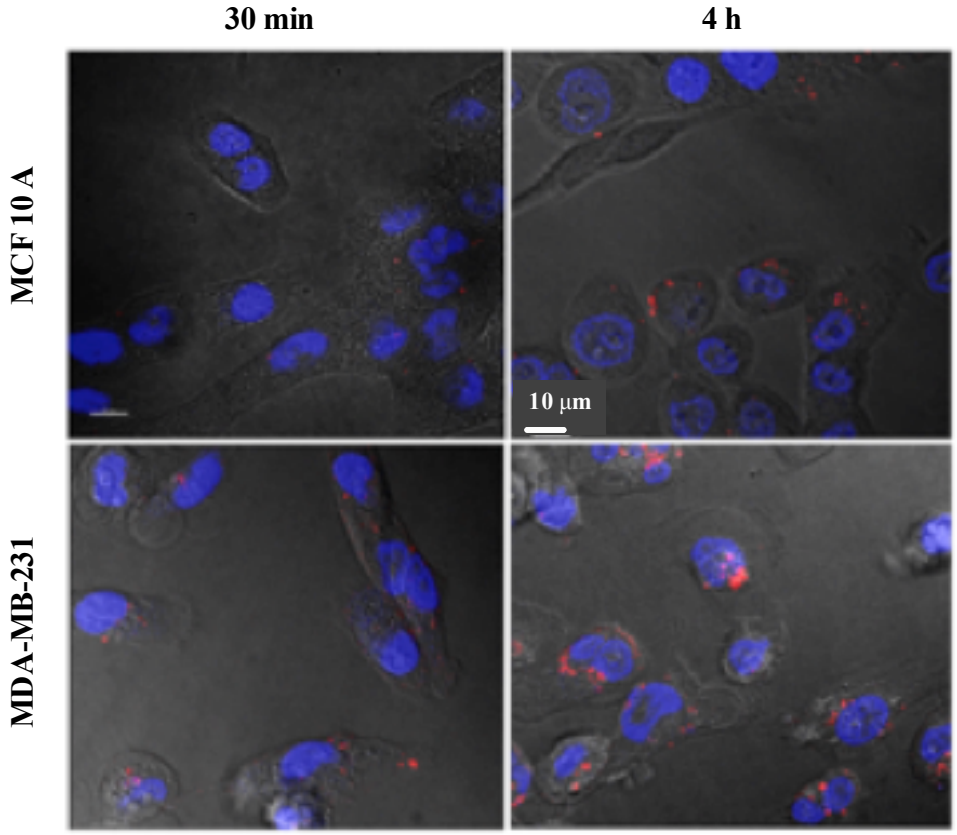

Figure 15. In vitro aptamer uptake.

Representative images of Cy5-NucA (Table 11, red) internalization after 30 min and 4 h incubation with MCF-10A (top) and MDA-MB-231 cells (bottom). Cell nuclei were labeled with Hoecsht dye (blue). All images are single z-slices taken at highest observed aptamer fluorescence.

4.4 A review of aptamer drug delivery systems in literature

The success and limitations of antibody drug conjugates (ADC) have sparked a tremendous interest in developing a wide range of aptamer drug conjugates. Aptamers, alternatively

known as ‘chemical antibodies’ were used to impart cancer specificity to chemotherapeutics and simultaneously offer better tumor penetration. Some examples include conjugating a targeting aptamer to a modified protein nanoparticle for the delivery of chemotherapeutics [152], aptamer-doxorubicin physical conjugates [153], aptamer micelles and aptamer coated liposomes[129] and other aptamer functionalized nanocarriers [119,120,Table 6].

The field of aptamer drug conjugates is relatively nascent and *in vivo* performances are not evaluated in most cases. Of the few systems whose tumor reductions in pre-clinical models were studied, majority of them reported poor *in vivo* efficacies, which leaves room for significant improvement. However, some outstanding results have also been reported validating the targeting potential of aptamers. For example, an aptamer targeted docetaxel nanoparticle provided 100% survival in a prostate cancer mouse model for over 120 days. This was however an intratumoral injection at the maximum tolerated dose of docetaxel, not a very attractive way to cure late stage cancers [155].

To improve efficacies, researchers took inspiration from second generation ADCs and have attempted conjugating potent payloads such as monomethyl auristatin E (MMAE) and derivative of maytansine 1 (DM1) to aptamers but unfortunately these conjugates suffer from low therapeutic indices [156,157]. The other alternative, conjugating a synergistic combination of commonly employed chemotherapeutics, is impeded by current designs that permit no more than one molecule to be conjugated per aptamer [156–160] or constrain loading to just DNA intercalating type drugs such as DOX [153,161–163].

Table 9. Aptamer systems developed to deliver chemotherapeutic drugs

Carrier type [Ref]	*Aptamer, Cancer*	*Drug (molecules / aptamer)*	*Evaluation*
Physical complex [153]	A10, Prostate	DOX (0.83)	*In vitro*, 18% increase in toxicity to target cells over control cells
Nanoparticle [155]	A10, Prostate	Docetaxel	*In vivo*, >85% tumor reduction & 100% survival for 120 days
Conjugate [158]	Sgc8c, ALL	DOX (0.5)	*In vitro*, 7-fold toxicity increase to target cells over control cells
Conjugate [159]	AS1411, Ovarian	Paclitaxel (1)	*In vivo*, >60% tumor reduction & no paclitaxel toxicity
Conjugate [160]	CD117 specific aptamer, AML	Methotrexate (1)	*In vitro*, selective AML killing in cell co-culture
Physical complex [161]	CD38 specific aptamer, multiple myeloma	DOX (5)	*In vivo*, >60% tumor reduction & no tumor reduction with free drug
Physical complex [162]	AS1411, Breast	DOX	*In vivo*, avoids drug efflux & >60% tumor reduction
Nanotrains [163]	Sgc8c, ALL	DOX (50)	*In vivo*, comparable efficacy to free drug treatment
Aptamer-polymer hybrids [164]	AS1411, Breast	DOX	*In vitro*, similar toxicity to free drug & no uptake in control cells

4.5 Dual drug delivery considerations with aptamers

The main challenge of delivering a synergistic drug combination with aptamers is to efficiently conjugate multiple drug molecules per aptamer. These restrictions have thus far prevented aptamer drug conjugates from delivering potent drug combinations in synergistic molar ratios.

Delivering drug combinations with aptamers as targeting agents has been demonstrated before with nanoparticles. [165–167] While a larger number of ratios can potentially be incorporated into nanoparticles, it must be noted that advantages such as small size of aptamer, improved tumor penetration and cellular uptake no longer pertain to these systems. Further, no attempt has been made to deliver a combination of drugs via covalent attachment to the aptamer. This is not surprising since covalently attaching a drug molecule directly to the aptamer can be quite challenging and particularly expensive if more than one molecule has to be attached. However, simultaneous covalent attachment of drugs is crucial for unifying their distinct pharmacokinetic properties and retaining the appealing targeting properties of an aptamer. Conjugating drugs directly to the aptamer backbone can not only be challenging but can also affect the aptamer folding, thereby compromising its affinity. A novel strategy to conjugate multiple different types of drug molecules without compromising the physical and chemical properties of an aptamer will be discussed in the next chapter.

Chapter 5

Aptamer conjugates for simultaneous dual drug delivery

Antibody-mediated targeting has been used extensively for enhancing delivery of cytotoxic payloads to tumors over healthy tissues. Aptamers offer a promising alternative to antibodies, as they can target a wide range of tumor ligands with affinities and specificities that are comparable to antibodies and also possess the capacity to penetrate into deeper areas of the tumor mass because of their smaller size [Figure 12, 108–110]. Several aptamer drug conjugates have been developed to date that can impart cancer specificity to chemotherapeutics and enable better tumor penetration relative to antibodies [153,156–163].

In Chapter 3, DOX and CPT, a combination that exhibits collateral drug sensitivity, were identified to synergistically inhibit tumor growth at extremely low doses in a human TNBC mouse model [47,71,72,158]. However, this drug pair posed a few translational issues. DOX is routinely employed in the clinic, but CPT has not been as successful in its translation due to its poor solubility properties. It has been shown that covalent conjugation of CPT to water-soluble polymers at the 20-OH position can improve the drug's solubility [93,94]. Secondly, this drug pair was synergistic on a control epithelial cell line and did not display cancer specific toxicity *in vitro*. The use of antibodies to target delivery of DOX and CPT has resulted in significantly decreased off-target binding and improved antitumor

activity [96,97,120]. Aptamers are made up oligonucleotides and are hence extremely hydrophilic. Thus the targeting advantages of aptamers over antibodies and their hydrophilicity provides a sound basis for employing them as alternative targeting agents. Using a TNBC recognizing aptamer, the issues with indiscriminate cytotoxicity and poor drug solubility of DOX and CPT can be overcome and ultimately result in effective targeting and treatment of TNBC.

However, current aptamer-drug conjugates permit no more than one molecule to be conjugated per aptamer [156–160] or are compatible only with DNA-intercalating drugs such as doxorubicin (DOX) [153,161–163], limiting targeted delivery of potent drug combinations. A novel strategy was developed for targeted and controlled combination drug dosing with aptamers and to achieve a potent anti-tumor response at doses far below individual drug MTDs.

To overcome drug conjugation limitations to aptamers, the tumor-targeting aptamer was coupled to inert hydrophilic carrier peptides, pre- loaded with combinations of drug molecules in a synergistic fashion with defined stoichiometry (Figure 16). As discussed in Chapter 4, AS1411, an aptamer that targets its payload to tumor cells via recognition of nucleolin (a receptor which is overexpressed on the cell surface of several cancers) was used [168]. The resultant construct, Aptamer-targeted DOX and CPT in Therapeutically Optimal Ratio (Ap-DOCTOR), is a relatively small macromolecular construct (~9.5 nm). It demonstrated targeted delivery of the combination drug agents—including CPT infamous for its solubility issues—with highly controlled stoichiometry, and achieved therapeutic efficacy *in vivo* at extremely low drug doses—500 μg/kg/dose of DOX and 350 μg/kg/dose of CPT. This represents the lowest effective DOX dose reported in the

literature, and these doses are about 8-fold and 21-fold lower than what is required of free DOX and CPT, respectively, to induce similar anti-tumor effect at similar dosing regimens. Furthermore, these drug levels are about 20–30-fold lower than the reported MTD values of these drugs [66,68,169,170]. The approach, entailing the generation of aptamer-peptide drug constructs for effective delivery of multiple therapeutic agents at defined molar ratios, is detailed in this chapter.

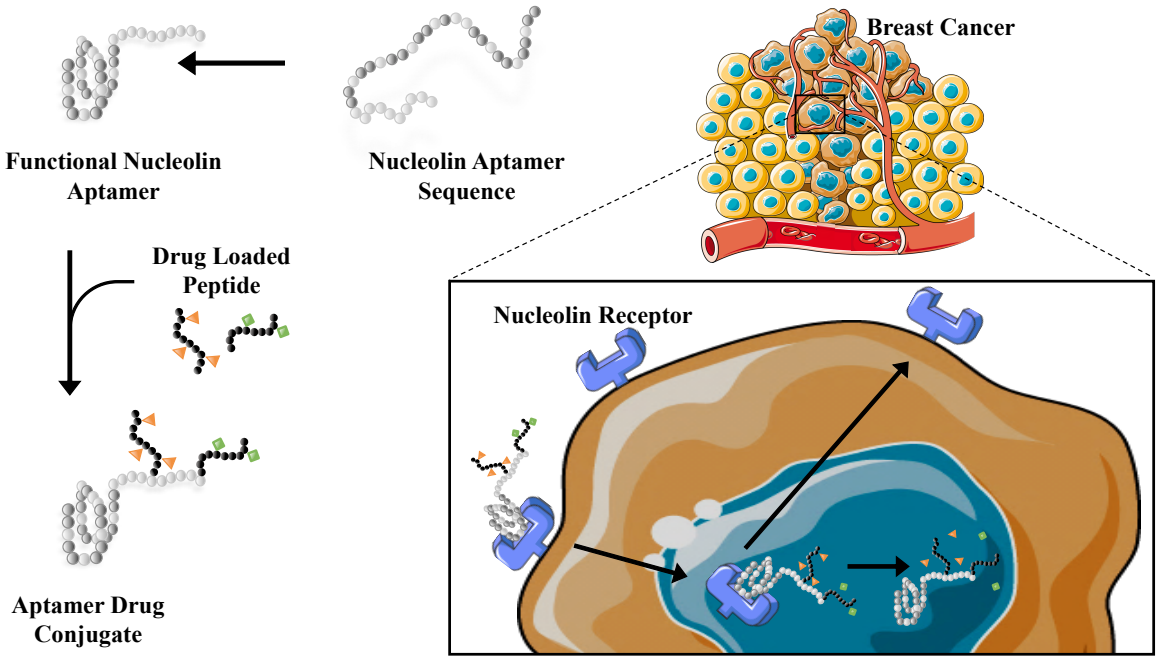

Figure 16. Schematic of TNBC specific and controlled delivery of DOX and CPT using nucleolin-targeting aptamer.

Image templates made freely available by Servier Medical Art (http://smart.servier.com) were used for preparing this figure.

5.1 Design and synthesis of single-drug loaded aptamers

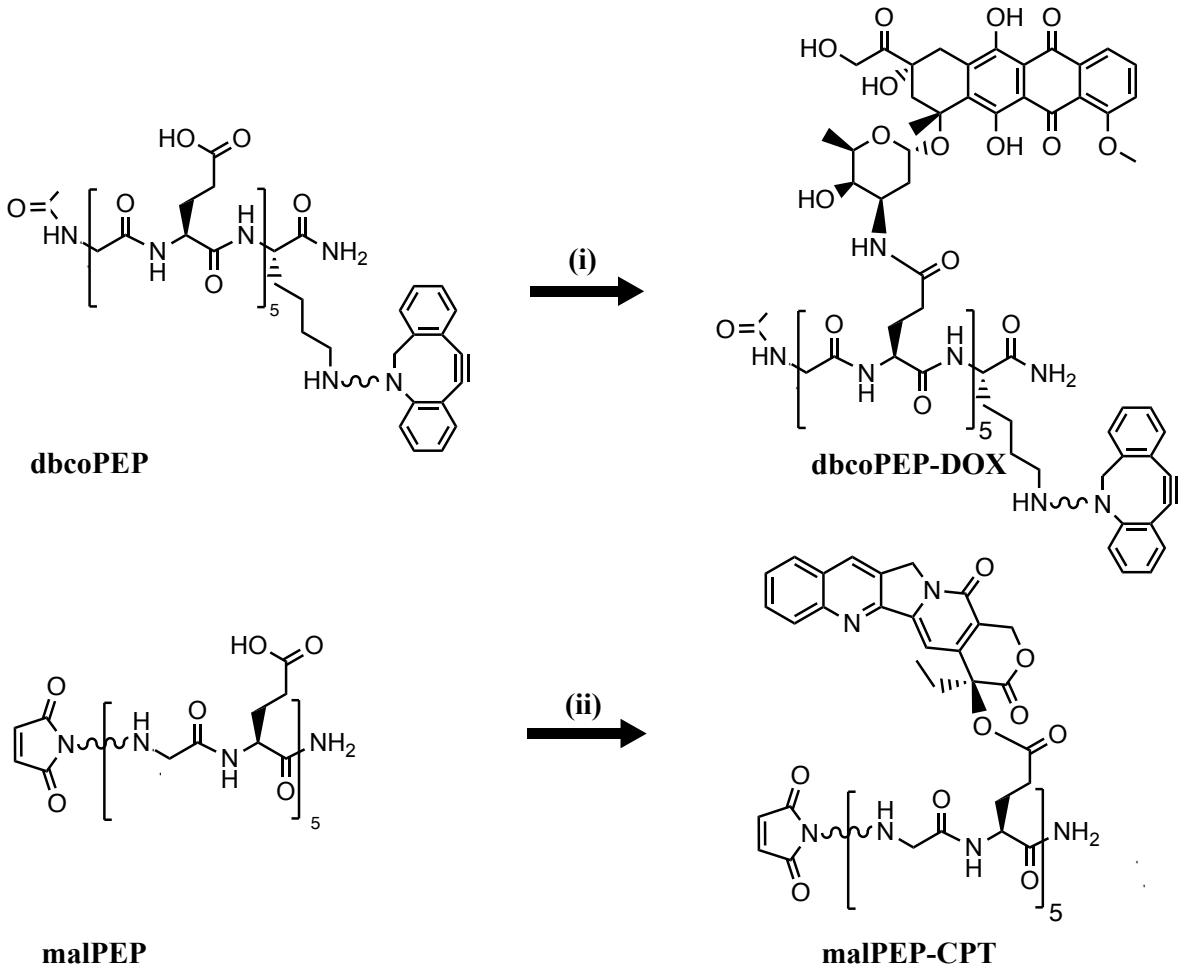

Figure 17. Schematic representation of drug-peptide conjugation chemistries.

Conditions (i) DOX, BOP-Cl, DMAP, DIPEA and DMF (ii) CPT, BOP-Cl, DMAP, DIPEA and DMF.

To achieve synergistic drug combination delivery with aptamers, the main challenge is to efficiently conjugating multiple drug molecules on a single aptamer molecule. This task is relatively easier with antibodies due to the availability of several amino acid and sugar

moieties in the Fc region that are compatible with orthogonal drug conjugation chemistries [171]. To make aptamers amenable to such conjugation techniques, aptamer-peptide constructs were devised wherein the aptamer serves as the targeting moiety and the peptide enables drug loading at a defined molar ratio.

A short peptide sequence was attached to the 3' end of the aptamer and drugs were conjugated to this peptide sequence instead of the aptamer. Given the vast set of natural and modified amino acids available, a large number of covalent conjugation schemes can be employed to conjugate drugs [172]. Peptide backbone was chosen instead of a polymer backbone because of its small size and thus negligible impact on the size of the final construct. Also, if two different drugs have to be loaded but have orthogonal conjugation chemistry sites, then the backbone can be easily customized to incorporate suitable amino acids in desired quantities. Peptides additionally have the following advantages: tissue penetration capability, lack of immunogenicity and ease of production.[103]

Since DOX and CPT have free primary amine and hydroxyl groups, a peptide scaffold with glutamic acid was employed in order to covalently conjugate both DOX and CPT via nucleophilic acyl substitution (Figure 17). Peptides were synthesized to consist ten alternating glutamic acid and glycine amino acid monomers (GEGEGEGE). The number of drug molecules conjugated per peptide was confirmed using MALDI-TOF mass spectrometry (Figure 18). CPT was conjugated to a maleimide-functionalized peptide (malPEP, Table 11) with up to two CPT molecules per chain, while DOX was conjugated to a dibenzocyclooctyne (DBCO)-functionalized peptide (dbcoPEP, Table 11) with up to three DOX molecules per chain. The exact loading efficiencies of the reactions are summarized in Table 10.

These drug-loaded peptides were then conjugated to the previously-described AS1411 nucleolin aptamer (NucA) [168] via copper-free 'click' chemistry (Figure 19). 'Click' chemistries are highly selective reactions that form extremely stable bonds in benign reaction conditions. Recently, several advances have been made in improving the efficiency, biocompatibility and kinetics of these reactions, making them a facile way to modify biologics including, peptides, proteins and oligonucleotides [173].

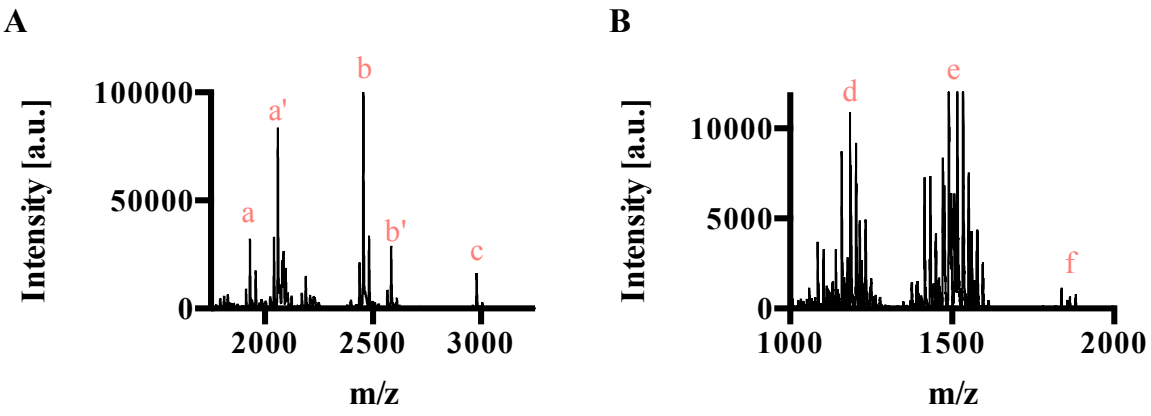

Figure 18. Representative MALDI-TOF MS spectrum

(1000 shots averaged) obtained from purified final product of (A) dbcoPEP-DOX conjugate (110 wt% drug loading), peaks identified in the spectrum (m/z): a, dbcoPEP conjugated to one DOX molecule, $M+H^+$ = 1931.8; b, dbcoPEP conjugated to two DOX molecules, $M+H^+$ = 2456.8; c, dbcoPEP conjugated to three DOX molecules, $M+H^+$ = 2982.6; a' and b' are M+130.9 adducts of a and b (B) malPEP-CPT conjugate (26.6 wt% drug loading), peaks identified in the spectrum (m/z): d, malPEP, $M+2K+H^+$ = 1176.9; e, malPEP conjugated to one CPT molecule, $M+2K+H^+$ = 1507.3; f, malPEP conjugated to two CPT molecules, $M+2K+H^+$ = 1837.6.

These drug-loaded peptides were then conjugated to the previously-described AS1411 nucleolin aptamer (NucA) [168] via copper-free 'click' chemistry (Figure 19). 'Click' chemistries are highly selective reactions that form extremely stable bonds in benign reaction conditions. Recently, several advances have been made in improving the efficiency, biocompatibility and kinetics of these reactions, making them a facile way to modify biologics including, peptides, proteins and oligonucleotides [173].

Table 10. Drug loading efficiencies on peptides

Peptide-drug conjugate	*Drug excess (moles/mole peptide)*	*Drug loading relative to peptide*	
		wt%	*moles*
malPEP-CPT	low (4)	9.3	0.3
	medium (8)	26.6	0.8
	high (12)	43.6	1.4
dbcoPEP-DOX	low (4)	11.8	0.3
	medium (8)	42.6	1.1
	high (12)	110	2.7

Drug loading was quantified by measuring drug concentrations via fluorescence and peptide concentrations via absorbance spectroscopy.

Hence, the drug-loaded peptide was conjugated to the aptamer using 'click' chemistry to minimize drug loss during peptide conjugation and purification steps. The CPT-loaded

malPEP was conjugated to thiol-functionalized nucleolin aptamer (th-NucA; Table 11) via a thiol-maleimide reaction, to produce Ap-CPT (CPT conjugated to Aptamer) and DOX-loaded dbcoPEP was conjugated to azide functionalized nucleolin aptamer (az-NucA; Table 11) by strain-promoted azide-alkyne click (SPAAC) chemistry (Figure 19) to produce Ap-DOX (DOX conjugated to Aptamer).

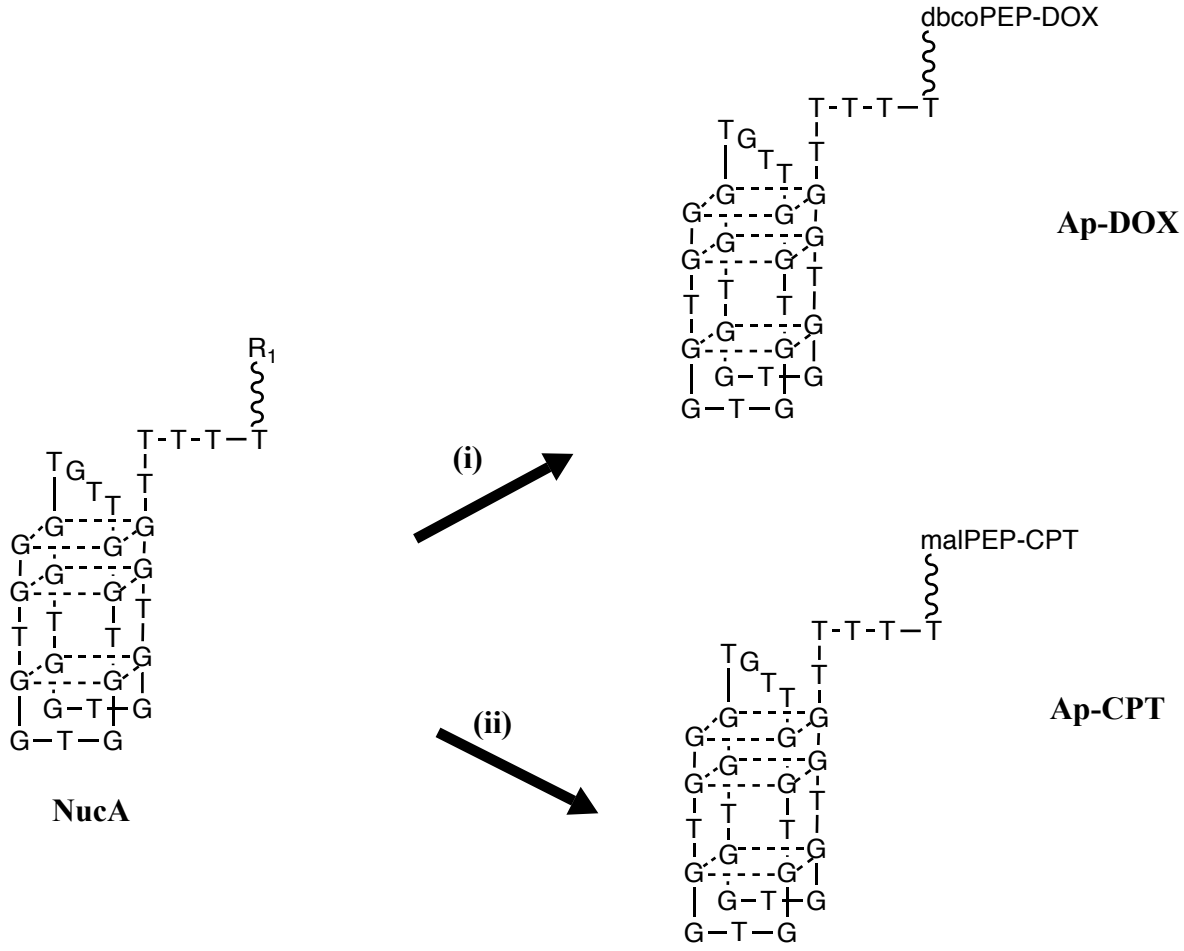

Figure 19. Schematic representation of drug-loaded peptide-aptamer conjugation chemistries.

(i) R_1 = --N_3,; dbcoPEP-DOX (ii) R_1 = --SH,; TCEP, malPEP-CPT.

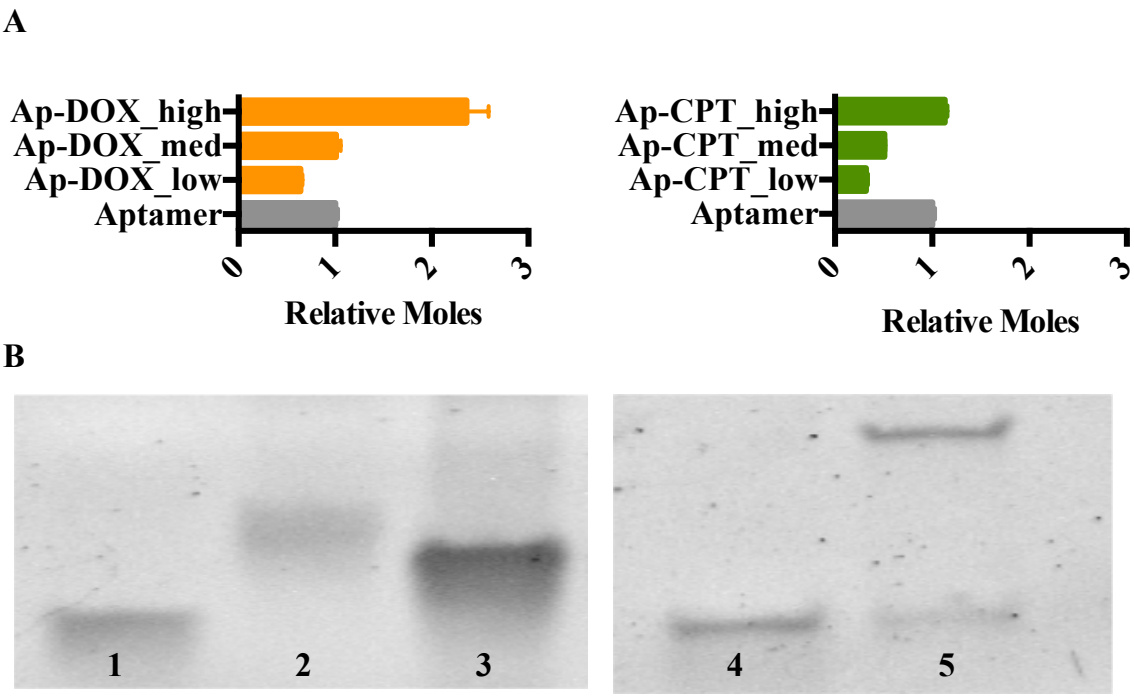

Figure 20. Assessing aptamer-peptide-drug conjugation.

(A) DOX and CPT conjugated per mole of aptamer. DOX and CPT concentrations in the final aptamer drug constructs were measured via fluorescence spectroscopy, and aptamer concentrations were determined by OliGreen ssDNA assay. Data are expressed as mean ± SD (n = 3). (B) Representative gel electrophoresis images for qualitative confirmation of click conjugation to aptamer. Lanes: 1, unconjugated az-NucA; 2, Ap-DOX, az-NucA conjugated to dbcoPEP-DOX; 3, az-NucA conjugated to dbcoPEP; 4, unconjugated th-NucA; 5, Ap-CPT, th-NucA conjugated to malPEP-CPT.

Successful peptide-aptamer conjugation was confirmed via denaturing gel electrophoresis, as indicated by a shift in the band for Ap-DOX relative to bands corresponding to unconjugated aptamer and aptamer conjugated to a peptide without drug.

The same was observed for Ap-CPT, confirming effective chemical conjugation of the peptides to the aptamer (Figure 20B). Further, there were no obvious signs of aptamer degradation. Hence, the proposed conjugation chemistry works well for loading drugs without causing any apparent damage to the aptamer.

The DOX and CPT concentrations were measured after purification and the molar amounts of these drugs relative to the aptamer are plotted (Figure 20A). While DOX mostly remains conjugated to the peptide post 'click' conjugation and purification (relative molar excess to peptide ≈ relative molar excess to aptamer), between 20 – 38 mol% of CPT conjugated to peptide was lost either due to unsuccessful conjugation of malPEP-CPT to aptamer or owing to drug hydrolysis during 'click' conjugation and purification steps.

5.2 Synergistic interactions between single-drug aptamer conjugates

Combination index (CI) was calculated to identify molar ratios of aptamer loaded DOX and CPT that exhibit favorable synergistic interactions. Previous studies have observed widely different combination indices for same molar drug ratios being delivered as free drug mixtures or with the aid of a delivery platform. The drug release kinetics, conjugate uptake mechanisms and a variety of other factors could affect the final outcome of identifying ideal synergistic molar ratios [46,47]. Since the final intent is to deliver drugs as aptamer conjugates, examination of the CI of aptamer drug conjugate cocktails over free drug cocktails was sought.

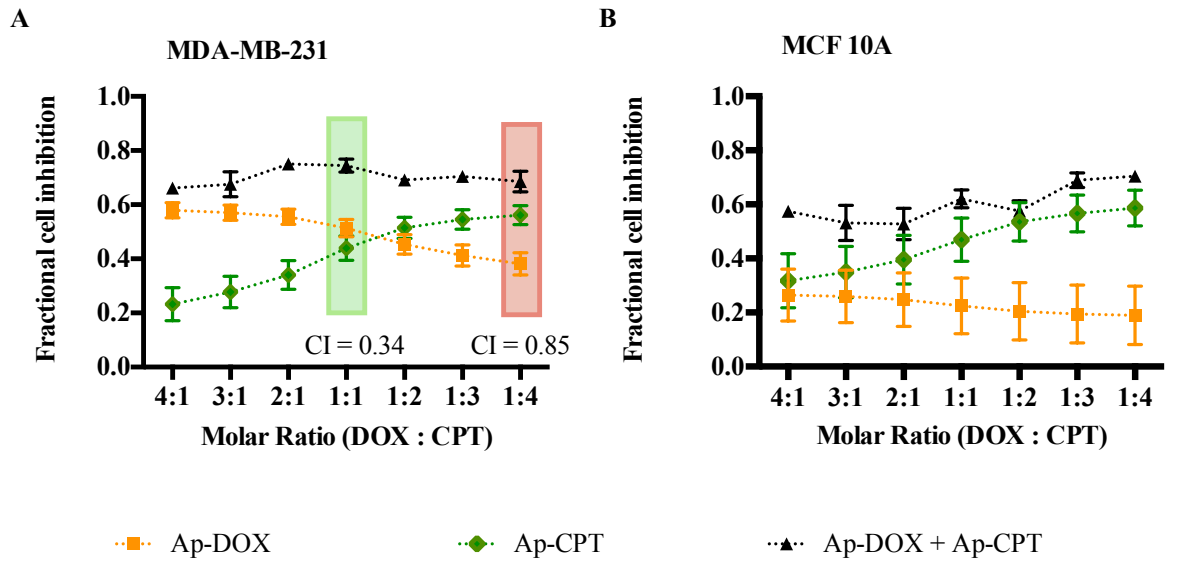

Figure 21. Effects of varying molar ratio treatments of Ap-DOX and Ap-CPT on MDA-MB-231 and MCF 10A cell growth.

The MTT assay was used to measure fractional cell inhibition of (A) MDA-MB-231 cells and (B) MCF 10A cells for the combination treatment (black) and the corresponding Ap-DOX (orange) and Ap-CPT (green) concentrations. The total drug concentration was kept constant at 2 μM for MDA-MB-231 cells and at 200 nM for MCF 10A cells at all ratios. Data are expressed as mean ± SD ($n \geq 12$). Combination index (CI) was calculated by the Chou-Talalay method for each drug ratio.

TNBC MDA-MB-231 cells and control MCF 10A were treated with cocktails of Ap-DOX and Ap-CPT (~1 drug molecule per aptamer) corresponding to various molar ratios of DOX and CPT, and the resulting fractional cell inhibition was assessed using the MTT (3-(4,5-dimethylthiazol-2-yl)-2,5-diphenyltetrazolium bromide) assay (Figure 21). Total drug

concentrations were selected to be around the IC_{50} values of each drug, so that the resulting combination index (CI) values used to assess synergy were not heavily influenced by the toxicity of either individual drug and any non-linear contributions from the median-effect model were avoided.

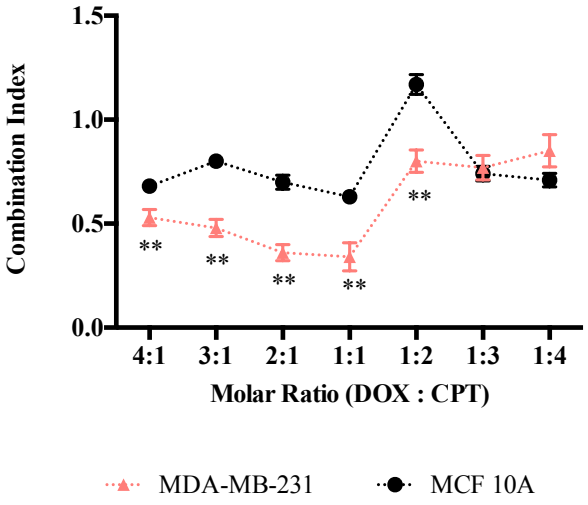

Drug Ratio [DOX:CPT]	Combination Index	
	MDA-MB-231	MCF 10A
4:1	0.53 ± 0.04	0.68 ± 0.02
3:1	0.48 ± 0.04	0.80 ± 0.02
2:1	0.36 ± 0.04	0.70 ± 0.03
1:1	0.34 ± 0.7	0.63 ± 0.02
1:2	0.80 ± 0.05	1.17 ± 0.05
1:3	0.77 ± 0.06	0.74 ± 0.04
1:4	0.85 ± 0.07	0.71 ± 0.03

Figure 22. Combination Index (CI) calculated by the Chou-Talalay method for each drug ratio on MDA-MB-231 and MCF-10A cells.

*Errors are propagated from corresponding errors in cell viability data and standard error of the individual drug model fits ($n \geq 12$). ** $p<0.01$*

All ratios of DOX and CPT tested displayed synergistic interactions in MDA-MB-231 cells (CI < 1) (Figure 22). More strikingly, significantly enhanced synergy for MDA-MB-231 cells compared to MCF-10A cells was observed at 5 of the 7 ratios tested. Coupling the drug pair to an aptamer, indeed led to an enhancement in the selectivity of the drug pair.

Consistent with a previous report on DOX and CPT hyaluronic acid conjugates [47], decreasing synergy (i.e. higher CI) with decreasing molar ratio of DOX:CPT was observed. High DOX:CPT molar ratios were significantly and consistently more synergistic towards the cancer cell line as compared to the control breast epithelial MCF 10A cell line. The lowest CI (0.34 ± 0.07) was obtained for molar ratio 1:1 (DOX:CPT) and hence it was deemed as the most synergistic molar drug ratio while molar drug ratio 1:4 (DOX:CPT) displayed the least synergy (CI = 0.85 ± 0.08). This is in contrast to the synergy trend witnessed earlier with the free drug cocktails (Figure 7) where higher DOX:CPT molar ratios were antagonistic towards MDA-MB-231 cells. This reemphasizes the point that it is prudent to examine combination effects in the final format in which the drugs will be delivered since several factors like drug uptake and drug release kinetics might influence the final outcomes. Previously, enhanced killing in MCF 10A cells was recorded at higher molar amounts of CPT in the free drug cocktail combination. However, by conjugating this drug onto a targeting aptamer, the trend is reversed and the therapeutic index of CPT is increased since higher molar amounts of CPT are more antagonistic to control cells.

5.3 Synthesis and characterization of aptamer dual drug conjugates (Ap-DOCTOR)

A drug ratio exhibiting high synergy (low CI) towards the cancer cell line and low synergy (high CI) towards a control cell line enhances the drug specificity towards cancer. While, antagonism towards MCF 10A cells at a molar ratio of 1:2 (DOX: CPT) was observed, 1:1

DOX:CPT- the molar ratio with highest synergy of the two drugs (CI of 0.34 ± 0.07) was used for further testing to retain the potency of DOX and CPT as a drug pair.

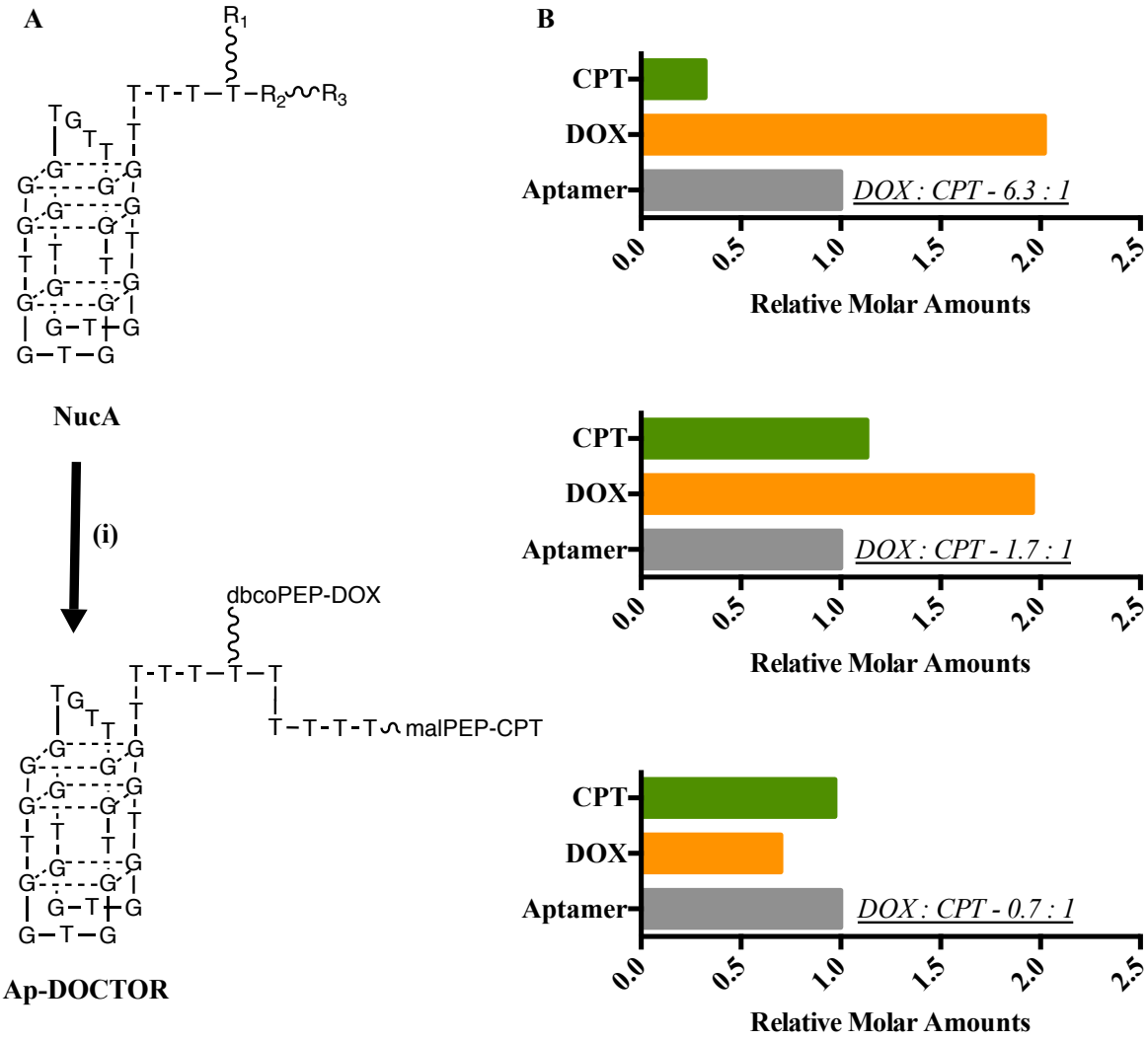

Figure 23. (A) Schematic representation of drug-loaded peptide-aptamer conjugation chemistries and molar amounts of DOX and CPT conjugated per mole of aptamer.

(i) R1 = --N3, R2 = --T5-- and R3 = --SH; TCEP, dbcoPEP-DOX and malPEP-CPT (B) Drug concentrations were measured using fluorescence spectroscopy and aptamer concentrations were determined using OliGreen ssDNA Assay.

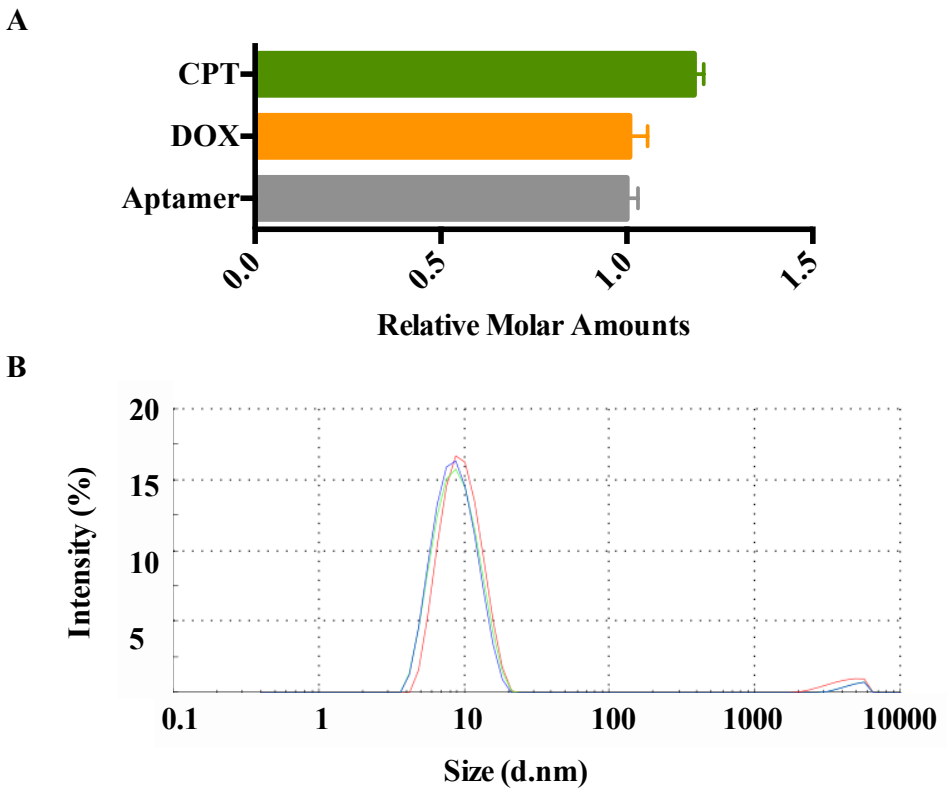

Figure 24. Size measurement and molar amounts of DOX and CPT conjugated per mole of Ap-DOCTOR.

(A) Drug concentrations were measured using fluorescence spectroscopy and aptamer concentrations were determined using OliGreen ssDNA Assay. (B) Distribution analysis by intensity of size measurement performed on Ap-DOCTOR using DLS in triplicate. Z-average = 9.5 ± 2.9 nm, and polydispersity index = 0.207.

Subsequently, aptamer dual drug conjugates that incorporate both drug compounds into a single targeted molecule were developed. The rationale behind co-loading drugs on a same construct is to deliver therapeutically optimal ratios *in vivo* and prevent separate pharmacokinetic fates of two chemically distinct drugs. DOX and CPT were conjugated at

defined molar ratios to a single aptamer molecule via the same 'click' chemistry reactions described above (Figure 23A). DOX and CPT were loaded onto different peptides, as it was easier to control drug loading efficiencies and consequently molar drug ratios in the final construct. Using this method several constructs carrying different ratios of DOX and CPT were synthesized (Figure 23B).

After careful optimization, performing both thiol maleimide 'click' and SPAAC as one-pot one-step synthesis (using malPEP loaded with 43.6 wt% CPT and dbcoPEP loaded with 42.6 wt% DOX) produced 1:1.2 molar ratio loading of DOX:CPT onto the aptamer. The yield obtained was > 90% (Figure 24A). This construct carries DOX and CPT in the optimal synergistic ratio regime that is both potent and specific to MDA-MB-231 cells, and will from now on be referred to as Ap-DOCTOR (Aptamer-targeted DOX & CPT in Therapeutically Optimal Ratio). Dynamic light scattering (DLS) measurements revealed that the average construct size was 9.5 ± 2.9 nm (Figure 24B). Thus large aggregates, which could compromise the penetration efficiency of the Ap-DOCTOR formulation, are not present.

Individual drug release kinetics from Ap-DOCTOR were also examined to ensure that drugs could detach from the peptide backbone to elicit toxicity. Release at neutral (pH 7.5) and acidic (pH 5) conditions at 37 °C was measured. These were chosen to mimic the temperature and pH conditions that the drug construct would encounter while in circulation and in case it underwent endocytosis and gets exposed to acidic environments in the endosome [72]. Release of DOX from aptamer via hydrolysis was slow, but occurred at a slightly higher rate at pH 5 ($t_{1/2}$ = 98.4 h) than pH 7.5 ($t_{1/2}$ = 125.4 h) as described in other studies [31,47]. CPT was released much faster than DOX at both pH 7.5 ($t_{1/2}$ = 3 h) and 5 ($t_{1/2}$

= 2.3 h). However, at longer time points, total release was higher at a higher pH (Figure 25), as seen in other studies [174].

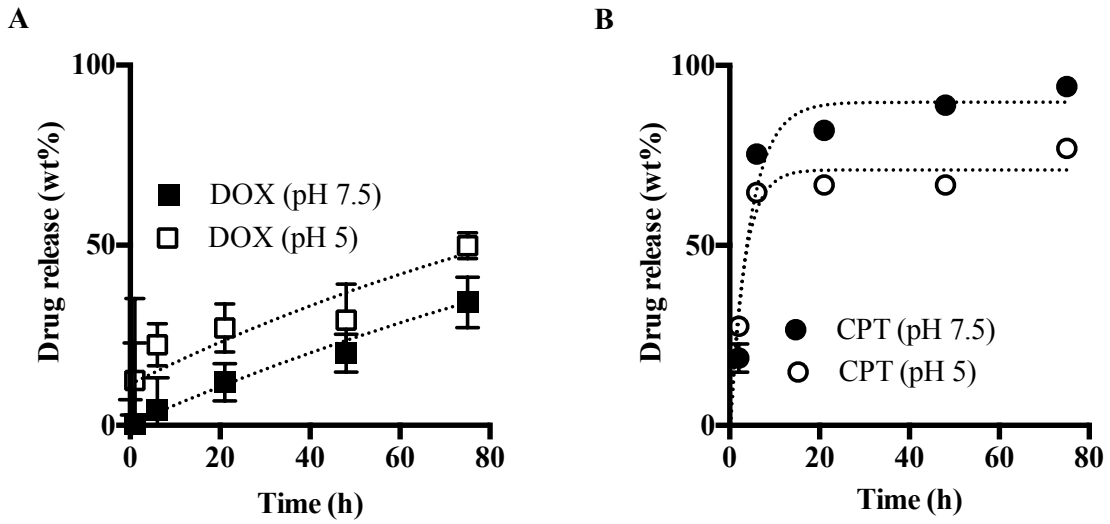

Figure 25. Release kinetics of (A) DOX and (B) CPT from Ap-DOCTOR at 37 °C. Dotted lines represent exponential fits to release profiles. DOX and CPT concentrations were measured using fluorescence spectroscopy, and aptamer concentrations were determined using the OliGreen ssDNA assay. Data are expressed as mean ± SD (n = 3).

Moreover, Ap-DOCTOR was also readily soluble in saline and demonstrated superior solubility as compared to an unconjugated DOX+CPT solution (Figure 26). Conjugating CPT to a hydrophilic carrier aptamer improved its solubility, making it a more translatable formulation compared to its free drug counterpart.

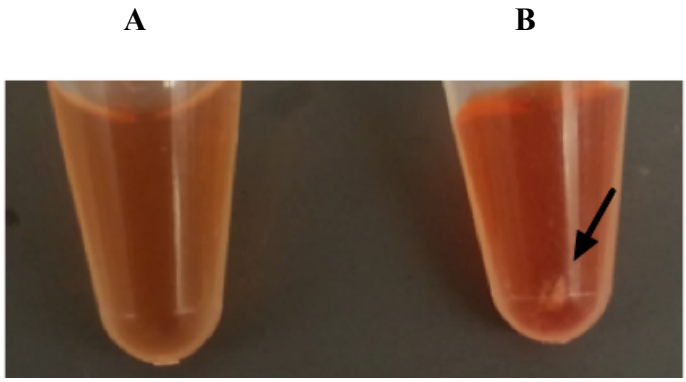

Figure 26. Improved solubility of (A) Ap-DOCTOR over (B) DOX + CPT in saline.

Both samples contain DOX at 3 mg/mL and CPT at 1.7 mg/mL, roughly 10-fold higher than in vivo injection concentrations. Samples were centrifuged for 5 min at 10,000 rpm after vortexing and sonicating for 2 min and 5 min, respectively. Black arrow indicates CPT pellet formed post-centrifugation (CPT solubility in water is < 1 mg/mL).

5.4 Antiproliferative activity of Ap-DOCTOR *in vitro*

The cytotoxicity of Ap-DOCTOR was next evaluated by incubating it *in vitro* for 72 hours with both MDA-MB-231 breast cancer cells and control MCF-10A breast epithelial cells. In parallel, these cell lines were also incubated with cocktails of Ap-DOX + Ap-CPT or Ctl-DOX + Ctl-CPT (in which DOX and CPT were coupled to a control non-nucleolin binding th-CRO aptamer, Table 11); both of these cocktails were mixed to correspond to the molar drug ratio of our Ap-DOCTOR (DOX:CPT = 1:1.2).

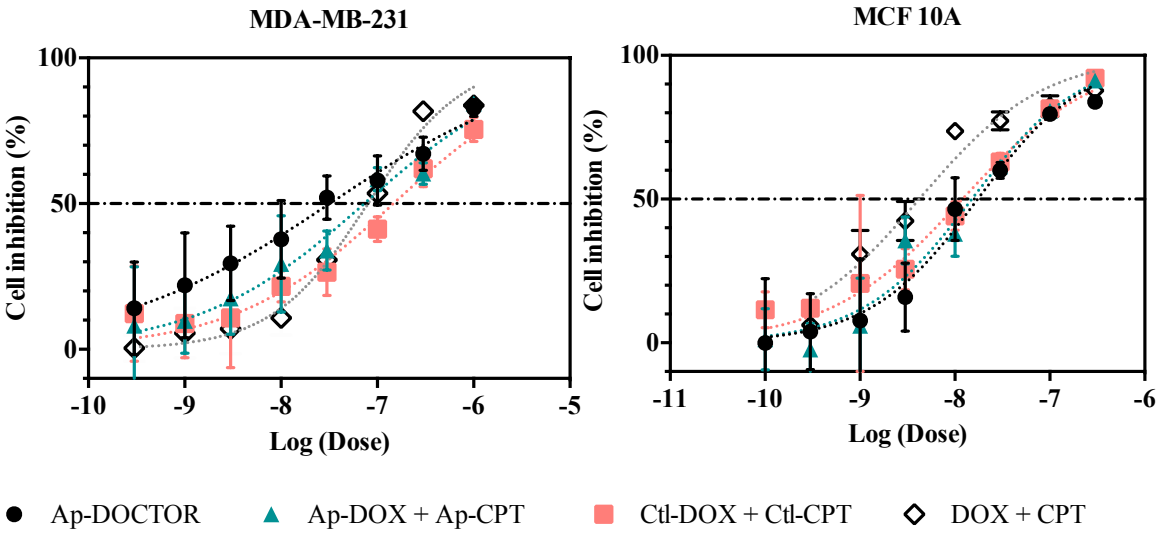

Treatment	IC_{50} DOX (nM)		IC_{50} CPT (nM)	
	MDA-MB-231	MCF 10A	MDA-MB-231	MCF 10A
Ap-DOCTOR	31.9 ± 7.8	17.3 ± 3.3	38.3 ± 9.4	20.8 ± 3.9
Ap-DOX + Ap-CPT	73.3 ± 15.8	15.1 ± 2.3	87.9 ± 18.9	18.1 ± 2.8
Ctl-DOX + Ctl-CPT	146.9 ± 29.9	12.0 ± 2.3	176.3 ± 35.8	14.4 ± 2.8
DOX + CPT	79.6 ± 6.7	4.2 ± 0.5	95.5 ± 8.0	5.0 ± 0.6
DOX	495.4 ± 44.6	31.3 ± 5.1	-	-
CPT	-	-	220.3 ± 30.1	13.4 ± 2.7

Figure 27. In vitro assays to evaluate aptamer and aptamer drug conjugate toxicity.

Cell inhibition on MDA-MB-231 (A) and MCF-10A (B) in the presence of Ap-DOCTOR (black circles), Ap-DOX and Ap-CPT (blue triangles), Ctl-DOX and Ctl-CPT (salmon squares) and DOX+CPT (open diamonds) for 72h. Cell viability data were fitted to the median-effect model to obtain IC_{50} values. Data are expressed as mean ± standard error of individual drug model fits ($n \geq 4$).

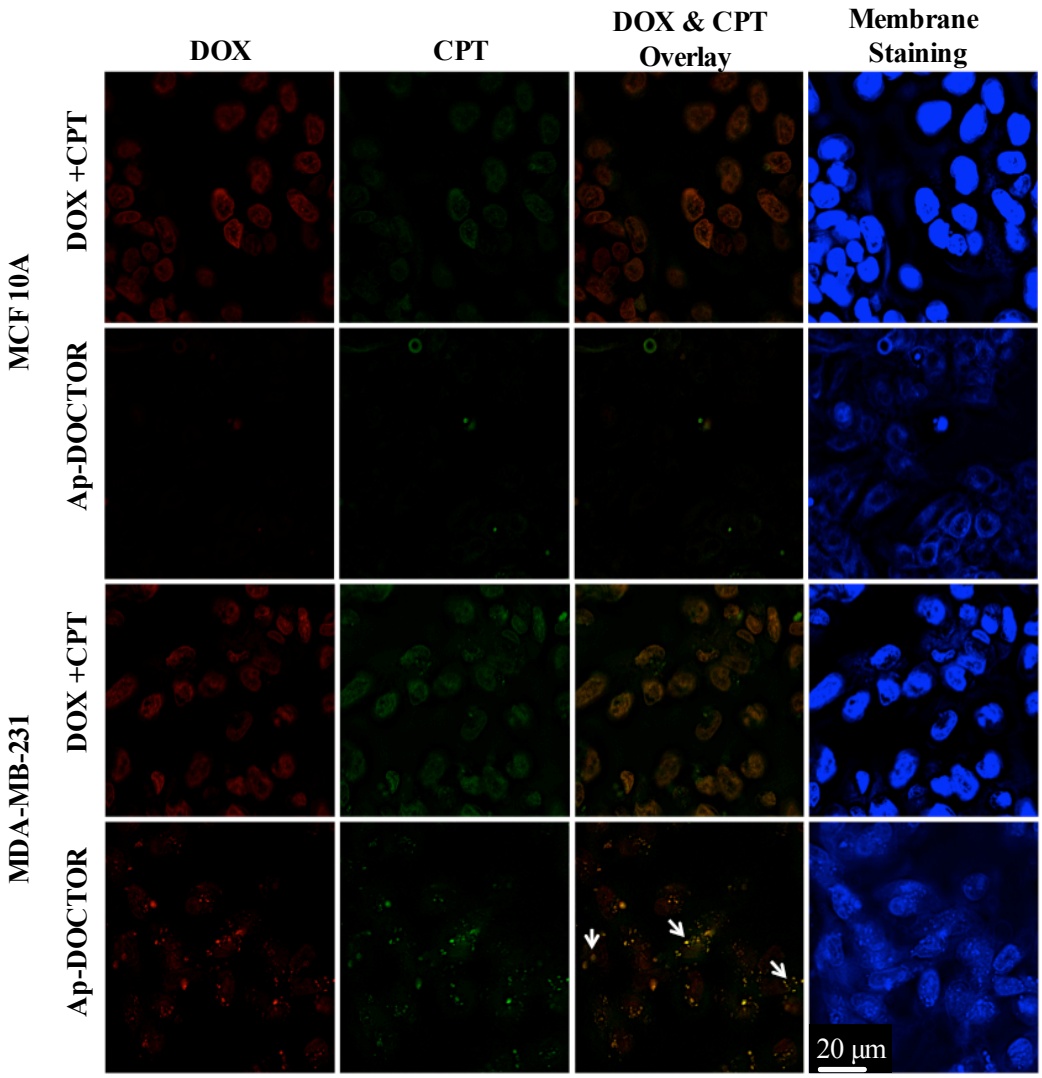

Figure 28. In vitro assessment of internalization of Ap-DOCTOR and free drug cocktails. Representative images of fluorescence signals from DOX (red) and CPT (green) after 2.5 h incubation of MDA-MB-231 cancer cells and MCF-10A breast epithelial cells with a cocktail of DOX and CPT or with Ap-DOCTOR loaded with both drugs. Plasma membranes were labeled using CellLight Plasma Membrane-RFP, BacMam 2.0 (blue). Nuclear fluorescence in the drug cocktail-treated cells is likely due to bleed-through of DOX signal into the RFP channel. White arrows indicate punctae from DOX/CPT signal overlap.

Drug combinations delivered via nucleolin aptamer to MDA-MB-231 breast cancer cells exhibited higher cytotoxicity, because they can be efficiently internalized upon binding to cell-surface nucleolin [151,168]. This trend is corroborated by the cocktail of single-drug-loaded NucA aptamer formulations (Ap-DOX + Ap-CPT) being more effective than a cocktail of control aptamer formulations (Ctl-DOX + Ctl-CPT), where the drugs must presumably diffuse after being released extracellularly in order to induce toxicity.

Most notably, Ap-DOCTOR displayed the highest potency (IC_{50} = 31.9 ± 7.8 nM, Figure 27) amongst all treatments. There was an approximate doubling in efficacy against MDA-MB-231 breast cancer cells when the drug combination was delivered on a single targeting molecule rather than as a cocktail combination of single-drug-loaded aptamers. Since more amount of drug was conjugated per aptamer molecule in the former configuration than in the latter, more amount of drug was likely being internalized with the Ap-DOCTOR as a result of the same level of aptamer uptake, causing more toxicity.

Additionally, no improvements in IC_{50} values for the nucleolin-targeted formulation in MCF 10A cells, which do not overexpress nucleolin, were observed (Figure 27). Upon direct comparison to MDA-MB-231 cells, Ap-DOCTOR is essentially more toxic to the control cells. However, it has to be pointed out that unconjugated DOX and CPT are extremely toxic to the control cells. In fact, the free drug combination is ~ 20-fold more toxic to the MCF 10A control cells (IC_{50} = 4.2 ± 0.5 nM) than MDA-MB-231 breast cancer cells (IC_{50} = 79.6 ± 6.7 nM). Nonetheless, by incorporating the aptamer, this difference was brought down to less than 2-fold. This corresponds to an approximate 10-fold increase in the therapeutic index of the drugs delivered via the aptamer form. The decrease in potency to the

control epithelial cells can again be attributed to the delay caused by extracellular drug release and the delivery of a less synergistic molar ratio of the drug combination.

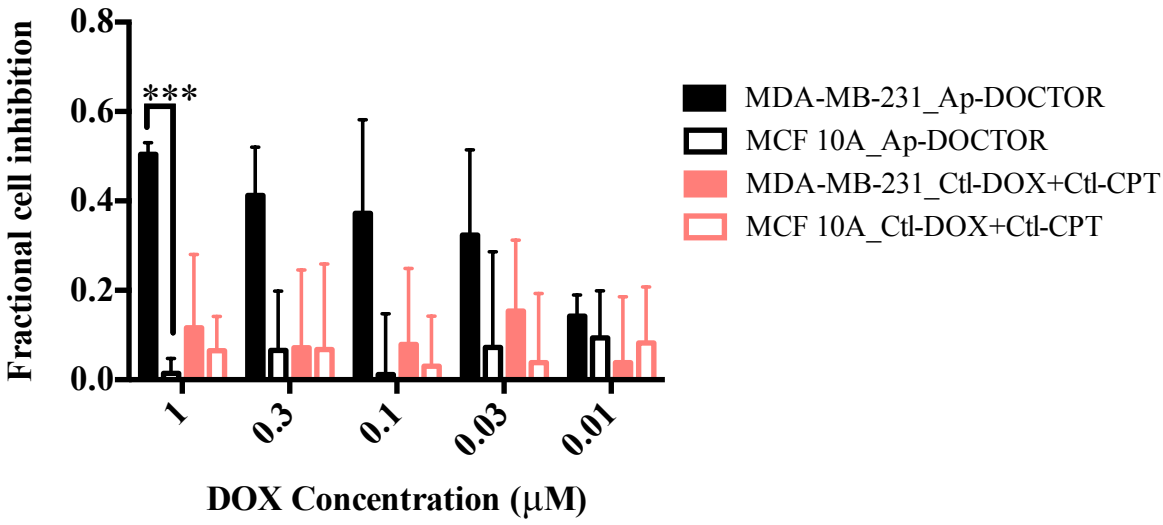

*Figure 29. Comparison of anti-proliferative activity of MDA-MB-231 and MCF-10A cells after brief (2.5 h) exposure to Ap-DOCTOR or cocktails of Ctl-DOX + Ctl-CPT. Fractional cell inhibitions were assessed with the MTT assay and formulation concentrations are represented via total DOX concentration present. Data are expressed as mean ± SD ($n \geq 4$). *** $p<0.005$.*

Next, to validate our cytotoxicity findings, increased internalization of our Ap-DOCTOR formulation in MDA-MB-231 cells was qualitatively confirmed by microscopy. After a 2.5 h incubation with Ap-DOCTOR, considerable DOX and CPT uptake was observed, as indicated by yellow-orange punctae throughout the cell, in MDA-MB-231 cells (Figure 28). In contrast, only a weak green signal in the cytoplasm was observed, potentially due to CPT uptake after extracellular release, for MCF-10A cells. In unconjugated free drug

cocktail incubations under the same conditions, irrespective of the cell type, fluorescent signals corresponding to DOX and CPT were observed mainly in the nucleus and the staining was more diffusely distributed throughout the cytoplasm. This striking difference in the staining pattern between free drug versus the Ap-DOCTOR strongly indicates that the efficacy of this combination therapy vehicle is achieved through specific internalization via nucleolin-mediated endocytosis [151]

In vivo, aptamer-drug conjugates are rapidly cleared from the body and are therefore exposed to the cells only for a brief amount of time. Based on previously described clearance rates for the AS1411 nucleolin aptamer [168], an *in vivo*-like drug exposure condition was simulated in which cells were treated with drug formulations for 2.5 h and then allowed to grow in fresh media. At the end of 72 h, cell viability using the MTT assay was assessed. Even after this brief drug exposure, highly selective toxicity by our Ap-DOCTOR in MDA-MB-231 cancer cells was observed, without any significant toxicity to MCF-10A breast epithelial cells (Figure 29). At the highest drug concentration tested, Ap-DOCTOR was 36-fold more toxic to MDA-MB-231 cells relative to MCF-10A cells. In contrast, minimal cytotoxicity to either cell type after equivalent treatment with a cocktail of the control aptamer-drug conjugates (Ctl-DOX + Ctl-CPT) was observed. This suggests that a nucleolin targeting aptamer can cause significant improvement in the rate of drug internalization only to cells overexpressing the nucleolin receptor, thereby simultaneously improving potency and selectivity. To cross verify, the fraction of cells that undergo apoptosis after a brief amount of drug exposure was also measured (Figure 30). The trend was in keeping with all observations thus far. The free drug mixture indiscriminately attacked both cancer and control cells, and in fact, greater apoptosis was observed in MCF 10A control cells.

However, when the same drug pair was exposed in the aptamer format, negligible to no apoptosis in control cells was realized but similar extent of apoptosis between free drug and aptamer conjugate was on MDA-MB-231 cells. This implies that DOX and CPT still retain their potency and elicit cell-death similar to the naïve-uncoupled drugs but with enhanced specificity when coupled to an aptamer.

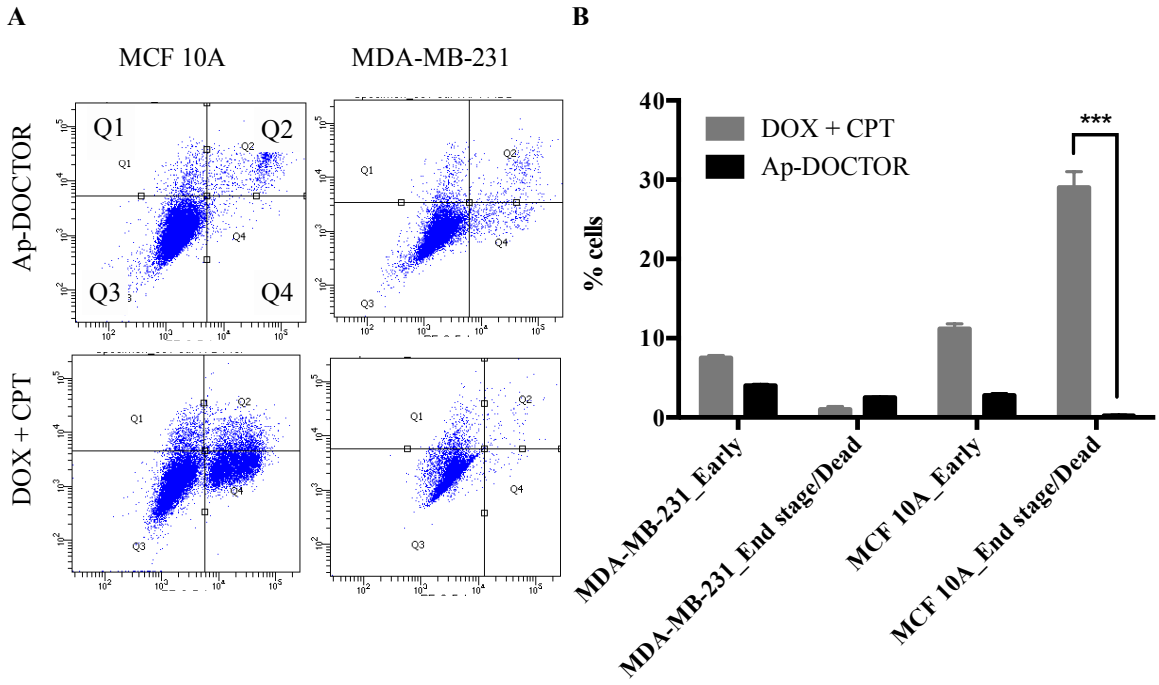

Figure 30. Apoptotic assessment of CPT+DOX-treated cells.

*Annexin V/Sytox Green assay was utilized to detect percentage of early and late apoptotic cells in various drug-treated MDA-MB-231 and MCF 10A cells. Cells were treated Ap-DOCTOR or free DOX+CPT for 3 hours prior to staining and analysis via flow cytometry. (A) Representative flow cytometry plots are shown, Q1 and Q2 – quadrants for early stage apoptosis, Q4 – quadrant for end stage apoptosis and Q3 – quadrant for live cells. (B) Cell populations were quantified via flow cytometry for early and end stage apoptosis. Data represents mean ± SD (n=3). *** p<0.005.*

Although Ap-DOCTOR consistently outperformed the control formulations, no significant difference in its toxicity relative to cocktails of single-drug-loaded aptamers was observed, unlike the results form the long incubation studies (Figure 31). It can be speculated that for short incubation studies, the nucleolin receptors may not have been sufficiently saturated leading to efficient internalization of both dual-drug and single-drug constructs and uniform toxicity in both cases. Another reason could be that the nucleolin receptor recycling occurs at longer time scales making it difficult to distinguish the more efficient drug delivery of a dual drug conjugate over a single drug conjugate.

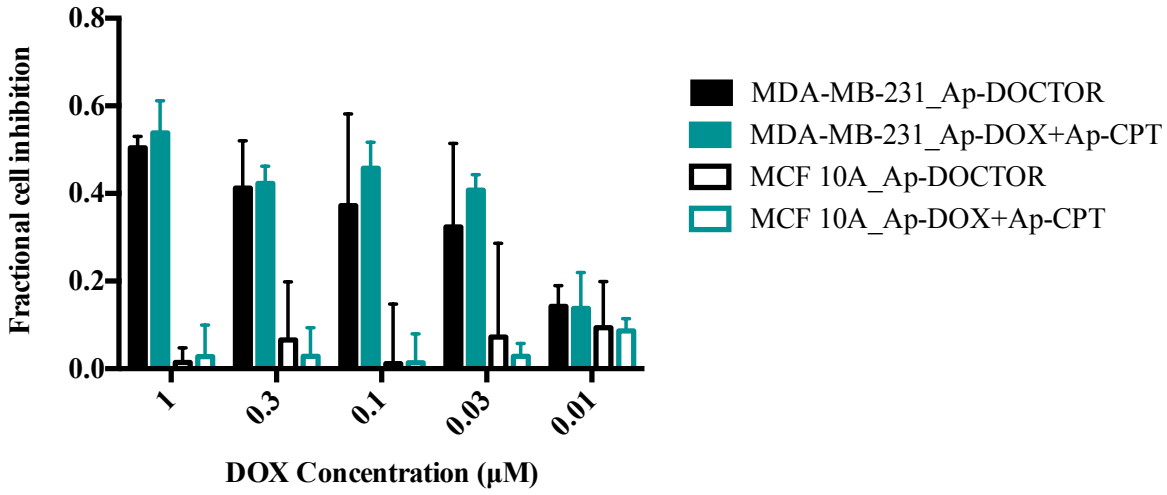

Figure 31. In vitro anti-proliferative activity of Ap-DOCTOR and Ap-DOX + Ap-CPT formulations.

Fractional cell inhibitions were assessed, after a brief 2.5 h exposure to MDA-MB-231 and MCF 10A cells, with the MTT assay and formulation concentrations are represented via total DOX concentration present. Data are expressed as mean ± SD ($n \geq 4$).

Additionally, It was also confirmed that all of the above results were not a mere addition in toxicity from the NucA aptamer. No apparent toxicity was observed for either cell line incubated for 72 hours with free unconjugated NucA aptamer at any concentration used for determining IC_{50} values of the drug constructs (Figure 32).

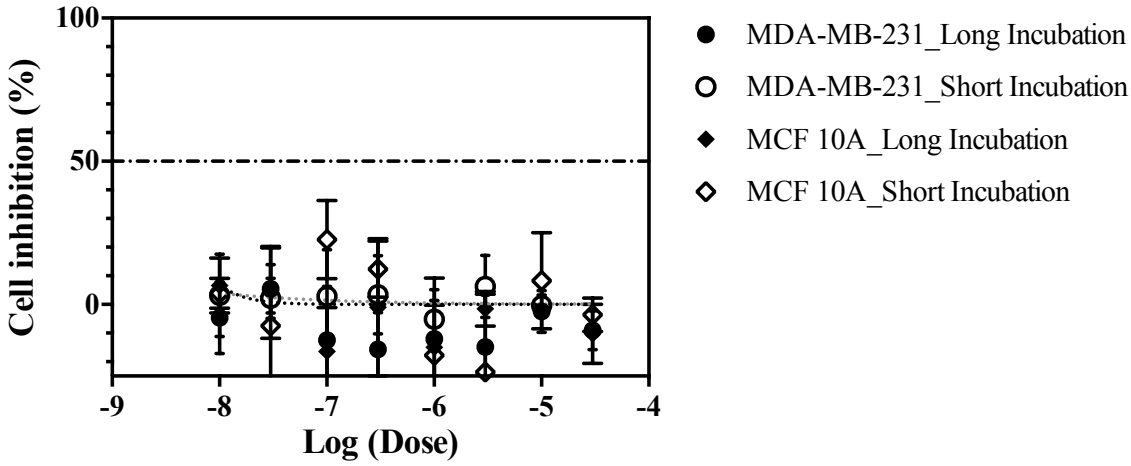

Figure 32. Cell inhibition of NucA (Table 11, free unconjugated aptamer) on MDA-MB-231 cells

after long 72 h incubation (closed circles) and short 2.5 h incubation (open circles) and on MCF-10A after long 72 h incubation (closed diamonds) and short 2.5 h incubation (open diamonds) of NucA. Cell viability data were fitted to the median-effect model to obtain IC_{50} values. Data are expressed as mean ± standard error of individual drug model fits ($n \geq 4$).

5.5 Antitumor activity and pharmacokinetics of Ap-DOCTOR *in vivo*

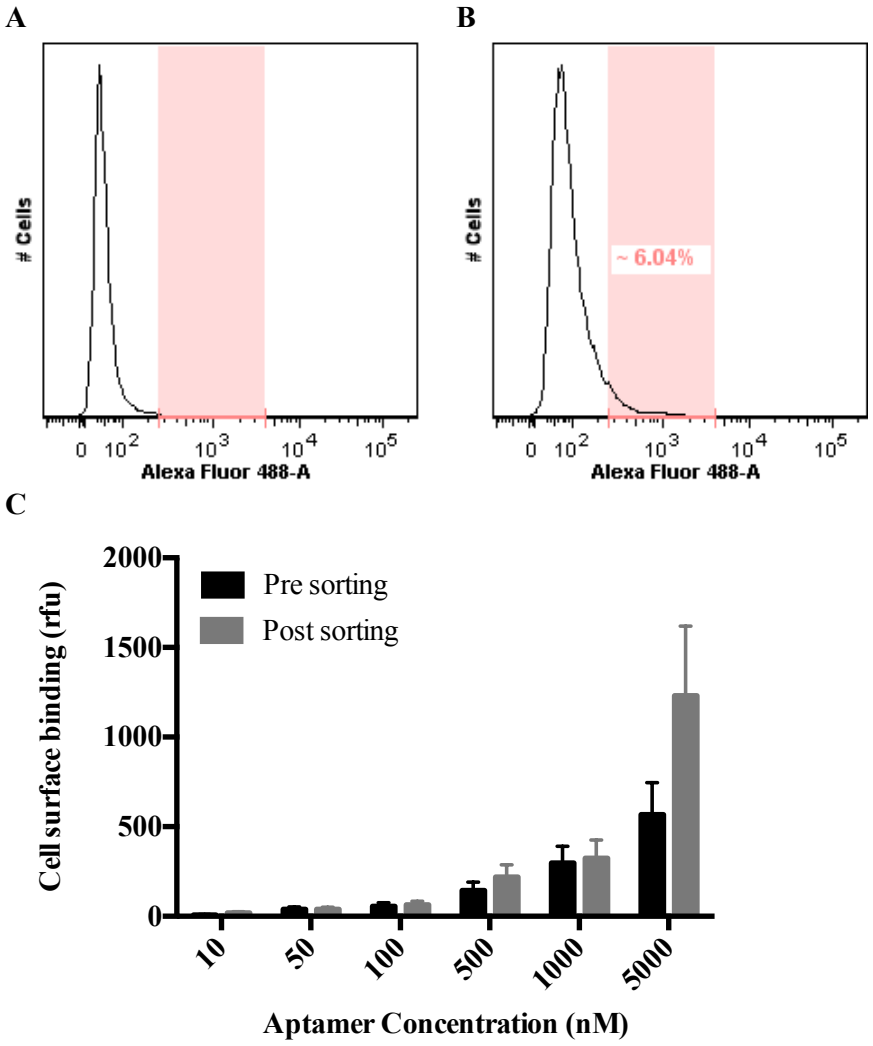

Figure 33. Isolation and characterization of cell surface nucleolin-rich MDA-MB-231 cells. FACS plots and sort gates to acquire nucleolin-rich cells from a single-cell suspension of MDA-MB-231 cells stained with (A) AlexaFluor 488-anti-nucleolin antibody [364-5] or (B) AlexaFluor 488-Mouse IgG1, kappa monoclonal - isotype control. Cells residing within the highlighted gate (red) of anti-nucleolin antibody-treated cells were collected. (C) Cy5-AS1411 binding to pre- and post-sorted MDA-MB-231 cells confirms enhanced cell surface nucleolin expression post-isolation.

Encouraged by the *in vitro* results, subsequent demonstration of improved therapeutic efficacy and enabling of synergistic combinatorial drug dosing in an *in vivo* tumor model by Ap-DOCTOR formulation was pursued. High-density expression of cell-surface nucleolin on MDA-MB-231 cells is correlated with more aggressive tumorigenic properties and an increased capacity to generate orthotopic tumors [175]. Therefore nucleolin-rich MDA-MB-231 cells were isolated via flow cytometry to generate robust orthotopic tumors in athymic nude mice (Figure 33), and then treatments to these animals were applied.

A total of four injections of either saline, an unconjugated DOX + CPT cocktail, or Ap-DOCTOR were administered i.v. every other day, starting 11 days post-tumor inoculation. Drug doses of DOX (500 μg/kg) and CPT (350 μg /kg) were constant in all treatment groups.

At the end of 44 days, tumor volumes for the drug cocktail-treated group exhibited a statistically insignificant 36% size reduction relative to the saline-treated group (Figure 34). In contrast, significantly smaller tumor volumes were seen at day 44 after treatment with Ap-DOCTOR compared to both the saline- and cocktail-treated groups (73% and 58%, respectively). No apparent signs of toxicity or any body weight changes for either the drug cocktail or the Ap-DOCTOR treatment were observed (Figure 34).

As a control, the *in vivo* cytotoxicity of the AS1411 nucleolin aptamer in the absence of DOX or CPT was evaluated to ensure that the significant differences in tumor growth rates for free drug combination treatments vs. Ap-DOCTOR treatments were not due to a mere addition in toxicity form the anti-nucleolin AS1411 aptamer (Figure 35). Mice were treated with four i.v. injections of the aptamer every other day at a dose of 30.4 mg/kg, equivalent to four times the dose of aptamer used in the experiment above. No significant difference in

tumor growth compared to saline treatment were observed, indicating that the tumor reduction previously observed was directly attributable to the combination therapy being selectively delivered to cancer cells via Ap-DOCTOR.

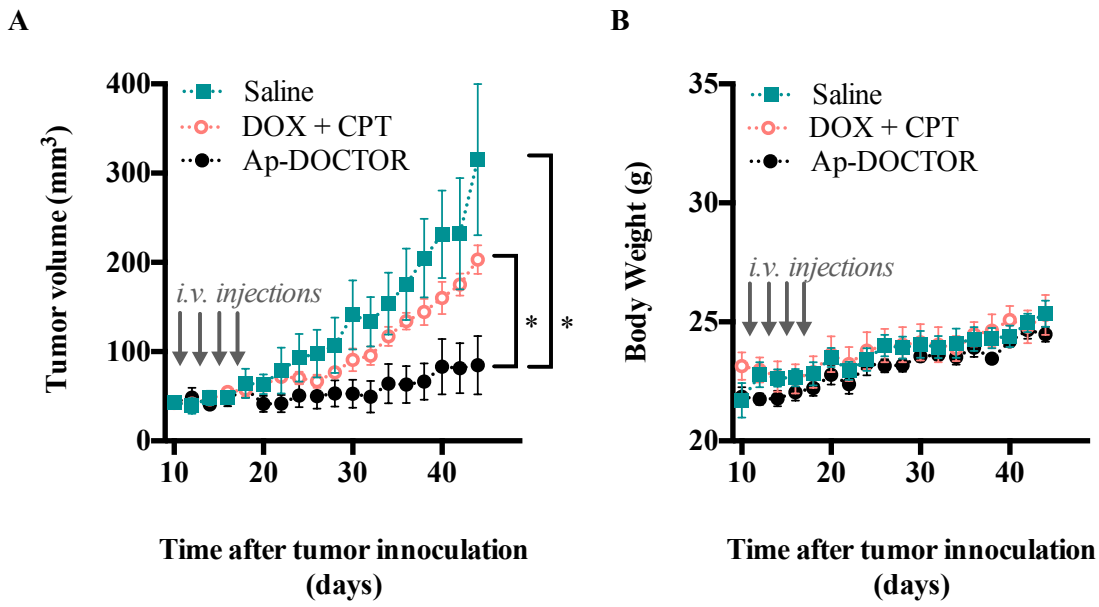

Figure 34. In vivo efficacy of Ap-DOCTOR treatments in athymic nude mice.

*(A) Tumor growth curves in an orthotopic MDA-MB-231 mouse breast cancer model treated with saline (squares), a cocktail of DOX and CPT (open circles), or Ap-DOCTOR (black circles) at drug equivalent doses of 0.5 mg/kg DOX and 0.35 mg/kg CPT. Four injections (grey arrows) were administered i.v. every other day starting on day 11 post-tumor inoculation. Statistical significance as determined using the Holm-Sidak method (α = 5%) is provided for the last day on the curve (day 44). * = p <0.05. (B) Body weight changes for all treatment groups. Data are expressed as mean ± SEM (n = 4 for drug cocktail, n = 5 for other groups).*

Safety of the free drug cocktail (DOX at 2 mg/kg/dose and CPT at 1.4 mg/kg/dose) was also tested at four times the dose administered in the Ap-DOCTOR treatment and negligible body weight changes were observed (Figure 36). This observation suggests that the MTD for CPT+DOX is at least 4-fold higher than our treatment dose for Ap-DOCTOR.

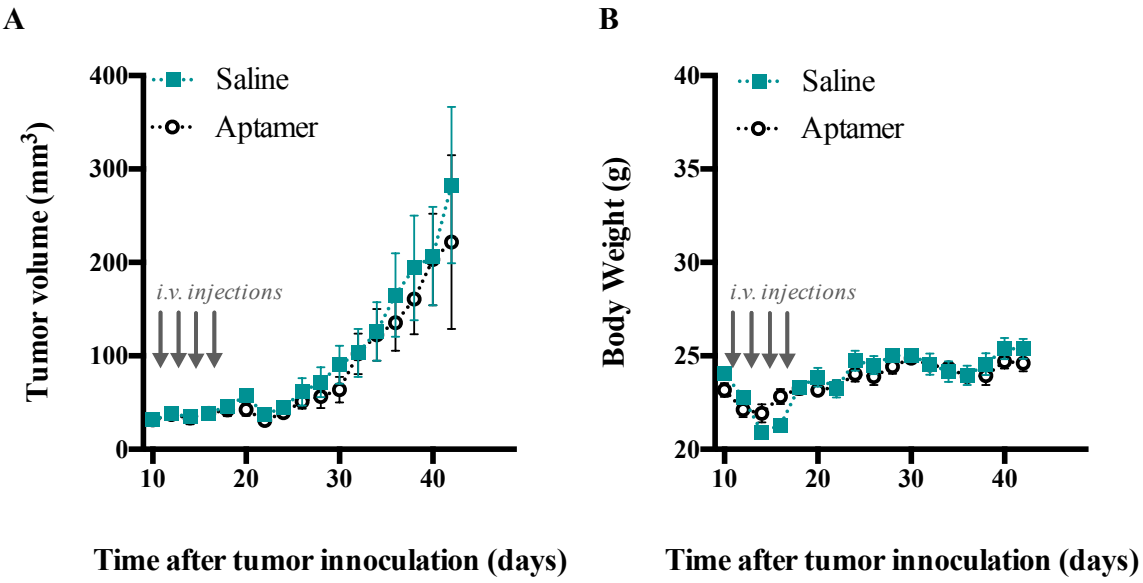

Figure 35. In vivo efficacy and toxicity assessment of aptamer-only and drug cocktail treatment in nude mice.

(A) Tumor growth curves in an orthotopic MDA-MB-231 mouse breast cancer model treated with saline (blue squares) and aptamer (black circles) at a dose of 30.4 mg/kg. A total of four injections (grey arrows) were administered every other day starting on day 11 post-tumor inoculations. (B) Corresponding body weight changes of tumor-bearing mice for all groups. Data are expressed as mean ± SEM (n = 5).

Critically, it was also noted that animals receiving Ap-DOCTOR exhibited similar clearance patterns for both DOX and CPT, whereas DOX was cleared faster than CPT after administration of the unconjugated drug cocktail at equivalent doses (Figure 37). This confirms that this novel Ap-DOCTOR construct is better suited for achieving synergistic treatment of multiple drugs at defined dosage levels, an attribute that is most likely an important factor contributing to its superior performance in preventing tumor growth.

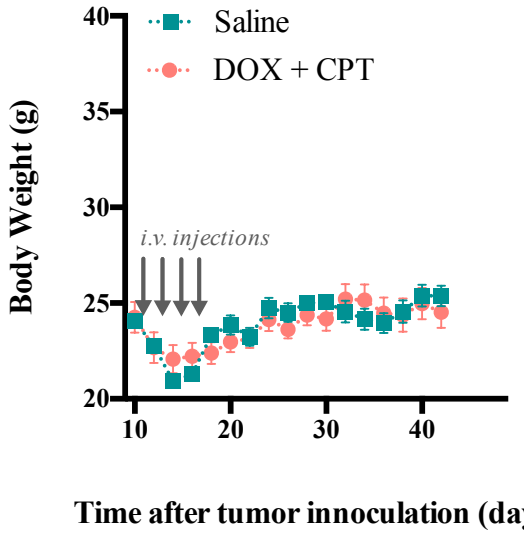

Figure 36. Body weight changes of nude mice following i.v. administration of an unconjugated DOX and CPT cocktail (salmon) and saline (blue squares).

Drug doses of 2 mg/kg DOX and 1.4 mg/kg CPT were used. Data are mean ± SEM (n = 5).

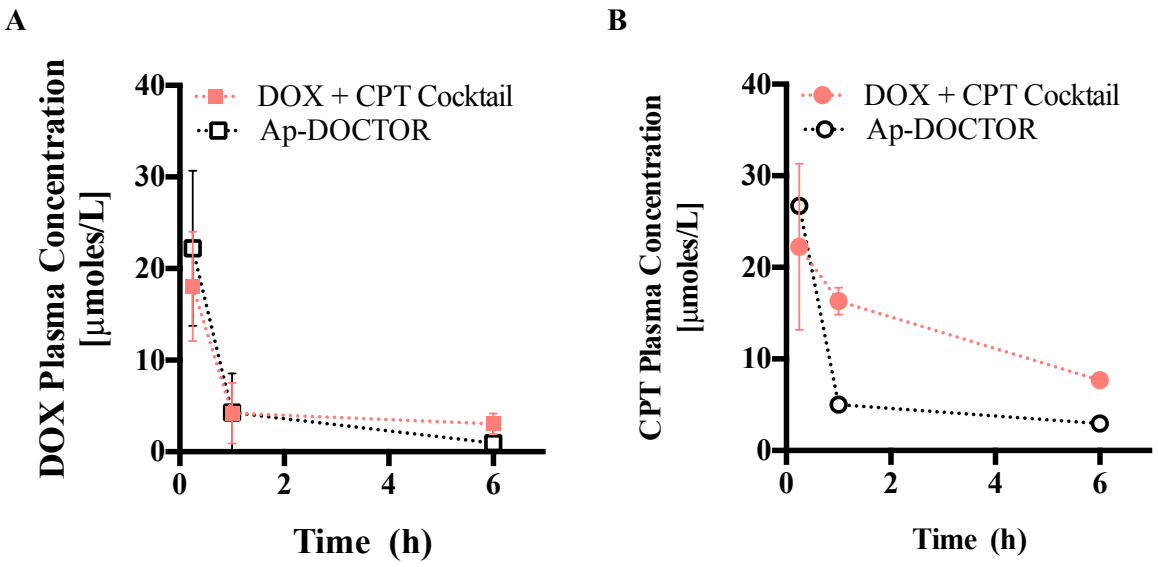

Figure 37. Plasma concentration of DOX (squares) and CPT (circles) after i.v. administration of DOX and CPT.

Injection was either a free drug cocktail (salmon) or Ap-DOCTOR (black) at drug equivalent doses of 2 mg/kg DOX and 1.4 mg/kg CPT. Data are expressed as mean ± SEM (n = 5).

5.6 Discussion on aptamer-mediated drug delivery

A strategy for achieving improved chemotherapeutic efficacy by enabling simultaneous targeted delivery of defined doses of multiple drugs was demonstrated. Briefly, an aptamer that recognizes a tumor-specific cell-surface marker was coupled with a peptide backbone that can be efficiently conjugated to therapeutic agents via a straightforward 'click' chemistry procedure. These designer constructs facilitated synergistic treatment at optimal molar ratios of drug while minimizing the toxicity that can otherwise arise in non-targeted chemotherapy.

As a demonstration, nucleolin aptamer AS1411 was attached to short peptides coupled to a 1:1 molar ratio of DOX and CPT to recognize and deliver the payload to a nucleolin-expressing metastatic breast cancer cell line MDA-MB-231 [151].

Optimizing drug ratio and targeting simultaneously for low dose cancer treatment

This study demonstrated that by systematic *in vitro* screening, it is possible to identify molar ratios that are selectively more potent to cancer cells and less potent to normal cells [46,47]. Hence, it is possible to engineer constructs with optimized therapeutic indices, maximizing their toxicity to cancer cells while minimizing risk of adverse events. At a molar ratio of 1:1 for DOX:CPT, a drug reduction index (inverse of combination index) of 3 was observed for MDA-MB-231 cancer cells compared to 1.6 for MCF 10A epithelial cells (Figure 22). While Ap-DOCTOR delivers DOX and CPT at a molar ratio of roughly 1:1, several constructs that can deliver DOX and CPT at other molar ratios were synthesized (Figure 23).

The targeting aspect of the vehicle design improves its apparent safety profile along with enhancing uptake specifically in cancer cells. *In vitro,* Ap-DOCTOR enhanced the toxicity of free DOX and CPT by 15-fold and 7-fold, respectively. Further, in long incubation studies, Ap-DOCTOR treatment enhanced cancer cell cytotoxicity by 2.5-fold relative to a simple drug cocktail, but also decreased the cytotoxicity seen in normal epithelial cells (MCF-10A) by 4-fold. These results are comparable to an aptamer targeted nanoparticle delivering Docetaxel and Cisplatin synergistically, where targeting led to a 2.5-fold increase in cytotoxicity to cancer cells and a 1.8 fold decrease in cytotoxicity to control cells [167].

When constructs were evaluated for cytotoxicity after short incubation times, a more realistic comparison to *in vivo* conditions, Ap-DOCTOR displayed negligible cytotoxicity to MCF 10A control cells even though the drug combination was extremely potent in long incubation studies. This is most likely a result of targeting differences emphasized after a short incubation and several wash steps that follow. Nevertheless, this is of great significance since the results demonstrate elimination of toxicity of DOX + CPT on control MCF 10A cells that were 20× more sensitive to the free drug combination compared to MDA-MB-231 cells. Prostate cancer targeting nanoparticles loaded with DOX and DTX were delivered to cancer cells and control cells in a comparable short incubation fashion. Similar to results shown with Ap-DOCTOR, negligible toxicity was observed for the control cell line; however, no synergistic effects of the drug combination were observed at the molar ratio delivered [165].

A clear enhancement of tumor-targeted cytotoxicity *in vivo* was demonstrated, using a nude mouse model with highly aggressive orthotopic tumors derived from nucleolin-enriched MDA-MB-231 cells. Ap-DOCTOR treatment produced a statistically significant 58% reduction in tumor volumes in this model relative to animals that were treated with a cocktail of equivalent doses of the same two drugs, and a 73% reduction relative to untreated mice. Notably, this reduction was achieved at an extremely low cumulative dose of 2 mg/kg DOX and 1.4 mg/kg CPT; to our knowledge, this is the lowest cumulative dose of DOX reported to date to achieve such drastic tumor volume reduction with an aptamer-targeted delivery system [161,163,166,176,177]. No additional toxicity was observed to mice with this delivery system relative to the standard drug cocktail.

DOX-based drug combinations have been previously tested on MDA-MB-231 mouse models. The most effective systems found were a polymerosome comprising DOX and Paclitaxel (3 mg/kg and 7.5 mg/kg, respectively) and PEGylated hyaluronic acid polymer conjugated to 10 mg/kg CPT. Since the starting tumor volumes for these studies are different to ones reported here, a direct comparison is difficult [178–182]. Nevertheless, the studies performed here show that DOX and CPT at optimal ratios are extremely potent against MDA MB 231 cells at a much lower DOX dose of 2mg/kg, and further studies at higher drug doses can validate their therapeutic efficacy for triple negative breast cancer.

Need for conjugating both drugs on a single carrier

Dual drug loaded systems have been previously shown to improve potencies over cocktail mixtures of single drug loaded systems in the same ratio [72,167]. This superior potency can be explained by consistent delivery of optimal therapeutic ratios by dual-drug delivery systems not guaranteed by a cocktail of single drug systems whose components can undergo different pharmacokinetics and cellular uptake [47,72]. Hence, to ensure that aptamers were carrying both drugs, each peptide was attached via highly efficient orthogonal chemistries in a site-specific fashion.

In agreement, the dual drug conjugation was noted to be critical for efficient drug uptake *in vitro* and in turn enhanced toxicity in the cancer cells (Figure 27). *In vitro* testing showed clear superiority of Ap-DOCTOR over a cocktail of single drug-aptamer conjugates (Ap-DOX + Ap-CPT). Likewise, the superior tumor reduction seen *in vivo* with Ap-DOCTOR relative to an unconjugated drug cocktail was paralleled by much stronger correlation in the circulating plasma levels of the two drugs (Figure 37) indicating that the

Ap-DOCTOR formulation offers a more robust means for attaining controlled, synergistic effects in combination therapy.

Targeting tumor subpopulations overexpressing nucleolin with AS1411

Studies have linked tumorigenicity, metastatic ability, relapse and drug evasive properties of triple negative breast cancers to cell surface nucleolin overexpression [39]. Thus, being able to deliver drugs to these aggressive subpopulations in a targeted fashion is of great interest. Since nucleolin overexpression plays an impact on tumor metastasis and progression, nucleolin overexpressing highly tumorigenic MDA-MB-231 triple negative breast cancer cell populations were identified and isolated for treatment in the present work.

AS1411 (NucA) is a well-characterized aptamer that targets overexpressed cell surface nucleolin and is currently the most advanced oncology aptamer in clinical trials [131]. Even though a 50 to 100-fold increase in binding of the nucleolin aptamer compared to a control aptamer on MDA-MB-231 cells was observed, it did not elicit *in vitro* or *in vivo* cytotoxic effect on these cells at the concentration ranges where DOX and CPT inhibited cell growth. This behavior is consistent with other reports and it can be concluded that the aptamer did not contribute to any cytotoxicity and was purely a targeting moiety [159].

Translation of *in vitro* results of aptamer efficacy into *in vivo* benefits has remained a major challenge since aptamers are rapidly cleared from the blood stream because they are degraded by nucleases *in vivo* [131]. AS1411 however, offers remarkable resistance to serum nucleases and is stable in blood due to its 3-dimensional G quadraplex structure [151]. Although, AS1411 has been extensively used in several targeted delivery applications, it has never been used to target a drug combination, much less a drug combination in

therapeutically optimal molar ratios [124]. These results demonstrate two key concepts: AS1411 aptamer guided delivery of a synergistic drug combination and an aptamer conjugate that is able to deliver drug combinations in predetermined molar ratios. On a side note, this is also the first study to report an aptamer system for targeted CPT delivery.

Comparison to previous aptamer dual drug delivery systems

Several notable studies have demonstrated the use of aptamers for combination drug delivery, however those studies were largely focused on using aptamers for surface modification of nanoparticles [165–167]. While a larger number of ratios can potentially be incorporated into nanoparticles, it must be noted that advantages such as small size of aptamer, improved tumor penetration and cellular uptake are no longer exhibited by these particulate systems. Ap-DOCTOR, on the other hand, is a molecular entity (<10 nm), which may facilitate its deep penetration into tumors. The design of Ap-DOCTOR also provides precise control of drug loading via orthogonal click chemistries, and finally, Ap-DOCTOR provides a soluble molecular design that facilitates its formulation and use (Figure 26). The potency of Ap-DOCTOR is a result of the highly selective tumor targeting and its internalization, along with the capacity to achieve effective synergy between multiple drugs with the peptide framework.

Modularity of the design strategy

It is believed that this approach should be broadly generalizable. A wide variety of tumor-specific protein biomarkers have been identified to date, for which aptamers are either already available or can readily be generated via well-established techniques

[123,126,127,131,148]. Furthermore, the chemistries described are easily extendable to any aptamer, which can theoretically allow for targeting several cancer markers. There is a wide range of additional linker technologies that can be designed and optimized for distinct drug combinations, and by taking advantage of facile peptide synthesis technologies, one can readily switch out glutamic acid residues for cysteine, lysine or other natural/unnatural amino acids that are suitable for conjugating drugs using other chemistries [172]. Overall, the design is highly modular and can be used with a large library of targeting moieties and cytotoxic molecules to suit several cancer therapeutic applications.

Chapter 6

Experimental Methods

6.1 Materials

Non-enzymatic cell dissociation solution, MDA-MB-231, 4T1, NIH-3T3 and MCF-10A cell lines were acquired from ATCC (Manassas, VA). RPMI-1640 media, DMEM media, fetal bovine serum (FBS), penicillin-streptomycin (pen-strep), Quant-iT OliGreen ssDNA Assay, 3-(4,5-dimethylthiazol-2-yl)-2,5-diphenyltetrazolium bromide (MTT), CellLight plasma membrane-RFP, BacMam 2.0, heparin-coated plasma preparation tubes and 7000 MWCO Slide-A-Lyzer dialysis devices were purchased from Thermo-Fisher Scientific (Waltham, MA). Cell culture flasks, microplates and Matrigel were obtained from Corning (Corning, NY). MEBM Medium and Gelstar staining dye were purchased from Lonza (Walkersville, MD). Accumax™ was purchased from Innovative Cell Technologies (San Diego, CA). AlexaFluor 488-anti-nucleolin antibody (364-5), AlexaFluor 488-Mouse IgG_1, kappa monoclonal - isotype control were obtained from Abcam (Cambridge, MA). malPEP peptide was custom synthesized at GenScript (Piscataway, NJ), and dbcoPEP peptide at New England Peptide (Gardner, MA). All aptamers were custom synthesized by Integrated DNA Technologies (Coralville, IA). DSPC (1,2-distearoyl-sn-glycero-3-phosphocholine) and mPEG-DSPE (1,2-distearoyl-sn-glycero-3- phosphoethanolamine-N-[methoxy(polyethylene glycol)-2000) were obtained from Avanti Polar Lipids (Alabaster, AL) and hyaluronic acid was sourced from Creative PEGWorks (Durham, NC). 15% TBE-urea polyacrylamide gel,

TBE buffer and micro bio-spin P-6 gel columns were obtained from Bio-Rad (Hercules, CA). Sephadex G-25 PD-10 desalting columns (5,000 MWCO) were purchased from GE Healthcare Life Sciences (Marlborough, MA). DOX was obtained from LC Laboratories (Woburn, MA) and Sep-Pak C18 cartridges were obtained from Waters (Milford, MA). CPT, cholera toxin, sodium azide, bis(2-oxo-3-oxazolidinyl)phosphinic chloride (BOP-Cl), 4-(dimethylamino)pyridine (DMAP), N,N-diisopropylethylamine (DMAP), Tris(2-carboxyethyl)phosphine hydrochloride (TCEP), Cholesterol and all other chemicals were purchased from Sigma-Aldrich (St. Louis, MO).

Table 11. Peptide and DNA sequences used in the experiment

Name	*Sequence/Structure*	*Description / Comments*
malPEP	GEGEGEGEGE	Peptide backbone of alternating Glycine and Glutamic acid amino acids. The N terminus is conjugated to maleimide and the C terminus is amidated.
dbcoPEP	GEGEGEGEGEK’	Peptide backbone of alternating Glycine and Glutamic acid amino acids with a modified azido lysine at position 11 from the N terminal. The N terminus is acetylated and the C terminus is amidated.
th-NucA	5’-GGT GGT GGT GGT TGT GGT GGT GGT GGT TTT TT/3ThioMC3-D/-3’	Nucleolin aptamer, AS1411 sequence [183] followed by a T_5 spacer and a thiol modification at the 3’ end.

th-CRO	5’-CCT CCT CCT CCT TCT CCT CCT CCT CCT TTT TT/3ThioMC3-D/-3’	Cystine-rich oligonucleotide, Control Aptamer sequence [184] followed by a T_5 spacer and a thiol modification at the 3’ end.
az-NucA	5’-GGT GGT GGT GGT TGT GGT GGT GGT GGT TTT TT/3AzideN /-3’	Nucleolin aptamer, AS1411 sequence [183] followed by a T_5 spacer and an azide modification at the 3’ end.
az-CRO	5’-CCT CCT CCT CCT TCT CCT CCT CCT CCT TTT TT/3AzideN/-3’	Cystine-rich oligonucleotide, Control Aptamer sequence [184] followed by a T_5 spacer and an azide modification at the 3’ end.
dc-NucA (dual click)	5’-GGT GGT GGT GGT TGT GGT GGT GGT GGT TTT T/iAzideN/TT TTT/3ThioMC3-D/-3’	Nucleolin aptamer, AS1411 sequence followed by a T_9 spacer with an internal azide modification at position 31 from the 5’ end and a thiol modification at the 3’ end.
Cy5-NucA	5’-GGT GGT GGT GGT TGT GGT GGT GGT GGT T/iCy5/TT TTT/3ThioMC3-D/-3’	Nucleolin aptamer, AS1411 sequence followed by a T_6 spacer with an internal Cy5™ modification at position 28 from the 5’ end of the sequence and a thiol modification at the 3’ end.
Cy5-CRO	5’-CCT CCT CCT CCT TCT CCT CCT CCT CCT	Cystine-rich oligonucleotide, Control Aptamer sequence followed by a T_6 spacer

	T/iCy5/TT TTT/3ThioMC3-D/-3’	and with an internal Cy5™ modification at position 28 from the 5’ end of the sequence and a thiol modification at the 3’ end.

6.2 Synthesis of drug delivery vehicles

Peptide-Drug Conjugates

DOX and CPT were conjugated to glutamic acid moieties on the peptide backbone via nucleophilic acyl substitution. To obtain CPT-peptide conjugates, 9 μmol malPEP and 8–26 μmol CPT (molar excess based on target loading) were solubilized in 3 mL of anhydrous dimethylformamide (DMF) and cooled in an ice bath. A solution of BOP-Cl (1.8× molar excess to CPT), DMAP (3.8× molar excess to CPT) and DIPEA (1.5× molar excess to CPT) in 1 mL anhydrous DMF was added drop-wise. The mixture was gradually warmed 40 °C and the reaction was carried out under nitrogen and stirring at 40 °C for two days. For DOX peptide conjugates, 9 μmol dbcoPEP and 8–26 μmol DOX (molar excess based on target loading) were used in the first step of conjugation. Molar excess amounts of other reactants and reaction conditions were otherwise the same as for CPT.

After two days, reverse-phase chromatography was used to purify conjugates. Briefly, the reaction mixture was diluted 20-fold in DI water and adsorbed on C18 cartridges (pre-washed thrice with pure acetonitrile followed by DI water). Next, the cartridges were washed five times each with DI water, 5% and 10% (v/v) acetonitrile in water to flush out unreacted peptides and hydrophilic impurities. Fractions eluted during subsequent washes at higher volume concentrations of acetonitrile in water (20–40%) were collected, combined and dried

under vacuum (<100 mTorr, 2 days) to yield purified powders of peptide-drug conjugates. Concentrations of DOX and CPT were quantified via fluorescence spectroscopy (DOX $\lambda_{ex}/\lambda_{em}$: 479/590 nm, CPT $\lambda_{ex}/\lambda_{em}$: 370/450 nm) and peptide concentrations were determined via absorbance at 270 nm after eliminating absorbance contributions of conjugated drug (Tecan Infinite M1000). MALDI-TOF mass spectrometry was performed to qualitatively confirm multiple drug conjugations on a single peptide backbone.

Attachment to aptamer via 'click' chemistry to make aptamer drug conjugates

Thiol-maleimide click chemistry: 3'-end disulfide linkage was reduced to free thiol on th-NucA or th-CRO aptamer by treating 100 nmol aptamer with 10 μmol TCEP (100× molar excess to aptamer) in 1 mL PBS (pH 7.4) for 1 h at room temperature under nitrogen. 1 μmol CPT-loaded malPEP in 1 mL dimethyl sulfoxide (DMSO) was added to the reduced aptamer mixture and allowed to react overnight at 4 °C under nitrogen.

Strain-promoted azide-alkyne click chemistry (SPAAC): 100 nmol az-NucA or az-CRO aptamer (Table S1) dissolved in 1 mL of PBS (pH 7.4) was added to 0.5 μmol DOX-loaded dbcoPEP in 1 mL DMSO and allowed to react overnight at 4 °C under nitrogen.

For dual drug-loading, reactions were carried out in a one-pot synthesis step. 100 nmol dc-NucA was treated with 10 μmol (100× molar excess of aptamer) TCEP in 1 mL PBS (pH 7.4) for 1 h at room temperature under nitrogen to reduce the 3'-end disulfide linkage to a free thiol. Then, 1 μmol CPT-loaded malPEP and 0.5 μmol DOX-loaded dbcoPEP dissolved in 1 mL DBCO were added simultaneously and allowed to react overnight at 4 °C under nitrogen.

After all reactions, unreacted excess peptides were removed by an initial overnight dialysis using a 7,000 MWCO Slide-A-Lyzer dialysis device followed by size-exclusion chromatography through a Sephadex G-25 PD-10 desalting column (5,000 MWCO). To determine the extent of drug conjugation to the aptamer, concentrations of CPT and DOX in the purified sample were measured via fluorescence and aptamer concentrations were determined using Quant-iT OliGreen ssDNA assay. Briefly, purified constructs diluted in TE buffer were incubated with equal volumes of aqueous working solution of Quant-iT OliGreen reagent for 5 minutes, protected from light. Post-incubation, fluorescence corresponding to the aptamer concentration was measured (Tecan Infinite M1000, $\lambda_{ex}/\lambda_{em}$: 480/520 nm).

Synthesis of hyaluronic acid drug conjugate

DOX was conjugated to Hyaluronic Acid (HA) via nucleophilic acyl substitution, by coupling the carboxylic acid of HA were conjugated to the primary amine or alcohol groups present on DOX. 10 mg of 250kDa molecular weight HA was dissolved in a 1 mL mixture of DMSO/water (1:1 by volume) under stirring and slight heating (40 °C). DMAP and EDC were added at a molar ratio of 1:1 relative to HA monomers, and were allowed to activate the polymer for 1 h under stirring. DOX was dissolved in the reaction mixture in a molar ratio of 0.5:1 DOX:HA. The reactions proceeded under slight heating (40 °C) for 3days. Then, DOX–HA was separated from unreacted free drugs, EDC and DMAP via overnight dialysis using a 5000 MW exclusion membrane. For further purification, a size exclusion chromatography step, through Sephadex G-25 PD-10 desalting columns (5000 MW exclusion limit) equilibrated in PBS (pH 7.4), was performed. Concentration of DOX in the purified sample was measured via fluorescence.

DOX loaded liposome preparation

A mixture of DSPC:mPEG-DSPE:Cholesterol in 56.3:5.3:38.4 molar equivalents is dissolved in chloroform and placed in a rotary evaporator and the pressure is first reduced to 250 mbar and subsequently reduced by 30 mbar in two five minute segments, and then by 50 mbar every 5 minutes to reach 140 mbar. Once the solvent was completely evaporated and a lipid film was visible, the flask was submerged in a 65°C water bath and the pressure was set to 0 mbar. It was left under this condition for 5 min. Leave for an additional five minutes. Meanwhile an extruder was assembled and membranes were allowed to be in water contact at 70°C. The lipids were then rehydrated with 1.1 ml of ammonium sulfate solution (250 mM, pH 5.5) and placed in a 65°C water bath at ambient pressure for 5 min until the lipids formed a white opaque solution. The rehydrated lipid solution was transferred to an extruder syringe and returned to a water bath in the oven at 80°C for 30 m. The lipid solution was passed through the membrane 21 times and collected for further purification in a Sephadex G-25 PD-10 column. Briefly, the columns were washed with 25 ml of PBS (pH 7.4) and ~1 ml liposomes were let to sink into the column. Then, another 1.5 ml of PBS was added to attain the bed volume (2.5 ml) of the column. By adding 1 mL of PBS, pure liposomes were collected. DOX was encapsulated by adding 50 ul of 70 mM DOX (in PBS pH 7.4) dropwise to 500 ul of liposomes under stirring at 65°C in the oven. They are kept under those conditions for 2.5 hours and removed. The liposomes were passed through a size exclusion column to separate the free drugs from the drug-encapsulated liposomes as described above. To quantify amount of DOX, 30 ul liposomes were added to 270 ul methanol and vortexed

and sonicated 30 min to disturb the liposomes. Lipids were centrifuged out at 12000 g for 5 min, and then the DOX concentration was read via fluorescence.

6.3 Construct characterization assays

Gel electrophoresis

All constructs were analyzed via denaturing gel electrophoresis on a 15% TBE-urea polyacrylamide gel stained with 1× Gelstar dye. Each lane contained a loading solution that comprised of 4 μL of purified construct or unconjugated aptamer, 2 μL of 5× loading dye and 6 μL of formamide. Loading solutions were heated to 95 °C for 5 min and cooled to room temperature. Gels were pre-run for 10 min at 150 V after which wells were washed with running buffer and loaded with 5 μL of each sample and run for an additional 80 min at 150 V in 1× TBE buffer (89 mM Tris borate, 2 mM Na_2-EDTA, pH 8.3). Gel images were taken with Gel-Doc EZ system (BioRad) equipped with Image Lab software.

Dynamic light scattering (DLS) measurements

Drug conjugates were diluted 20-fold in PBS prior to analysis and dust particles were removed by centrifuging at 500 rpm for 1 min. Samples were read on a Malvern ZetaSizer Nano ZS and an average of three independent measurements of at least 13 runs each ± SD are reported.

Release studies

We determined drug release kinetics from the aptamer construct via hydrolysis from the peptide scaffold at pH 7.4 and 5.0. Constructs were dissolved in PBS at pH 7.4 or at pH 5 and kept under stirring at 37 °C. At indicated time points, released drugs were separated from constructs via size-exclusion chromatography by passing the mixture through micro bio-spin P-6 gel columns (6,000 MW exclusion limit). Following removal, we determined the amounts of drug conjugated to the construct by measuring concentrations of CPT and DOX in the recovered sample via fluorescence. Drug release (wt%) was fit to exponential release profiles to determine time required for 50% drug release ($t_{1/2}$).

6.4 In vitro cell assays

Cell culture

All cells were cultured in a humidified incubator with 5% CO_2 at 37 °C. MDA-MB-231 was maintained in RPMI-1640 medium supplemented with 10% FBS and 1% pen-strep. MCF-10A cells were maintained in MEBM media supplemented with hydrocortisone, hEGF, insulin, BPE, and 100 ng/mL cholera toxin. 4T1 and NIH-3T3 were maintained in DMEM medium supplemented with 10% FBS and 1% pen-strep. Nucleolin-overexpressing MDA-MB-231 cells were obtained as previously described [175]. Briefly, 1×10^7 cells were stained with AlexaFluor 488-anti-nucleolin antibody [364-5] or Alexa Fluor 488-mouse IgG_1, kappa monoclonal - isotype control for 1 h at 4 °C in PBS buffer containing 10% FBS and 1% pen-strep. Cells were then washed twice and sorted via flow cytometry (BD FACSAria II) into a sterile FBS-coated tube. Isolated cells were resuspended in culture media and grown as described above.

Internalization studies with confocal microscopy

To verify specific internalization of the targeting aptamer (NucA), we used confocal laser scanning microscopy. 4.5×10^4 MDA-MB-231 cells and 9×10^4 MCF-10A cells were seeded and allowed to adhere overnight in a 48-well coverslip bottom culture plate. The coverslip bottom was coated with fibronectin prior to cell seeding. Cells were exposed to either a labeled nucleolin-specific aptamer (Cy5-NucA) or a labeled control aptamer (Cy5-CRO) at a concentration of 1 μM in fresh media for 30 m or 4h in a humidified incubator at 37 °C and 5% CO_2. Cells were then washed twice with PBS warmed to 37 °C and fixed with 4% formaldehyde for 15 min at 37 °C. The cells were then counterstained with 1 μg/ml Hoechst dye for 5 min and washed twice with PBS to remove excess dye. All cells were imaged with an Olympus Fluoview 1000 spectral confocal equipped with a 60 × silicon oil objective. 405-nm 50 mW and 635-nm 20 mW diode lasers were used to excite Hoechst (420–460 nm emission filter) and aptamer (>630 nm emission filter), respectively. 6-μm *z*-stacks were captured and subsequently analyzed with ImageJ software (NIH).

For visualizing drug uptake with or without a targeting aptamer, cells were grown as described above. Cells were incubated with formulations consisting of DOX and CPT at a final concentration of 5 μM for 2.5 h and later washed and fixed following the protocol above. Plasma membranes were stained using CellLight plasma membrane-RFP, BacMam 2.0. All cells were imaged with a Zeiss CellDiscoverer 7 microscope equipped with a 50 × water objective. 385-nm, 470-nm, and 567-nm diode lasers were used to excite CPT (460-nm emission filter), DOX (555-nm emission filter) and plasma membrane (568-nm emission filter) labeling, respectively. *z*-stacks were captured and subsequently analyzed with ZenPro software.

In vitro tumor penetration study with tumor spheroids

Tumor spheroids were developed using the hanging-drop method described previously [185]. Briefly, a total of 1.1×10^4 cells/mL of 4T1 and NIH-3T3 cells harvested and resuspended in DMEM at a ratio of 1:5 4T1:NIH-3T3 cells were prepared. A 45 μL aliquot of the cell mixture was added to the top of each well and the plates were sealed. Cells were allowed to grow and form spheroids in the incubator for 4 days. Media was replenished on day 2 by removing 15 μL of media from each droplet and adding equivalent amount of fresh DMEM media. Spheroids that grew in droplets were harvested at the end of 96 hours into a non-adherent 96 well plate. Each spheroid was incubated with different drug delivery vehicles dissolved in 70 μL DMEM at a DOX equivalent dose of 25 μM. Drug vehicle solutions were removed at pre-determined time points and the spheroids were washed with PBS twice and disintegrated in 70 μL Accumax™ and further dissolved in equal volume of DMSO. To quantify the amount of penetration, DOX concentration was measured via fluorescence.

In vitro cell toxicity assay and synergy analysis

To identify optimal therapeutic ratios for DOX and CPT, we used the Combination Index (CI) method [31,44,46,47]. 5×10^3 MDA-MB-231 cells or 1×10^4 MCF-10A cells in 100 μL media were seeded per well in a 96-well culture plate and allowed to adhere overnight. After aspirating old media, serial dilutions of individual aptamer drug formulations (*i.e.,* Ap-DOX or Ap-CPT) in fresh media were added and incubated for 72 h. Cell viability was then assessed by the MTT assay. Drug formulations were replaced with 100 μL of MTT solubilized in media (0.5 mg/mL) and, following a 3.5 h incubation, the solution was aspirated and replaced with DMSO. Finally, the plates were shaken for 20 min and cell

viability was measured by reading the absorbance of each well at 570 nm with a Tecan Infinite M1000. To obtain *in vitro* cytotoxicity curves and IC_{50} values, experimental cell viability data were fitted to the median-effect model. [186] Cell viabilities were also assessed for different molar ratios of aptamer drug cocktails by the same method. For all ratios, total drug concentrations were kept constant (2 μM for MDA-MB-231 cells and 200 nM for MCF-10A cells). Synergy was assessed by calculating CI values, where synergism, additivism, and antagonism are respectively indicated by CI values less than 1, equal to 1, and greater than 1 [8,44]. CI errors are reported by propagating the corresponding errors in cell viability data after a combination treatment and standard error of the individual drug model fits.

For direct comparison of *in vitro* toxicities, formulations were tested for their ability to inhibit cancer cell proliferation. Cells seeded as described above were exposed to drug formulations for either the full 72 h incubation period or for a brief window of 2.5 h at the start, washed twice and incubated with fresh media for an additional 69.5 h. At the end of 72 h, the MTT assay was performed to obtain cell viability data, and fractional cell inhibitions were calculated.

Apoptosis Assay

Apoptosis patterns of Ap-DOCTOR and free DOX+CPT were studied in MDA-MB-231 and MCF 10A cells by Annexin V and Sytox Green counterstaining, following the Life Technologies Apoptosis Assay protocol. Briefly, cells were seeded at a concentration of 100 x 10^4 cells per 25 cm^2 cell culture flask, and allowed to adhere overnight. Cells were exposed to drug solutions for 3 hours. After drug exposure, all adherent and floating cells were harvested at a concentration of 1 x 10^6 cells/mL in Annexin V binding buffer, and 200 μL of

each sample were incubated with 5 μL of Annexin V- 647 and 1 μL of 1 μM Sytox Green. After 15 minutes of dye incubation, cells were diluted 5X in ice cold Annexin V Binding Buffer, and immediately analyzed via flow cytometry (BD FACSAria II). Cells gated as Annexin V^-/Sytox $Green^-$ were live, cells with Annexin V^+/Sytox $Green^-$ were early-apoptotic, and cells gated as Annexin V^+/Sytox $Green^+$ were either end-stage apoptotic or dead.

6.5 *In vivo* studies

In vivo tumor growth inhibition

Orthotopic MDA-MB-231 xenografts in nude mice obtained from Charles River laboratories were used to evaluate the efficacy of the aptamer conjugates *in vivo*. The Institutional Animal Care and Use Committees of the University of California Santa Barbara and Harvard University approved all experimental procedures pertaining to the use of animals. MDA-MB-231 cells (2.5×10^6 in 100 μL of 1:1 Matrigel and saline, > 98% cell viability) were injected subcutaneously into the inguinal mammary fat pad of 6–8 week old athymic nu/nu mice. The mice were randomized into groups of five and monitored for tumor growth and body weight changes. Treatments began 11 days post-implantation. Cocktails of unconjugated CPT and DOX were dissolved in 10% tween-80 in sterile saline (0.9 wt/vol% NaCl) and all other treatments were solubilized directly in sterile saline. Mice received a total of 4 intravenous treatments of saline, free drug cocktail, aptamer, or Ap-DOCTOR every other day via tail vein injections. All formulations were injected at drug-equivalent doses of 0.5 mg/kg DOX and 0.35 mg/kg CPT. Separate aptamer and drug cocktail treatments were injected at a drug-

equivalent dose of 2 mg/kg DOX and 1.4 mg/kg CPT. Tumor volumes were calculated using the following equation: $V = ½ (l) \times (w)^2$, where l and w are the longest and shortest dimensions of the tumor, respectively. Mice were euthanized if tumor length exceeded 15 mm, or after body weight loss exceeded 15%, or after necrotic ulcers appeared in the tumor core.

Plasma Pharmacokinetics

A cocktail of CPT and DOX was dissolved in 10% tween-80 in sterile saline (0.9 wt/vol% NaCl) and Ap-DOCTOR was solubilized directly in sterile saline. Mice received intravenous treatments of drug cocktail or Ap-DOCTOR every other day via tail vein injections at a drug-equivalent dose of 2 mg/kg DOX and 1.4 mg/kg CPT. Whole blood was collected via tail nicking, and plasma was isolated with heparin-coated plasma preparation centrifuge tubes and split into two separate aliquots. DOX was dissociated from the peptide backbone by acid hydrolysis. Briefly, 50 μL of sample was treated with 50 μL of 1 M HCl at 85 °C for 20 min. After cooling to room temperature, the solution was neutralized with 50 μL of 1 M NaOH, and 50 μL of 1× PBS was added. Proteins were precipitated by incubating the mixture with 1 mL of a 9:1 acetonitrile:methanol mixture for 1 h at room temperature. The suspension was centrifuged at 14,000 rpm for 10 min and the supernatant was dried under vacuum at 45 °C. The second aliquot was treated according to a previously described method to determine the total CPT amount [70]. Briefly, 33 μL of 0.1 N NaOH was added to 50 μL of sample and stored at room temperature for 1 h. 50 μL of 0.1 N HCl was then added and proteins were precipitated by incubating the mixture with 367 μL of methanol at room temperature for 3 h. The suspension was centrifuged at 14,000 rpm for 10 min and the supernatant was dried

under vacuum at 45 °C. Drug amounts were determined by measuring concentrations of CPT and DOX in treated samples via fluorescence.

Chapter 7

Conclusion and future outlook

7.1 Reflections

Are two drugs better than one?

While severe toxicity issues have impaired the clinical progress of combination chemotherapy, several preclinical studies and clinical studies outlining ways to mitigate the toxicity foreshadow its reemergence. By controlling the drug molar ratios and schedules of chemotherapeutics, higher efficacies at low doses have been obtained [7,20,31]. Here, DOX and CPT were found to be an extremely potent drug pair against TNBC that exhibited molar ratio-dependent synergy. High efficacies at extremely low doses in an *in vivo* orthotopic mouse model were obtained by optimizing molar ratios of the drug pair through systematic screening. For the entire length of the study (44 days), progression free survival was achieved at doses that were roughly 4-fold lower than individual drug MTD values. Though remarkable, the combination was also extremely toxic *in vitro* on a control epithelial cell line and moreover the drug ratios were not preserved during circulation. Hence, drug combinations can be extremely beneficial, but careful engineering is necessary to translate them into the clinic.

What is the benefit of targeting?

Traditionally, imparting successful cancer-targeting properties to non-selective payloads was considered to be a 'cancer-binding' optimization problem i.e. if the drugs were somehow coupled to a carrier that could effectively and specifically recognize the tumor, it could deliver the payload efficiently to the tumor. However, increasingly, the roles of several transport barriers are gaining importance in targeted drug delivery, especially for advanced solid cancers that are metastasized and largely unvascularized. Along with superior tumor recognition, the targeting agents have to also efficiently penetrate into such tumors, be retained and taken up effectively. Hence, more emphasis is currently being laid on the physical and pharmacological properties of a targeting agent.

To allow the drug pair of DOX and CPT to discriminate between cancer and healthy cells, tumor-targeting aptamers were explored as an option. A cell surface nucleolin recognizing aptamer, AS1411 (NucA), was found to have excellent cancer binding affinities and a drug conjugate prepared using this aptamer was also small enough to penetrate more efficiently into tumor spheroids compared to other delivery agents. Further, it localized to the nucleus, the desired intracellular destination for DOX and CPT, which can assist in more efficient toxicity production of the payload after accumulation. Further, the aptamer carrier undergoes nucleolin-mediated endocytosis, which would also prevent cancer cells from acquiring drug resistance through efflux mechanisms. Anthracyclines like DOX are especially prone to such phenomena, where cancer cells with p53 mutations become less sensitive to chemotherapy due to constant expulsion of the drugs that have non-specifically accumulated inside the cell [187].

Thus, targeting agents that could efficiently bind and internalize into cancer cells and simultaneously penetrate into deep tumor tissues are highly desirable. Here, DOX and CPT

were carried by the cell surface nucleolin targeting aptamer for efficient TNBC specific uptake and mitigation of their indiscriminate toxicity to healthy cells.

How can drug combinations be translated more effectively to the clinic?

Several properties have to be simultaneously and rationally optimized for effective clinical translation. First, identifying ways to have good tumor responses with low drug doses can help reduce the clinical failure rates of combinations arising from dose limiting toxicities. Secondly, providing targeting properties to efficacious drug pairs could improve the safety profile of a treatment. Lastly, identifying a drug carrier with physical and pharmacological properties most suitable for any given cancer is extremely crucial. For example long circulating drug vehicles like liposomes and other stealth nanoparticles might be more suitable for hematologic cancers or highly 'leaky' tumors where repeated exposure during circulation can enhance tumor accumulation [188,189]. In contrast, small and efficiently penetrating carriers might be suitable for dense cancers like pancreatic and breast cancer [190,191].

In this work an approach to fabricate effective combination therapy is proposed, which is to combine highly potent drug molar ratios to suitable targeting agents like aptamers. A novel aptamer drug conjugate design was devised that unlike previous designs allows conjugation of several drug molecules of different types onto a single aptamer molecule while still retaining the attractive targeting and biochemical properties of this class of affinity reagents. A small peptide scaffold was used to conjugate DOX and CPT to the nucleolin-targeting aptamer and an optimal molar ratio was identified via systematic screening. The resulting optimal drug formulation, Ap-DOCTOR, was small (< 10 nm) for

effective penetration, cancer recognition and uptake. The construct exhibited cancer specific killing in vitro and was also more effective at inhibiting tumor growth in an in vivo MDA-MB-231 tumor model compared to an uncoupled drug cocktail. Remarkable potency at unprecedentedly low drug doses was obtained, marking this approach as a feasible way to effectively translate drug combinations.

7.2 Further design improvements of aptamer-peptide conjugates

Overcoming drug conjugation limitations

While a limited number of molar ratios were presented in this framework, it is worthwhile to note that, the drug conjugation sites can be nearly doubled without significantly affecting the overall construct size. Additionally, more sophisticated linker technologies to conjugate CPT, demonstrated in other works, can improve overall CPT yield and allow more ratios to be loaded on to aptamers [93,94]. Controlling drug release rates using such linkers and others will enable engineering aptamer constructs that could release drugs sequentially, which is also known to impact the synergy of a drug pair [31].

As a separate goal, additional studies to fundamentally assess the impact of specificity (largest difference in CI between cancer and control cells) or potency (lowest CI on cancer cells), will help design targeted systems that are more beneficial and can realize their full therapeutic potential. Further preclinical and clinical evaluation will be required to verify the applicability of Ap-DOCTOR approach in treating triple-negative breast cancer, but this work demonstrates the feasibility of achieving controlled delivery of defined ratios of potent drug combinations using aptamer-peptide vectors as a therapeutic option for cancer.

Improving aptamer circulation properties

Aptamers are short circulating in nature and prone to rapid nuclease degradation and these problems are the main reasons limiting their use in targeted drug delivery [191]. Although AS1411 aptamer is resistant to serum nucleases due to its G-quadraplex structure, the aptamer is eliminated rapidly. Over 80% of Ap-DOCTOR was removed from the blood stream within an hour of circulation (Figure 37). Fortunately, several solutions have been engineered to enhance the circulation and limit aptamer degradation properties.

Polyethylene glycol (PEG) is commonly attached to aptamers to extend the circulation times of an aptamer in the blood stream [192]. It has been shown that conjugating aptamers to PEG of various sizes (20-80 kDa) can reduce the renal clearance rates and enhance the plasma pharmacokinetics [193]. However, one has to bear in mind that as a consequence of increasing the molecular weight of an aptamer construct the tumor penetration capacities could be diminished. Thus the molecular weight of PEG has to be optimized accordingly.

Several strategies have been discovered to limit aptamer degradation due to nucleases. Spiegelmers, which are oligonucleotide chains made from enantiomeric mirror-images of naturally occurring DNA and RNA, have been shown to have high serum nuclease resistance and extremely stable structures in complex biological environments [194,195]. Modifying the nucleobases to synthetic derivatives of nucleotides such as 2'-fluoropyrimdines and 2'-O-methyl purines has also been shown to confer extreme resistance to nuclease activity [196,197]. Similarly, using a 3' -3' inverted deoxythymidine cap also reduces the extent of nuclease degradation [198,199].

7.3 Designing interventions against different TNBC subtypes and cancers.

Modifying the chemotherapy combination

An obvious extension of the current work would be to test other combinations of drugs that are approved for use against breast cancer (previously discussed in Section 3.2). Several clinical trials are underway to identify chemotherapy drug combinations to which TNBC patients respond. This task is challenging since different TNBC subtypes respond differently to different chemotherapy drug classes [200,201]. Nevertheless, by using these combinations, a panel of aptamer dual-drug conjugates can be engineered to appropriately dose patients according to the subtype of TNBC they present. Table 12 lists other combination chemotherapy examples tested against different TNBC subtypes.

As a proof of concept, a combination using Gemcitabine (GEM), the drug that was found to be the least potent on the MDA-MB-231 cancer cell line (Figure 4), and DOX were tested to see if other drug pairs exhibited molar-ratio dependent synergy. There is prior evidence for synergy between DOX and GEM. GEM is a DNA antimetabolite and DOX is a topoisomerase II inhibitor. Since their mode of action is through two different pathways, the drug pair is expected to be synergistic [208,209]. Moreover, this drug pair was also found to have schedule dependent synergy [31].

Table 12. Drug combinations for different TNBC subtypes.

TNBC subtype	*Characteristics* [202–204]	*Drug Combinations*	
Basal-like	▪ Make up to 50-75% of all tumors ▪ Highly proliferative ▪ Favorable overall survival compared to other subtypes ▪ Respond poorly to anthracyclines.	Cyclophosphamide, Methotrexate and 5-Fluorouracil (CMF)	[205]
Claudin-low	▪ Primitive tumors, 5-10% of tumors ▪ Progenitor to other subtypes ▪ Linked to BRCA 1 mutation ▪ Respond well to anthracyclines and platinum drugs.	Doxorubicin and Cyclophosphamide (AC)	[206]
Luminal	▪ High BCL2 expression ▪ Extremely poor patient outcomes ▪ Respond poorly to taxanes	Fluorouracil, Doxorubicin and Cyclophosphamide (TAC)	[207]

Several different molar ratios of this drug combination were tested on the triple negative breast cancer cell line and indeed found the synergy to be a function of the ratio exposed. All ratios except 4:1 DOX:CPT was found to be synergistic. At the 3:2 DOX:CPT ratio, a dramatic 98.2% reduction of the IC_{50} value of GEM was observed and at the most

synergistic ratio (1:4 DOX:GEM; CI = 0.41±0.05), a 92% reduction in the IC_{50} value of GEM was observed. This warrants the further exploration of DOX and GEM and other drug pairs for TNBC treatment. Further studies on their cancer-selectivity and performance after conjugation to a tumor-targeting agent could lead to the discovery of other exciting therapies.

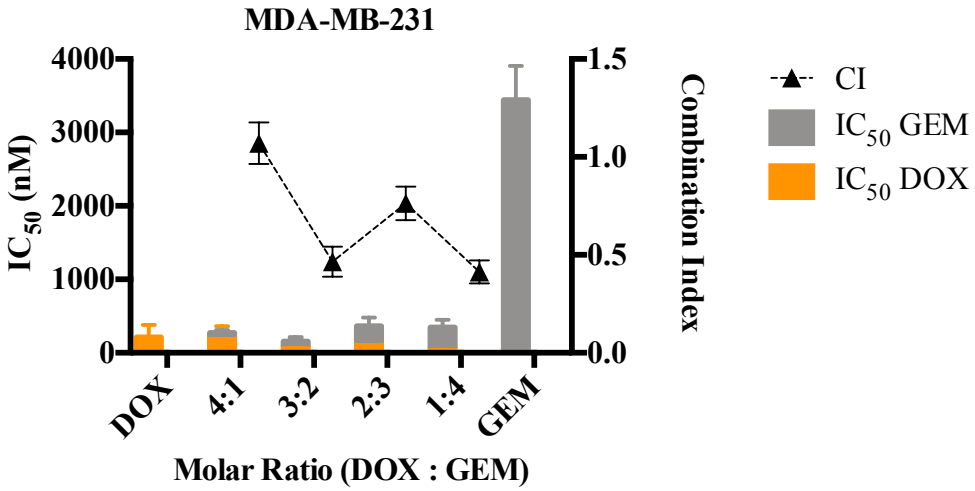

Figure 38. Effects of varying molar ratio in DOX and GEM combination treatments on MDA-MB-231 cell growth.

The MTT assay was used to measure fractional cell inhibition of MDA-MB-231 cells due to the combination treatment after 72 h incubations. Cell viability data were fitted to the median-effect model to obtain IC50 values corresponding to DOX (orange) and GEM (grey). CI was calculated by the Chou-Talalay method for each drug ratio tested. Errors were propagated from corresponding errors in cell viability data and standard errors of the drug model fits. Data are expressed as mean ± standard error of individual drug model fits (n ≥ 5).

Additional TNBC targeting aptamers

Cancer cells constantly mutate to form sub-clones that have a survival advantage under stressful conditions, like the presence of cytotoxic agents, so that they can continue proliferating. Resistance mechanisms developed by cancer cells to targeted drugs that are akin to development of resistance to chemotherapy drugs have been reported [50]. While one approach to circumvent this problem would be to use a co-targeting strategy, another approach could be to identify an alternative target on the cancer cell [210].

Aptamer identification technology, SELEX, is well suited for rapid generation of novel cancer recognizing aptamers. One advantage of aptamers is that unlike other targeting agents, they can be generated against cells, tissues or even whole organs without knowing the fundamental surface composition of the target cell [211–214]. In a first of its kind experiment, brain-penetrating aptamer was identified by isolating aptamers that selectively homed into the brain of a live mouse [147]. Thus aptamers being easy to generate are an extremely versatile choice for a targeting agent against cancer. Moreover, several other aptamers against TNBC have also been reported, like the 5TR1 aptamer that binds to MUC1 protein, a CD44 binding aptamer and a novel breast cancer internalizing aptamer generated by Cell-SELEX [215–217], which can be tested for the delivery of chemotherapeutic drug pairs. New technologies at our disposal like next generation sequencing, computer modeling, systems biology and patient derived xenografts can further revolutionize aptamer discovery technologies.

Expanding to other cancer types

The strategy of delivering potent drugs using aptamers can be utilized to target other advanced solid cancers. We have already shown targeting of AS1411 aptamer to nucleolin

overexpressing TNBC but this aptamer was advanced to phase II clinical trials against metastatic renal cell carcinoma and acute myeloid leukemia. Unfortunately, it showed limited activity in the former disease and was terminated against the latter [134]. Hence, conjugating cytotoxic agents to AS1411 could improve the poor clinical response witnessed in the clinical trials.

Further, small drug delivery vehicles like aptamer drug conjugates, hold great promise for treating cancers that have typically dense tumors due to enhanced penetration rates. Pancreatic cancers are one such example that have an almost impenetrable tumor microenvironment, which makes them one of most difficult cancers to treat [218]. Yoon et al. describe an aptamer drug conjugate to deliver either nucleoside analogs like GEM and 5-fluorouracil or cytotoxic agents like monomethyl auristatin E (MMAE) and derivative of maytansine 1 (DM1) using an RNA pancreatic cancer aptamer [157]. Using the aptamer dual drug conjugate framework described above, combination therapy for pancreatic cancer can be performed using the aptamer they describe. Similarly, other aptamer single drug conjugates have been described for prostate cancer targeting with A10 aptamer [219], colorectal and ovarian cancer targeting using 5TR1 aptamer [220,221] and hepatocellular carcinoma targeting using TLS11a aptamer [176].

7.4 Optimizing immunogenic effects of low dose combination treatments

The main dose limiting toxicities of most chemotherapy is myelosuppression and febrile neutropenia. Thus, dosing chemotherapeutic drugs at MTD results in such toxicities and makes them notorious for ‘immunosuppression’ [222]. However, several chemotherapeutic

drugs widely used in treating breast cancers are increasingly known to have anticancer immunogenic effects [223,224] (Table 13).

Lately, metronomic chemotherapy (MC), administering lower drug doses more frequently, is being advocated over the traditional MTD approach. This is because, while the MTD approach causes cell death mostly by apoptosis, MC can cause cell inhibition via several mechanisms like apoptosis, senescence, non-apoptotic cell death and also immunogenic cell death [225]. Further, due to tumor heterogeneity, highly immunogenic tumor cells are eradicated over time leaving behind a tumor composed of poorly immunogenic cells [226]. Thus dosing immune stimulating chemotherapeutic drugs could result in enhanced tumor responses. For example, Mastaria et. al. have shown that by formulating DOX, an immune stimulating agent, appropriately in a nanoparticle, the host immune system can be enabled and subsequently higher tumor responses can be achieved *in vivo* [227].

Immunogenic chemotherapy can also have huge implications in designing combination therapies with other cancer treatment modalities like immunotherapy and cell therapies. Immunotherapy and chemotherapy combinations are generally designed empirically and often fail in clinical trials. But with proper understanding of the anti-cancer immune effects generated by chemotherapies, synergistic immunotherapy and chemotherapy combinations for better cancer treatments can be designed [228].

'Low-dose' chemotherapy regimens identified in this work, by optimizing relative molar ratios and schedules of drug components, could be beneficial towards achieving potent immunogenic cell death effects. While immune effects are not always directly cytotoxic, they are very beneficial to establish a long-term therapeutic response

[229]. Hence, it would be a worthwhile exercise to study the immune effects produced by a chemotherapy combination and establish strong anticancer immune properties to the combination by iterative optimization.

Table 13 Immune stimulating chemotherapeutic drugs

Drug	Disease studied	Description of immune stimulating effect
Doxorubicin (Anthracycline)	Leukemia	▪ Enhanced dendritic cell (DC) uptake and maturation ▪ CD8+ T cells are critical for response
Paclitaxel (Taxane)	Breast cancer	▪ Enhanced T-cell and NK-cell function
Gemcitabine (Antimetabolite)	Pancreatic, non-small cell lung and colon cancer	▪ Inhibits B-cell proliferation – promotes favorable T-cell immunity ▪ Reduces myeloid suppressor cells ▪ Gemcitabine-induced apoptosis – enhanced DC cross-presentation of tumor antigens
5-Fluorouracil (Antimetabolite)	Breast and gastrointestinal cancer	▪ Expresses heat shock proteins (HSP) ▪ HSP facilitate DC uptake and cross-presentation of tumor antigens

References

[1] L. a Torre, F. Bray, R.L. Siegel, J. Ferlay, J. Lortet-tieulent, A. Jemal, Global Cancer Statistics, 2012, CA. Cancer J. Clin. 65 (2015) 87–108. doi:10.3322/caac.21262.

[2] F. Alexis, E.M. Pridgen, R. Langer, O.C. Farokhzad, Nanoparticle Technologies for Cancer Therapy, 2010. doi:10.1007/978-3-642-00477-3.

[3] American Cancer Society, Cancer Facts & Figures 2018., Am. Cancer Soc. (2018). doi:10.3322/caac.21442.

[4] A. Bosch, P. Eroles, R. Zaragoza, J.R. Viña, A. Lluch, Triple-negative breast cancer: Molecular features, pathogenesis, treatment and current lines of research, Cancer Treat. Rev. 36 (2010) 206–215. doi:10.1016/j.ctrv.2009.12.002.

[5] Types of Treatment, Natl. Cancer Inst. Natl. Institutes Heal. (2015). http://www.who.int/mediacentre/factsheets/fs310/en/.

[6] B.A. Chabner, T.G. Roberts, Timeline: Chemotherapy and the war on cancer, Nat. Rev. Cancer. 5 (2005) 65–72. doi:10.1038/nrc1529.

[7] L.D. Mayer, A.S. Janoff, Optimizing Combination Chemotherapy by Controlling Drug Ratios, Mol. Interv. 7 (2007) 216–223.

[8] A.C. Pinto, J.N. Moreira, S. Simões, Combination Chemotherapy in Cancer : Principles , Evaluation and Drug Delivery Strategies, in: P.O. Ozdemir (Ed.), Curr. Cancer Treat. - Nov. Beyond Conv. Approaches, 2011. doi:10.5772/22656.

[9] N. Howlader, M. Krapcho, D. Miller, K. Bishop, C. Kosary, M. Yu, J. Ruhl, Z. Tatalovich, A. Mariotto, D. Lewis, H. Chen, E. Feuer, K. Cronin, A. Noone, SEER Cancer Statistics Review 1975-2014 National Cancer Institute, (2017) 2012–2014.

[10] P. Yang, Epidemiology of Lung Cancer Prognosis: Quantity and Quality of Life, in: 2009: pp. 469–486. doi:10.1007/978-1-59745-416-2_24.

[11] G. Auclerc, E.C. Antoine, F. Cajfinger, A. Brunet-Pommeyrol, C. Agazia, D. Khayat, Management of Advanced Prostate Cancer, Oncologist. 5 (2000) 36–44. doi:10.1634/theoncologist.5-1-36.

[12] R. Siegel, C. Desantis, A. Jemal, Colorectal Cancer Statistics, 2014, CA Cancer J. Clin. 64 (2014) 104–17. doi:10.3322/caac.21220.

[13] D. Schadendorf, F.S. Hodi, C. Robert, J.S. Weber, K. Margolin, O. Hamid, D. Patt, T.T. Chen, D.M. Berman, J.D. Wolchok, Pooled analysis of long-term survival data from phase II and phase III trials of ipilimumab in unresectable or metastatic melanoma, J. Clin. Oncol. 33 (2015) 1889–1894. doi:10.1200/JCO.2014.56.2736.

[14] F. Abdollah, G. Gandaglia, R. Thuret, J. Schmitges, Z. Tian, C. Jeldres, N.M. Passoni, A. Briganti, S.F. Shariat, P. Perrotte, F. Montorsi, P.I. Karakiewicz, M. Sun, Incidence, survival and mortality rates of stage-specific bladder cancer in United States: A trend analysis, Cancer Epidemiol. 37 (2013) 219–225. doi:10.1016/j.canep.2013.02.002.

[15] K.D. Miller, R.L. Siegel, C.C. Lin, A.B. Mariotto, J.L. Kramer, J.H. Rowland, K.D. Stein, R. Alteri, A. Jemal, Cancer treatment and survivorship statistics, 2016, CA. Cancer J. Clin. 66 (2016) 271–289. doi:10.3322/caac.21349.

[16] W.P. Parker, J.C. Cheville, I. Frank, H.B. Zaid, C.M. Lohse, S.A. Boorjian, B.C. Leibovich, R.H. Thompson, Application of the Stage, Size, Grade, and Necrosis (SSIGN) Score for Clear Cell Renal Cell Carcinoma in Contemporary Patients, Eur. Urol. 71 (2017) 665–673. doi:10.1016/j.eururo.2016.05.034.

[17] B. Costa-Silva, N.M. Aiello, A.J. Ocean, S. Singh, H. Zhang, B.K. Thakur, A. Becker,

A. Hoshino, M.T. Mark, H. Molina, J. Xiang, T. Zhang, T.M. Theilen, G. García-Santos, C. Williams, Y. Ararso, Y. Huang, G. Rodrigues, T.L. Shen, K.J. Labori, I.M.B. Lothe, E.H. Kure, J. Hernandez, A. Doussot, S.H. Ebbesen, P.M. Grandgenett, M.A. Hollingsworth, M. Jain, K. Mallya, S.K. Batra, W.R. Jarnagin, R.E. Schwartz, I. Matei, H. Peinado, B.Z. Stanger, J. Bromberg, D. Lyden, Pancreatic cancer exosomes initiate pre-metastatic niche formation in the liver, Nat. Cell Biol. 17 (2015) 816–826. doi:10.1038/ncb3169.

[18] C. Holohan, S. Van Schaeybroeck, D.B. Longley, P.G. Johnston, Cancer drug resistance: An evolving paradigm, Nat. Rev. Cancer. 13 (2013) 714–726. doi:10.1038/nrc3599.

[19] Q. Hu, W. Sun, C. Wang, Z. Gu, Recent advances of cocktail chemotherapy by combination drug delivery systems, Adv. Drug Deliv. Rev. 98 (2016) 19–34. doi:10.1016/j.addr.2015.10.022.

[20] F. Greco, M.J. Vicent, Combination therapy: Opportunities and challenges for polymer-drug conjugates as anticancer nanomedicines, Adv. Drug Deliv. Rev. 61 (2009) 1203–1213. doi:10.1016/j.addr.2009.05.006.

[21] C. Le Tourneau, J.J. Lee, L.L. Siu, Dose escalation methods in phase I cancer clinical trials, J. Natl. Cancer Inst. 101 (2009) 708–720. doi:10.1093/jnci/djp079.

[22] S. Carrick, S. Parker, T. Ce, D. Ghersi, J. Simes, N. Wilcken, Single agent versus combination chemotherapy for metastatic breast cancer (Review), Cochrane Database Syst. Rev. (2009). doi:10.1002/14651858.CD003372.pub3.

[23] C. Delbaldo, S. Michiels, N. Syz, J.-C. Soria, T. Le Chevalier, J.-P. Pignon, Benefits of Adding a Drug to a Single-Agent or a 2-Agent Chemotherapy Regimen in Advanced Non–Small-Cell Lung Cancer, JAMA. 292 (2004) 470. doi:10.1001/jama.292.4.470.

[24] H.M. Resende, L.F.P. Jacob, L.V. Quinellato, D. Matos, E.M.K. da Silva, Combination chemotherapy versus single-agent chemotherapy during preoperative chemoradiation for resectable rectal cancer, Cochrane Database Syst. Rev. 2015 (2015). doi:10.1002/14651858.CD008531.pub2.

[25] X.-J. Wu, Y. Zhi, P. He, X.-Z. Zhou, J. Zheng, Z. Chen, Z.-S. Zhou, Comparison of single agent versus combined chemotherapy in previously treated patients with advanced urothelial carcinoma: a meta-analysis., Onco. Targets. Ther. 9 (2016) 1535–43. doi:10.2147/OTT.S97062.

[26] P. Johan Permert, Larsolof Hafström, A Systematic Overview of Chemotherapy Effects in Pancreatic Cancer, Acta Oncol. (Madr). 40 (2001) 361–370. doi:10.1080/02841860117846.

[27] A.C. Palmer, P.K. Sorger, Combination Cancer Therapy Can Confer Benefit via Patient-to-Patient Variability without Drug Additivity or Synergy, Cell. 171 (2017) 1678–1691.e13. doi:10.1016/j.cell.2017.11.009.

[28] A. Ocana, E. Amir, C. Yeung, B. Seruga, I.F. Tannock, How valid are claims for synergy in published clinical studies?, Ann. Oncol. 23 (2012) 2161–2166. doi:10.1093/annonc/mdr608.

[29] J.R. Kroep, G. Giaccone, C. Tolis, D.A. Voorn, W.J.P. Loves, C.J. va. Groeningen, H.M. Pinedo, G.J. Peters, Sequence dependent effect of paclitaxel on gemcitabine metabolism in relation to cell cycle and cytotoxicity in non-small-cell lung cancer cell lines, Br. J. Cancer. 83 (2000) 1069–1076. doi:10.1054/bjoc.2000.1399.

[30] E.K. Rowinsky, M.J. Citardi, D.A. Noe, R.C. Donehower, Sequence-dependent cytotoxic effects due to combinations of cisplatin and the antimicrotubule agents taxol and vincristine, J. Cancer Res. Clin. Oncol. 119 (1993) 727–733. doi:10.1007/BF01195344.

[31] D.R. Vogus, M.A. Evans, A. Pusuluri, A. Barajas, M. Zhang, V. Krishnan, M. Nowak, S. Menegatti, M.E. Helgeson, T.M. Squires, S. Mitragotri, A hyaluronic acid conjugate engineered to synergistically and sequentially deliver gemcitabine and doxorubicin to treat triple negative breast cancer, J. Control. Release. 267 (2017) 191–202. doi:10.1016/j.jconrel.2017.08.016.

[32] J.R. Bertino, W.L. Sawicki, C.A. Lindquist, Schedule-dependent Antitumor Effects of Methotrexate and Schedule-dependent Antitumor Effects of Methotrexate and 5-Fluorouracil, Cancer Res. 37 (1977) 327–328.

[33] M.J. Lee, A.S. Ye, A.K. Gardino, A.M. Heijink, P.K. Sorger, G. MacBeath, M.B. Yaffe, Sequential application of anticancer drugs enhances cell death by rewiring apoptotic signaling networks, Cell. 149 (2012) 780–794. doi:10.1016/j.cell.2012.03.031.

[34] M. a Shah, G.K. Schwartz, Cell Cycle-mediated Drug Resistance : An Emerging Concept in Cancer Therapy Cell Cycle-mediated Drug Resistance : An Emerging Concept in, Clin. Cancer Res. 7 (2001) 2168–2181.

[35] P. Brown, M. Levis, E. McIntyre, M. Griesemer, D. Small, Combinations of the FLT3 inhibitor CEP-701 and chemotherapy synergistically kill infant and childhood MLL-rearranged ALL cells in a sequence-dependent manner, Leukemia. 20 (2006) 1368–1376. doi:10.1038/sj.leu.2404277.

[36] B.L. Gianni, E. Munzone, G. Capri, F. Fulfaro, E. Tarenzi, F. Villani, C. Spreafico, A. Laffranchi, A. Caraceni, C. Martini, M. Stefanelli, P. Valagussa, G. Bonadonna, Paclitaxel by 3-hour infusion in combination with bolus doxorubicin in women with untreated metastatic breast cancer: high antitumor efficacy and cardiac effects in a dose-finding and sequence-finding study., J. Clin. Oncol. 13 (1995) 2688–2699.

[37] F.A. Holmes, T. Madden, R.A. Newman, V. Valero, R.L. Theriault, G. Fraschini, R.S. Walters, D.J. Booser, A.U. Buzdar, J. Willey, G.N. Hortobagyi, Sequence-dependent alteration of doxorubicin pharmacokinetics by paclitaxel in a phase I study of paclitaxel and doxorubicin in patients with metastatic breast cancer, J. Clin. Oncol. 14 (1996) 2713–2721. doi:10.1200/JCO.1996.14.10.2713.

[38] E.K. Rowinsky, S.H. Kaufmann, S.D. Baker, L.B. Grochow, T.L. Chen, D. Peereboom, M.K. Bowling, S.E. Sartorius, D.S. Ettinger, A.A. Forastiere, R.C. Donehower, Sequences of topotecan and cisplatin: Phase I, pharmacologic, and in vitro studies to examine sequence dependence, J. Clin. Oncol. 14 (1996) 3074–3084. doi:10.1200/JCO.1996.14.12.3074.

[39] D.R. Vogus, A. Pusuluri, R. Chen, S. Mitragotri, Schedule dependent synergy of gemcitabine and doxorubicin: Improvement of in vitro efficacy and lack of in vitro-in vivo correlation, Bioeng. Transl. Med. 3 (2018) 49–57. doi:10.1002/btm2.10082.

[40] R. Zhang, J. Yang, M. Sima, Y. Zhou, J. Kope ek, Sequential combination therapy of ovarian cancer with degradable N-(2-hydroxypropyl)methacrylamide copolymer paclitaxel and gemcitabine conjugates, Proc. Natl. Acad. Sci. 111 (2014) 12181–12186. doi:10.1073/pnas.1406233111.

[41] C. Brunetti, L. Anelli, A. Zagaria, G. Specchia, F. Albano, CPX-351 in acute myeloid

leukemia: can a new formulation maximize the efficacy of old compounds?, Expert Rev. Hematol. 10 (2017) 853–862. doi:10.1080/17474086.2017.1369400.

[42] P. Tardi, S. Johnstone, N. Harasym, S. Xie, T. Harasym, N. Zisman, P. Harvie, D. Bermudes, L. Mayer, In vivo maintenance of synergistic cytarabine:daunorubicin ratios greatly enhances therapeutic efficacy, Leuk. Res. 33 (2009) 129–139. doi:10.1016/j.leukres.2008.06.028.

[43] C.M.J. Hu, L. Zhang, Nanoparticle-based combination therapy toward overcoming drug resistance in cancer, Biochem. Pharmacol. 83 (2012) 1104–1111. doi:10.1016/j.bcp.2012.01.008.

[44] T. Chou, Theoretical Basis , Experimental Design , and Computerized Simulation of Synergism and Antagonism in Drug Combination Studies □, Pharmacol. Rev. 58 (2006) 621–681. doi:10.1124/pr.58.3.10.

[45] S. Eckhouse, G. Lewison, R. Sullivan, Trends in the global funding and activity of cancer research, Mol. Oncol. 2 (2008) 20–32. doi:10.1016/j.molonc.2008.03.007.

[46] K.M. Camacho, S. Menegatti, D.R. Vogus, A. Pusuluri, Z. Fuchs, M. Jarvis, M. Zakrewsky, M.A. Evans, R. Chen, S. Mitragotri, DAFODIL: A novel liposome-encapsulated synergistic combination of doxorubicin and 5FU for low dose chemotherapy, J. Control. Release. 229 (2016) 154–162. doi:10.1016/j.jconrel.2016.03.027.

[47] K.M. Camacho, S. Kumar, S. Menegatti, D.R. Vogus, A.C. Anselmo, S. Mitragotri, Synergistic antitumor activity of camptothecin-doxorubicin combinations and their conjugates with hyaluronic acid., J. Control. Release. 210 (2015) 198–207. doi:10.1016/j.jconrel.2015.04.031.

[48] L. Miao, S. Guo, J. Zhang, W.Y. Kim, L. Huang, Nanoparticles with Precise Ratiometric Co-Loading and Co-Delivery of Gemcitabine Monophosphate and Cisplatin for Treatment of Bladder Cancer, Adv. Funct. Mater. 24 (2014) 6601–6611. doi:10.1002/adfm.201401076.

[49] H. Meng, M. Wang, H. Liu, X. Liu, A. Situ, B. Wu, Z. Ji, C.H. Chang, A.E. Nel, Use of a lipid-coated mesoporous silica nanoparticle platform for synergistic gmcitabine and pclitaxel dlivery to hman pncreatic cncer in mice, ACS Nano. 9 (2015) 3540–3557. doi:10.1021/acsnano.5b00510.

[50] M. Stacey Ricci, W. Zong, Chemotherapeutic Approaches for Targeting Cell Death Pathways, Oncologist. 11 (2006) 342–357. doi:10.1634/theoncologist.11-4-342.Chemotherapeutic.

[51] S. Fulda, K.M. Debatin, Extrinsic versus intrinsic apoptosis pathways in anticancer chemotherapy, Oncogene. 25 (2006) 4798–4811. doi:10.1038/sj.onc.1209608.

[52] M.C. Berenbaum, Synergy, additivism and antagonism in immunosuppression, Clin. Exp. Immunol. 28 (1977) 1–18.

[53] L.D. Mayer, T.O. Harasym, P.G. Tardi, N.L. Harasym, C.R. Shew, S. a Johnstone, E.C. Ramsay, M.B. Bally, A.S. Janoff, Ratiometric dosing of anticancer drug combinations: controlling drug ratios after systemic administration regulates therapeutic activity in tumor-bearing mice., Mol. Cancer Ther. 5 (2006) 1854–63. doi:10.1158/1535-7163.MCT-06-0118.

[54] J. Ferlay, I. Soerjomataram, R. Dikshit, S. Eser, C. Mathers, M. Rebelo, D.M. Parkin, D. Forman, F. Bray, Cancer incidence and mortality worldwide: Sources, methods and major patterns in GLOBOCAN 2012, Int. J. Cancer. 136 (2015) E359–E386.

doi:10.1002/ijc.29210.
[55] F. Cardoso, A. Costa, E. Senkus, M. Aapro, F. André, C.H. Barrios, J. Bergh, G. Bhattacharyya, L. Biganzoli, M.J. Cardoso, L. Carey, D. Corneliussen-James, G. Curigliano, V. Dieras, N. El Saghir, A. Eniu, L. Fallowfield, D. Fenech, P. Francis, K. Gelmon, A. Gennari, N. Harbeck, C. Hudis, B. Kaufman, I. Krop, M. Mayer, H. Meijer, S. Mertz, S. Ohno, O. Pagani, E. Papadopoulos, F. Peccatori, F. Penault-Llorca, M.J. Piccart, J.Y. Pierga, H. Rugo, L. Shockney, G. Sledge, S. Swain, C. Thomssen, A. Tutt, D. Vorobiof, B. Xu, L. Norton, E. Winer, 3rd ESO-ESMO International Consensus Guidelines for Advanced Breast Cancer (ABC 3), Ann. Oncol. 28 (2017) 16–33. doi:10.1093/annonc/mdw544.
[56] D.L. Holliday, V. Speirs, Choosing the right cell line for breast cancer research., Breast Cancer Res. 13 (2011) 215. doi:10.1186/bcr2889.
[57] C. Liedtke, C. Mazouni, K.R. Hess, F. André, A. Tordai, J.A. Mejia, W.F. Symmans, A.M. Gonzalez-Angulo, B. Hennessy, M. Green, M. Cristofanilli, G.N. Hortobagyi, L. Pusztai, Response to neoadjuvant therapy and long-term survival in patients with triple-negative breast cancer, J. Clin. Oncol. 26 (2008) 1275–1281. doi:10.1200/JCO.2007.14.4147.
[58] G.N. Hortobdgyi, Anthracyclines in the Treatment of Cancer An Overview, Drugs. 54 (1997) 1–7. doi:10.2165/00003495-199700544-00003.
[59] J. Crown, M. O'Leary, The taxanes: An update, Lancet. 355 (2000) 1176–1178. doi:10.1016/S0140-6736(00)02074-2.
[60] S.B. Kaye, New antimetabolites in cancer chemotherapy and their clinical impact, Br J Cancer. 78 Suppl 3 (1998) 1–7. doi:10.1038/bjc.1998.747.
[61] L. Kelland, The resurgence of platinum-based cancer chemotherapy, Nat. Rev. Cancer. 7 (2007) 573–584. doi:10.1038/nrc2167.
[62] E. Sj, W. Ml, J. Morgan, W. Hs, S. Carrick, D. Ghersi, N. Wilcken, Platinum-containing regimens for metastatic breast cancer (Review), Cochrane Database Syst. Rev. (2017). doi:10.1002/14651858.CD003374.pub4.www.cochranelibrary.com.
[63] E.A. Perez, D.W. Hillman, J.A. Mailliard, J.N. Ingle, J.M. Ryan, T.R. Fitch, K.M. Rowland, C.G. Kardinal, J.E. Krook, J.W. Kugler, S.R. Dakhil, Randomized phase II study of two irinotecan schedules for patients with metastatic breast cancer refractory to an anthracycline, a taxane, or both, J. Clin. Oncol. 22 (2004) 2849–2855. doi:10.1200/JCO.2004.10.047.
[64] H. Hayashi, J. Tsurutani, T. Satoh, N. Masuda, W. Okamoto, R. Morinaga, M. Terashima, M. Miyazaki, I. Okamoto, Y. Nishida, S. Tominaga, Y. Tokunaga, M. Yamaguchi, J. Sakamoto, T. Nakayama, K. Nakagawa, Phase II study of bi-weekly irinotecan for patients with previously treated HER2-negative metastatic breast cancer: KMBOG0610B, Breast Cancer. 20 (2013) 131–136. doi:10.1007/s12282-011-0316-z.
[65] J.F. Pizzolato, L.B. Saltz, The camptothecins, Lancet. 361 (2003) 2235–2242. doi:10.1016/S0140-6736(03)13780-4.
[66] D. Iliopoulos, H.A. Hirsch, K. Struhl, Metformin decreases the dose of chemotherapy for prolonging tumor remission in mouse xenografts involving multiple cancer cell types, Cancer Res. 71 (2011) 3196–3201. doi:10.1158/0008-5472.CAN-10-3471.
[67] K.H. Min, K. Park, Y.S. Kim, S.M. Bae, S. Lee, H.G. Jo, R.W. Park, I.S. Kim, S.Y. Jeong, K. Kim, I.C. Kwon, Hydrophobically modified glycol chitosan nanoparticles-encapsulated camptothecin enhance the drug stability and tumor targeting in cancer

therapy, J. Control. Release. 127 (2008) 208–218. doi:10.1016/j.jconrel.2008.01.013.
[68] U. Vanhoefer, S. Cao, H. Minderman, K. Tóth, R.J. Scheper, M.L. Slovak, Y.M. Rustum, PAK-104P, a pyridine analogue, reverses paclitaxel and doxorubicin resistance in cell lines and nude mice bearing xenografts that overexpress the multidrug resistance protein, Clin. Cancer Res. 2 (1996) 369–377.
[69] B.C. Giovanella, H.R. Hinz, A.J. Kozielski, J.S.J. Stehlin, R. Silber, M. Potmesil, Complete Growth Inhibition of Human Cancer Xenografts in Nude Mice by Treatment with 20-S Camptothecin, Cancer Res. 51 (1991) 3052–3055. http://mcgill.on.worldcat.org/atoztitles/link ?sid=OVID:biopdb&id=pmid:&id=doi:&issn=0008-5472&isbn=&volume=51&issue=11&spage=3052&pages=3052-3055&date=1991&title=Cancer+Research&atitle=COMPLETE+GROWTH+INHIBITION+OF+HUMAN+CANCER+XENOGRAFTS+IN+NUDE+MICE+BY.
[70] T. Schluep, J. Cheng, K.T. Khin, M.E. Davis, Pharmacokinetics and biodistribution of the camptothecin-polymer conjugate IT-101 in rats and tumor-bearing mice, Cancer Chemother. Pharmacol. 57 (2006) 654–662. doi:10.1007/s00280-005-0091-7.
[71] L. Liao, J. Liu, E.C. Dreaden, S.W. Morton, K.E. Shopsowitz, P.T. Hammond, J. a. Johnson, A convergent synthetic platform for single-nanoparticle combination cancer therapy: Ratiometric loading and controlled release of cisplatin, doxorubicin, and camptothecin, J. Am. Chem. Soc. 136 (2014) 5896–5899. doi:10.1021/ja502011g.
[72] S. Aryal, C.-M.J. Hu, L. Zhang, Polymeric Nanoparticles with Precise Ratiometric Control over Drug Loading for Combination Therapy, Mol. Pharm. 8 (2011) 1401–1407. doi:10.1021/mp200243k.
[73] M. Oguro, Y. Seki, K. Okada, T. Andoh, Collateral drug sensitivity induced in CPT-11 (a novel derivative of camptothecin)-resistant cell lines, Biomed. Pharmacother. 44 (1990) 209–216. doi:10.1016/0753-3322(90)90026-6.
[74] V. Pavillard, D. Kherfellah, S. Richard, J. Robert, D. Montaudon, Effects of the combination of camptothecin and doxorubicin or etoposide on rat glioma cells and camptothecin-resistant variants., Br. J. Cancer. 85 (2001) 1077–83. doi:10.1038/sj.bjc.6692027.
[75] G. Pillai, Nanomedicines for Cancer Therapy : An Update of FDA Approved and Those under Various Stages of Development, (2014).
[76] Y. Pommier, Topoisomerase I inhibitors: Camptothecins and beyond, Nat. Rev. Cancer. 6 (2006) 789–802. doi:10.1038/nrc1977.
[77] J. V. McGowan, R. Chung, A. Maulik, I. Piotrowska, J.M. Walker, D.M. Yellon, Anthracycline Chemotherapy and Cardiotoxicity, Cardiovasc. Drugs Ther. 31 (2017) 63–75. doi:10.1007/s10557-016-6711-0.
[78] V.J. Venditto, E.E. Simanek, Cancer Therapies Utilizing the Camptothecins: A Review of the in Vivo Literature, Mol. Pharm. 7 (2010) 307–349. doi:10.1021/mp900243b.
[79] C. Oberhoff, D.G. Kieback, R. Wurstlein, H. Deertz, J. Sehouli, C. van Soest, J. Hilfrich, M. Mesrogli, G. von Minckwitz, H.J. Staab, A.E. Schindler, Topotecan chemotherapy in patients with breast cancer and brain metastases: results of a pilot study., Onkologie. 24 (2001) 256–260. doi:55088.
[80] A.A. Garcia, L. Roman, L. Muderspach, A. O'Meara, G. Facio, S. Edwards, A. Burnett, Phase I clinical trial of topotecan and pegylated liposomal doxorubicin, Cancer Invest. 23 (2005) 665–670. doi:10.1080/07357900500359877.

[81] D. Mirchandani, H. Hochster, A. Hamilton, L. Liebes, H. Yee, J.P. Curtin, S. Lee, J. Sorich, C. Dellenbaugh, F.M. Muggia, Phase I study of combined pegylated liposomal doxorubicin with protracted daily topotecan for ovarian cancer, Clin. Cancer Res. 11 (2005) 5912–5919. doi:10.1158/1078-0432.CCR-04-1240.

[82] D. Morgensztern, M.Q. Baggstrom, G. Pillot, B. Tan, P. Fracasso, R. Suresh, J. Wildi, R. Govindan, A phase i study of pegylated liposomal doxorubicin and irinotecan in patients with solid tumors, Chemotherapy. 55 (2009) 441–445. doi:10.1159/000264925.

[83] S. Nishimura, H. Tsuda, Y. Hashiguchi, K. Kokawa, R. Nishimura, O. Ishiko, S. Kamiura, K. Hasegawa, N. Umesaki, Phase II study of irinotecan plus doxorubicin for early recurrent or platinum-refractory ovarian cancer: Interim analysis, Int. J. Gynecol. Cancer. 17 (2007) 159–163. doi:10.1111/j.1525-1438.2006.00728.x.

[84] N. Xenidis, N. Vardakis, I. Varthalitis, S. Giassas, E. Kontopodis, N. Ziras, I. Gioulbasanis, G. Samonis, K. Kalbakis, V. Georgoulias, A multicenter phase II study of pegylated liposomal doxorubicin in combination with irinotecan as second-line treatment of patients with refractory small-cell lung cancer, Cancer Chemother. Pharmacol. 68 (2011) 63–68. doi:10.1007/s00280-010-1427-5.

[85] L.W. Goff, M.L. Rothenberg, A.C. Lockhart, B.J. Roth, W.L. VerMeulen, E. Chan, J.D. Berlin, A phase I trial of irinotecan alternating with epirubicin in patients with advanced malignancies, Am. J. Clin. Oncol. Cancer Clin. Trials. 31 (2008) 413–416. doi:10.1097/COC.0b013e318168ef2a.

[86] D. Lau, J. Johl, M. Huynh, A. Davies, M. Tanaka, P. Lara, D. Gandara, Population-based phase i trial of irinotecan and epirubicin, Am. J. Clin. Oncol. Cancer Clin. Trials. 31 (2008) 226–230. doi:10.1097/COC.0b013e3181605440.

[87] T. Harada, A. Hamada, M. Shimokawa, K. Takayama, S. Kudoh, K. Maeno, S. Saeki, H. Miyawaki, A. Moriyama, K. Nakagawa, Y. Nakanishi, A phase I/II trial of irinotecan plus amrubicin supported with G-CSF for extended small-cell lung cancer, Jpn. J. Clin. Oncol. 44 (2014) 127–133. doi:10.1093/jjco/hyt198.

[88] K. Hotta, N. Takigawa, K. Kiura, M. Tabata, S. Umemura, A. Ogino, A. Uchida, A. Bessho, Y. Segawa, T. Shinkai, N. Nogami, S. Harita, N. Okimoto, H. Ueoka, M. Tanimoto, Phase I Study of Irinotecan and Amrubicin in Patients with Advanced Non-Small-Cell Lung Cancer, Anticancer Res. 25 (2005) 2429–2434.

[89] N. Nogami, K. Hotta, Y. Segawa, N. Takigawa, S. Hosokawa, I. Oze, M. Fujii, E. Ichihara, T. Shibayama, A. Tada, N. Hamada, M. Uno, A. Tamaoki, S. Kuyama, G. Ikeda, M. Osawa, S. Takata, M. Tabata, M. Tanimoto, K. Kiura, Phase II study of irinotecan and amrubicin in patients with relapsed non-small cell lung cancer: Okayama Lung Cancer Study Group Trial 0402, Acta Oncol. (Madr). 51 (2012) 768–773. doi:10.3109/0284186X.2011.648342.

[90] C.W. Ryan, G.F. Fleming, L. Janisch, M.J. Ratain, A phase I study of liposomal doxorubicin (Doxil) with topotecan, Am. J. Clin. Oncol. Cancer Clin. Trials. 23 (2000) 297–300. doi:10.1097/00000421-200006000-00019.

[91] S. Wagner, O. Peters, C. Fels, G. Janssen, A.K. Liebeskind, A. Sauerbrey, M. Suttorp, P. Hau, J.E.A. Wolff, Pegylated-liposomal doxorubicin and oral topotecan in eight children with relapsed high-grade malignant brain tumors, J. Neurooncol. 86 (2008) 175–181. doi:10.1007/s11060-007-9444-x.

[92] P. Pantazis, Preclinical studies of water-insoluble camptothecin congeners:

cytotoxicity, development of resistance, and combination treatments, Clin. Cancer Res. 1 (1995) 1235–1244.
[93] S. Svenson, M. Wolfgang, J. Hwang, J. Ryan, S. Eliasof, Preclinical to clinical development of the novel camptothecin nanopharmaceutical CRLX101, J. Control. Release. 153 (2011) 49–55. doi:10.1016/j.jconrel.2011.03.007.
[94] R. Bhatt, P. De Vries, J. Tulinsky, G. Bellamy, B. Baker, J.W. Singer, P. Klein, Synthesis and in vivo antitumor activity of poly(L-glutamic acid) conjugates of 20(S)-camptothecin, J. Med. Chem. 46 (2003) 190–193. doi:10.1021/jm020022r.
[95] A. V. Yurkovetskiy, R.J. Fram, XMT-1001, a novel polymeric camptothecin pro-drug in clinical development for patients with advanced cancer, Adv. Drug Deliv. Rev. 61 (2009) 1193–1202. doi:10.1016/j.addr.2009.01.007.
[96] P.J. Burke, P.D. Senter, D.W. Meyer, J.B. Miyamoto, M. Anderson, B.E. Toki, G. Manikumar, M.C. Wani, D.J. Kroll, S.C. Jeffrey, Design, Synthesis , and Biological Evaluation of Antibody - Drug Conjugates Comprised of Potent Camptothecin Analogues, Bioconjugate Chem. 20 (2009) 1242–1250.
[97] M.A. Walker, G.M. Dubowchik, S.J. Hofstead, P.A. Trail, R.A. Firestone, Synthesis of an immunoconjugate of camptothecin, Bioorganic Med. Chem. Lett. 12 (2002) 217–219. doi:10.1016/S0960-894X(01)00707-7.
[98] N.E. Schoemaker, C. Van Kesteren, H. Rosing, S. Jansen, M. Swart, J. Lieverst, D. Fraier, M. Breda, C. Pellizzoni, R. Spinelli, M. Grazia Porro, J.H. Beijnen, J.H.M. Schellens, W.W. Ten Bokkel Huinink, A phase I and pharmacokinetic study of MAG-CPT, a water-soluble polymer conjugate of camptothecin, Br. J. Cancer. 87 (2002) 608–614. doi:10.1038/sj.bjc.6600516.
[99] E.K. Rowinsky, J. Rizzo, L. Ochoa, C.H. Takimoto, B. Forouzesh, G. Schwartz, L.A. Hammond, A. Patnaik, J. Kwiatek, A. Goetz, L. Denis, J. McGuire, A.W. Tolcher, A phase I and pharmacokinetic study of pegylated camptothecin as a 1-hour infusion every 3 weeks in patients with advanced solid malignancies, J. Clin. Oncol. 21 (2003) 148–157. doi:10.1200/JCO.2003.03.143.
[100] C.-M.J. Hu, S. Aryal, L. Zhang, Nanoparticle-assisted combination therapies for effective cancer treatment, Ther. Deliv. 1 (2010) 323–334. doi:10.4155/tde.10.13.
[101] P. Couvreur, C. Vauthier, Nanotechnology: intelligent design to treat complex disease., 2006. doi:10.1007/s11095-006-0284-8.
[102] E. Blanco, A. Hsiao, A.P. Mann, M.G. Landry, F. Meric-Bernstam, M. Ferrari, Nanomedicine in cancer therapy: Innovative trends and prospects, Cancer Sci. 102 (2011) 1247–1252. doi:10.1111/j.1349-7006.2011.01941.x.
[103] T. Sun, Y.S. Zhang, B. Pang, D.C. Hyun, M. Yang, Y. Xia, Engineered Nanoparticles for Drug Delivery in Cancer Therapy Angewandte, Angew. Chemie Int. Ed. 53 (2014) 12320–12364. doi:10.1002/anie.201403036.
[104] A. Schroeder, D. a. Heller, M.M. Winslow, J.E. Dahlman, G.W. Pratt, R. Langer, T. Jacks, D.G. Anderson, Treating metastatic cancer with nanotechnology, Nat. Rev. Cancer. 12 (2012) 39–50. doi:10.1038/nrc3180.
[105] J.D. Byrne, T. Betancourt, L. Brannon-Peppas, Active targeting schemes for nanoparticle systems in cancer therapeutics., Adv. Drug Deliv. Rev. 60 (2008) 1615–26. doi:10.1016/j.addr.2008.08.005.
[106] Y. Matsumura, H. Maeda, A new concept for macromolecular therapeutics in cnacer chemotherapy: mechanism of tumoritropic accumulatio of proteins and the antitumor

agents Smancs, Cancer Res. 46 (1986) 6387–6392. doi:10.1021/bc100070g.
[107] H. Maeda, K. Tsukigawa, J. Fang, A Retrospective 30 Years After Discovery of the Enhanced Permeability and Retention Effect of Solid Tumors: Next-Generation Chemotherapeutics and Photodynamic Therapy—Problems, Solutions, and Prospects, Microcirculation. 23 (2016) 173–182. doi:10.1111/micc.12228.
[108] Y. Nakamura, A. Mochida, P.L. Choyke, H. Kobayashi, Nanodrug Delivery: Is the Enhanced Permeability and Retention Effect Sufficient for Curing Cancer?, Bioconjug. Chem. 27 (2016) 2225–2238. doi:10.1021/acs.bioconjchem.6b00437.
[109] Y.H. Bae, K. Park, Targeted drug delivery to tumors: Myths, reality and possibility, J. Control. Release. 153 (2011) 198–205. doi:10.1016/j.jconrel.2011.06.001.
[110] M. Tabrizi, G.G. Bornstein, H. Suria, Biodistribution mechanisms of therapeutic monoclonal antibodies in health and disease., AAPS J. 12 (2010) 33–43. doi:10.1208/s12248-009-9157-5.
[111] P. Chames, M. Van Regenmortel, E. Weiss, D. Baty, Therapeutic antibodies: Successes, limitations and hopes for the future, Br. J. Pharmacol. 157 (2009) 220–233. doi:10.1111/j.1476-5381.2009.00190.x.
[112] J. Shi, P.W. Kantoff, R. Wooster, O.C. Farokhzad, Cancer nanomedicine: Progress, challenges and opportunities, Nat. Rev. Cancer. 17 (2017) 20–37. doi:10.1038/nrc.2016.108.
[113] J.P. Johnson, W.G. Dippold, Realizing Paul Ehrlich' s magic bullets, J. Cancer Res. Clin. Oncol. 115 (1989) 494–495.
[114] X. Xu, W. Ho, X. Zhang, N. Bertrand, O. Farokhzad, Cancer nanomedicine : from targeted delivery to combination therapy, Trends Mol. Med. 21 (2015) 223–232. doi:http://dx.doi.org/10.1016/j.molmed.2015.01.001 advantages.
[115] F. Kratz, I. a. Müller, C. Ryppa, A. Warnecke, Prodrug strategies in anticancer chemotherapy, ChemMedChem. 3 (2008) 20–53. doi:10.1002/cmdc.200700159.
[116] W. Cheng, L. Gu, W. Ren, Y. Liu, Stimuli-responsive polymers for anticancer drugs delivery, Mater. Sci. Eng. C. (2014). doi:10.1016/j.msec.2014.05.050.
[117] C.P. Leamon, S.R. Cooper, G.E. Hardee, Folate-liposome-mediated antisense oligodeoxynucleotide targeting to cancer cells: Evaluation in vitro and in vivo, Bioconjug. Chem. 14 (2003) 738–747. doi:10.1021/bc020089t.
[118] E. Ruoslahti, S.N. Bhatia, M.J. Sailor, Targeting of drugs and nanoparticles to tumors, J. Cell Biol. 188 (2010) 759–768. doi:10.1083/jcb.200910104.
[119] L.M. Bareford, P.W. Swaan, Endocytic mechanisms for targeted drug delivery, Adv. Drug Deliv. Rev. 59 (2007) 748–758. doi:10.1016/j.addr.2007.06.008.
[120] R.V.J. Chari, M.L. Miller, W.C. Widdison, Antibody-drug conjugates: An emerging concept in cancer therapy, Angew. Chemie - Int. Ed. 53 (2014) 3796–3827. doi:10.1002/anie.201307628.
[121] H.L. Perez, P.M. Cardarelli, S. Deshpande, S. Gangwar, G.M. Schroeder, G.D. Vite, R.M. Borzilleri, Antibody-drug conjugates: current status and future directions., Drug Discov. Today. 19 (2014) 869–81. doi:10.1016/j.drudis.2013.11.004.
[122] N. Diamantis, U. Banerji, Antibody-drug conjugates—an emerging class of cancer treatment, Br. J. Cancer. 114 (2016) 1–6. doi:10.1038/bjc.2015.435.
[123] A.D. Keefe, S. Pai, A. Ellington, Aptamers as therapeutics., Nat. Rev. Drug Discov. 9 (2010) 537–550. doi:10.1038/nrd3141.
[124] Y.H. Lao, K.K.L. Phua, K.W. Leong, Aptamer nanomedicine for cancer therapeutics:

Barriers and potential for translation, ACS Nano. 9 (2015) 2235–2254. doi:10.1021/nn507494p.
[125] Standardize antibodies used in research, Nature. 518 (2015) 27–29. doi:10.2146/ajhp070364.
[126] H. Sun, X. Zhu, P.Y. Lu, R.R. Rosato, W. Tan, Y. Zu, Oligonucleotide aptamers: new tools for targeted cancer therapy., Mol. Ther. Nucleic Acids. 3 (2014) e182. doi:10.1038/mtna.2014.32.
[127] H. Ma, J. Liu, M.M. Ali, M.A.I. Mahmood, L. Labanieh, M. Lu, S.M. Iqbal, Q. Zhang, W. Zhao, Y. Wan, Nucleic acid aptamers in cancer research, diagnosis and therapy, Chem. Soc. Rev. 44 (2015) 1240–1256. doi:10.1039/C4CS00357H.
[128] G. Zhu, G. Niu, X. Chen, Aptamer-Drug Conjugates, Bioconjug. Chem. 26 (2015) 2186–2197. doi:10.1021/acs.bioconjchem.5b00291.
[129] F. Radom, P.M. Jurek, M.P. Mazurek, J. Otlewski, F. Jeleń, Aptamers: molecules of great potential., Biotechnol. Adv. 31 (2013) 1260–74. doi:10.1016/j.biotechadv.2013.04.007.
[130] B.J. Hicke, A.W. Stephens, T. Gould, Y.-F. Chang, C.K. Lynott, J. Heil, S. Borkowski, C.-S. Hilger, G. Cook, S. Warren, P.G. Schmidt, Tumor targeting by an aptamer., J. Nucl. Med. 47 (2006) 668–78. http://www.ncbi.nlm.nih.gov/pubmed/16595502.
[131] J. Zhou, J. Rossi, Aptamers as targeted therapeutics: Current potential and challenges, Nat. Rev. Drug Discov. 16 (2017) 181–202. doi:10.1038/nrd.2016.199.
[132] V. Inhibition, O. Neovascularization, V.I.S.I.O.N.C. Trial, Year 2 Efficacy Results of 2 Randomized Controlled Clinical Trials of Pegaptanib for Neovascular Age-Related Macular Degeneration, Ophthalmology. 113 (2006) 1–25. doi:10.1016/j.ophtha.2006.02.064.
[133] E.W.M. Ng, D.T. Shima, P. Calias, E.T. Cunningham, D.R. Guyer, A.P. Adamis, Pegaptanib, a targeted anti-VEGF aptamer for ocular vascular disease, Nat. Rev. Drug Discov. 5 (2006) 123–132. doi:10.1038/nrd1955.
[134] J.E. Rosenberg, R.M. Bambury, E.M. Van Allen, H.A. Drabkin, P.N. Lara, A.L. Harzstark, N. Wagle, R.A. Figlin, G.W. Smith, L.A. Garraway, T. Choueiri, F. Erlandsson, D.A. Laber, A phase II trial of AS1411 (a novel nucleolin-targeted DNA aptamer) in metastatic renal cell carcinoma, Invest. New Drugs. 32 (2014) 178–187. doi:10.1007/s10637-013-0045-6.
[135] J. Hoellenriegel, D. Zboralski, C. Maasch, N.Y. Rosin, W.G. Wierda, M.J. Keating, A. Kruschinski, J.A. Burger, The Spiegelmer NOX-A12, a novel CXCL12 inhibitor, interferes with chronic lymphocytic leukemia cell motility and causes chemosensitization, Blood. 123 (2014) 1032–1039. doi:10.1182/blood-2013-03-493924.
[136] R. Marasca, R. Maffei, NOX-A12: Mobilizing CLL away from home, Blood. 123 (2014) 952–953. doi:10.1182/blood-2013-12-542480.
[137] O. Kulkarni, R.D. Pawar, W. Purschke, D. Eulberg, N. Selve, K. Buchner, V. Ninichuk, S. Segerer, V. Vielhauer, S. Klussmann, H.-J. Anders, Spiegelmer Inhibition of CCL2/MCP-1 Ameliorates Lupus Nephritis in MRL-(Fas)lpr Mice, J. Am. Soc. Nephrol. 18 (2007) 2350–2358. doi:10.1681/ASN.2006121348.
[138] C. Maasch, K. Buchner, D. Eulberg, S. Vonhoff, S. Klussmann, Physicochemical Stability of NOX-E36, a 40mer L-RNA (Spiegelmer) for Therapeutic Applications,

Nucleic Acids Symp. Ser. 52 (2008) 61–62. doi:10.1093/nass/nrn031.
[139] V. Ninichuk, S. Clauss, O. Kulkarni, H. Schmid, S. Segerer, E. Radomska, D. Eulberg, K. Buchner, N. Selve, S. Klussmann, H.J. Anders, Late onset of Ccl2 blockade with the Spiegelmer mNOX-E36-3′PEG prevents glomerulosclerosis and improves glomerular filtration rate in db/db mice, Am. J. Pathol. 172 (2008) 628–637. doi:10.2353/ajpath.2008.070601.
[140] F. Schwoebel, L.T. Van Eijk, D. Zboralski, S. Sell, K. Buchner, C. Maasch, W.G. Purschke, M. Humphrey, S. Zöllner, D. Eulberg, F. Morich, P. Pickkers, S. Klussmann, The effects of the anti-hepcidin Spiegelmer NOX-H94 on inflammation-induced anemia in cynomolgus monkeys, Blood. 121 (2013) 2311–2315. doi:10.1182/blood-2012-09-456756.
[141] P. Georgiev, M. Lazaroiu, L. Ocroteala, J. Grudeva-Popova, E. Gheorghita, M. Vasilica, S.M. Popescu, A. Cucuianu, L. Summo, F. Schwoebel, K. Riecke, The anti-hepcidin Spiegelmer® Lexaptepid Pegol (NOX-H94) as treatment of anemia of chronic disease in patients with multiple myeloma, low grade lymphoma, and CLL: A phase II pilot study., Cancer Res. (2014) 3847.
[142] K. Riecke, S. Zöllner, M. Boyce, S. Vauléon, D.W. Swinkels, T. Dümmler, L. Summo, C. Laarakkers, F. Schwoebel, F. Fliegert, Single and Repeated Dose First-in-Human Study with the Anti-Hepcidin Spiegelmer Nox-H94, Blood. 120 (2012) 2342.
[143] G. Mayer, F. Rohrbach, B. Pötzsch, J. Müller, Aptamer-based modulation of blood coagulation, Hamostaseologie. 31 (2011) 258–263. doi:10.5482/ha-1156.
[144] D. Xiang, C. Zheng, S.F. Zhou, S. Qiao, P.H.L. Tran, C. Pu, Y. Li, L. Kong, A.Z. Kouzani, J. Lin, K. Liu, L. Li, S. Shigdar, W. Duan, Superior performance of aptamer in tumor penetration over antibody: Implication of aptamer-based theranostics in solid tumors, Theranostics. 5 (2015) 1083–1097. doi:10.7150/thno.11711.
[145] S.L. Ham, R. Joshi, P.S. Thakuri, H. Tavana, Liquid-based three-dimensional tumor models for cancer research and drug discovery, Exp. Biol. Med. 241 (2016) 939–954. doi:10.1177/1535370216643772.
[146] D. Rama-Esendagli, G. Esendagli, G. Yilmaz, D. Guc, Spheroid formation and invasion capacity are differentially influenced by co-cultures of fibroblast and macrophage cells in breast cancer, Mol. Biol. Rep. 41 (2014) 2885–2892. doi:10.1007/s11033-014-3144-3.
[147] C. Cheng, Y.H. Chen, K. a Lennox, M. a Behlke, B.L. Davidson, In vivo SELEX for Identification of Brain-penetrating Aptamers., Mol. Ther. Nucleic Acids. 2 (2013) e67. doi:10.1038/mtna.2012.59.
[148] W. Tan, H. Wang, Y. Chen, X. Zhang, H. Zhu, C. Yang, R. Yang, C. Liu, Molecular aptamers for drug delivery., Trends Biotechnol. 29 (2011) 634–40. doi:10.1016/j.tibtech.2011.06.009.
[149] G.L. Nicolson, Tumor cell instability, diversification, and progression to the metastatic phenotype: From oncogene to oncofetal expression, Cancer Res. 47 (1987) 1473–1487.
[150] A.E. Dago, A. Stepansky, A. Carlsson, M. Luttgen, J. Kendall, T. Baslan, A. Kolatkar, M. Wigler, K. Bethel, M.E. Gross, J. Hicks, P. Kuhn, Rapid phenotypic and genomic change in response to therapeutic pressure in prostate cancer inferred by high content analysis of single Circulating Tumor Cells, PLoS One. 9 (2014). doi:10.1371/journal.pone.0101777.

[151] C.R. Ireson, L.R. Kelland, Discovery and development of anticancer aptamers., Mol. Cancer Ther. 5 (2006) 2957–62. doi:10.1158/1535-7163.MCT-06-0172.
[152] J. Wu, C. Song, C. Jiang, X. Shen, Q. Qiao, Y. Hu, Nucleolin Targeting AS1411 Modified Protein Nanoparticle for Antitumor Drugs Delivery, Mol. Pharm. 10 (2013) 3555–3563.
[153] V. Bagalkot, O.C. Farokhzad, R. Langer, S. Jon, An aptamer-doxorubicin physical conjugate as a novel targeted drug-delivery platform., Angew. Chem. Int. Ed. Engl. 45 (2006) 8149–52. doi:10.1002/anie.200602251.
[154] A.D. À, L. Tang, R. Tong, V.J. Coyle, Q. Yin, H. Pondenis, L.B. Borst, J. Cheng, T.M. Fan, Targeting Tumor Vasculature with Polylactide Nanoconjugates for Enhanced Cancer Therapy, (2015) 5072–5081.
[155] O.C. Farokhzad, J. Cheng, B. a Teply, I. Sherifi, S. Jon, P.W. Kantoff, J.P. Richie, R. Langer, Targeted nanoparticle-aptamer bioconjugates for cancer chemotherapy in vivo., Proc. Natl. Acad. Sci. U. S. A. 103 (2006) 6315–20. doi:10.1073/pnas.0601755103.
[156] C. Kratschmer, M. Levy, Targeted Delivery of Auristatin-Modified Toxins to Pancreatic Cancer Using Aptamers, Mol. Ther. - Nucleic Acids. 10 (2018) 227–236. doi:10.1016/j.omtn.2017.11.013.
[157] S. Yoon, K.W. Huang, V. Reebye, D. Spalding, T.M. Przytycka, Y. Wang, P. Swiderski, L. Li, B. Armstrong, I. Reccia, D. Zacharoulis, K. Dimas, T. Kusano, J. Shively, N. Habib, J.J. Rossi, Aptamer-Drug Conjugates of Active Metabolites of Nucleoside Analogs and Cytotoxic Agents Inhibit Pancreatic Tumor Cell Growth, Mol. Ther. - Nucleic Acids. 6 (2017) 80–88. doi:10.1016/j.omtn.2016.11.008.
[158] Y.F. Huang, D. Shangguan, H. Liu, J.A. Phillips, X. Zhang, Y. Chen, W. Tan, Molecular assembly of an aptamer-drug conjugate for targeted drug delivery to tumor cells, ChemBioChem. 10 (2009) 862–868. doi:10.1002/cbic.200800805.
[159] F. Li, J. Lu, J. Liu, C. Liang, M. Wang, L. Wang, D. Li, H. Yao, Q. Zhang, J. Wen, Z.K. Zhang, J. Li, Q. Lv, X. He, B. Guo, D. Guan, Y. Yu, L. Dang, X. Wu, Y. Li, G. Chen, F. Jiang, S. Sun, B.T. Zhang, A. Lu, G. Zhang, A water-soluble nucleolin aptamer-paclitaxel conjugate for tumor-specific targeting in ovarian cancer, Nat. Commun. 8 (2017). doi:10.1038/s41467-017-01565-6.
[160] N. Zhao, S.-N. Pei, J. Qi, Z. Zeng, S.P. Iyer, P. Lin, C.-H. Tung, Y. Zu, Oligonucleotide aptamer-drug conjugates for targeted therapy of acute myeloid leukemia, Biomaterials. 67 (2015) 42–51. doi:10.1016/j.biomaterials.2015.07.025.
[161] J. Wen, W. Tao, S. Hao, S.P. Iyer, Y. Zu, A unique aptamer-drug conjugate for targeted therapy of multiple myeloma, Leukemia. 30 (2016) 987–991. doi:10.1038/leu.2015.216.
[162] J. Liu, T. Wei, J. Zhao, Y. Huang, H. Deng, A. Kumar, C. Wang, Z. Liang, X. Ma, X.J. Liang, Multifunctional aptamer-based nanoparticles for targeted drug delivery to circumvent cancer resistance, Biomaterials. 91 (2016) 44–56. doi:10.1016/j.biomaterials.2016.03.013.
[163] G. Zhu, J. Zheng, E. Song, M. Donovan, K. Zhang, C. Liu, W. Tan, Self-assembled, aptamer-tethered DNA nanotrains for targeted transport of molecular drugs in cancer theranostics, Proc. Natl. Acad. Sci. 110 (2013) 7998–8003. doi:10.1073/pnas.1220817110.
[164] S.S. Oh, # Bongjae, F. Lee, F.A. Leibfarth, M. Eisenstein, M.J. Robb, N.A. Lynd, C.J.

Hawker, H.T. Soh, Synthetic Aptamer-Polymer Hybrid Constructs for Programmed Drug Delivery into Specific Target Cells, (2014). doi:10.1021/ja5079464.
[165] L. Zhang, A.F. Radovic-Moreno, F. Alexis, F.X. Gu, P. a. Basto, V. Bagalkot, S. Jon, R.S. Langer, O.C. Farokhzad, Co-delivery of hydrophobic and hydrophilic drugs from nanoparticle-aptamer bioconjugates, ChemMedChem. 2 (2007) 1268–1271. doi:10.1002/cmdc.200700121.
[166] K. Jiang, L. Han, Y. Guo, G. Zheng, L. Fan, Z. Shen, R. Zhao, J. Shao, A carrier-free dual-drug nanodelivery system functionalized with aptamer specific targeting HER2-overexpressing cancer cells, J. Mater. Chem. B. 5 (2017) 9121–9129. doi:10.1039/C7TB02562A.
[167] N. Kolishetti, S. Dhar, P.M. Valencia, L.Q. Lin, R. Karnik, S.J. Lippard, R. Langer, O.C. Farokhzad, Engineering of self-assembled nanoparticle platform for precisely controlled combination drug therapy, Proc. Natl. Acad. Sci. 107 (2010) 17939–17944. doi:10.1073/pnas.1011368107.
[168] P.J. Bates, D.A. Laber, D.M. Miller, S.D. Thomas, J.O. Trent, Discovery and Development of the G-rich Oligonucleotide AS1411 as a Novel Treatment for Cancera, Exp. Mol. Pathol. 86 (2010) 151–164. doi:10.1016/j.yexmp.2009.01.004.Discovery.
[169] K.H. Min, K. Park, Y.S. Kim, S.M. Bae, S. Lee, H.G. Jo, R.W. Park, I.S. Kim, S.Y. Jeong, K. Kim, I.C. Kwon, Hydrophobically modified glycol chitosan nanoparticles-encapsulated camptothecin enhance the drug stability and tumor targeting in cancer therapy, J. Control. Release. 127 (2008) 208–218. doi:10.1016/j.jconrel.2008.01.013.
[170] V.R. Caiolfa, M. Zamai, A. Fiorino, E. Frigerio, C. Pellizzoni, R. D'Argy, A. Ghiglieri, M.G. Castelli, M. Farao, E. Pesenti, M. Gigli, F. Angelucci, A. Suarato, Polymer-bound camptothecin: Initial biodistribution and antitumour activity studies, J. Control. Release. 65 (2000) 105–119. doi:10.1016/S0168-3659(99)00243-6.
[171] M.R. Levengood, X. Zhang, J.H. Hunter, K.K. Emmerton, J.B. Miyamoto, T.S. Lewis, P.D. Senter, Orthogonal Cysteine Protection Enables Homogeneous Multi-Drug Antibody–Drug Conjugates, Angew. Chemie - Int. Ed. 56 (2017) 733–737. doi:10.1002/anie.201608292.
[172] S. Majumdar, T.J. Siahaan, Peptide-mediated targeted drug delivery, Med. Res. Rev. 32 (2012) 637–658. doi:10.1002/med.20225.
[173] C.S. McKay, M.G. Finn, Click chemistry in complex mixtures: Bioorthogonal bioconjugation, Chem. Biol. 21 (2014) 1075–1101. doi:10.1016/j.chembiol.2014.09.002.
[174] J. Cheng, K.T. Khin, G.S. Jensen, A. Liu, M.E. Davis, Synthesis of linear, beta-cyclodextrin-based polymers and their camptothecin conjugates, Bioconjug. Chem. 14 (2003) 1007–1017. doi:10.1021/bc0340924.
[175] N.A. Fonseca, A.S. Rodrigues, P. Rodrigues-Santos, V. Alves, A.C. Gregório, Â. Valério-Fernandes, L.C. Gomes-da-Silva, M.S. Rosa, V. Moura, J. Ramalho-Santos, S. Simões, J.N. Moreira, Nucleolin overexpression in breast cancer cell sub-populations with different stem-like phenotype enables targeted intracellular delivery of synergistic drug combination, Biomaterials. 69 (2015) 76–88. doi:10.1016/j.biomaterials.2015.08.007.
[176] L. Meng, L. Yang, X. Zhao, L. Zhang, H. Zhu, C. Liu, W. Tan, Targeted Delivery of Chemotherapy Agents Using a Liver Cancer-Specific Aptamer, PLoS One. 7 (2012)

e33434. doi:10.1371/journal.pone.0033434.
[177] H. Xing, L. Tang, X. Yang, K. Hwang, W. Wang, Q. Yin, N.Y. Wong, L.W. Dobrucki, N. Yasui, J.A. Katzenellenbogen, W.G. Helferich, J. Cheng, Y. Lu, Selective delivery of an anticancer drug with aptamer-functionalized liposomes to breast cancer cells in vitro and in vivo, J. Mater. Chem. B. 1 (2013) 5288. doi:10.1039/c3tb20412j.
[178] K.Y. Choi, H.Y. Yoon, J.H. Kim, S.M. Bae, R.W. Park, Y.M. Kang, I.S. Kim, I.C. Kwon, K. Choi, S.Y. Jeong, K. Kim, J.H. Park, Smart nanocarrier based on PEGylated hyaluronic acid for cancer therapy, ACS Nano. 5 (2011) 8591–8599. doi:10.1021/nn202070n.
[179] Z. Yan, H. Bao, Q. Zhang, H. Xu, D. Press, Effects of nanoparticle size on antitumor activity of 10-hydroxycamptothecin-conjugated gold nanoparticles: in vitro and in vivo studies, Int. J. Nanomedicine. 0123 (2016) 929. doi:10.2147/IJN.S96422.
[180] N. Yoon, M.S. Park, G.C. Peltier, R.H. Lee, Pre-activated human mesenchymal stromal cells in combination with doxorubicin synergistically enhance tumor-suppressive activity in mice, Cytotherapy. 17 (2015) 1332–1341. doi:10.1016/j.jcyt.2015.06.009.
[181] L.E. Himmel, M.B. Lustberg, A.C. DeVries, M. Poi, C.S. Chen, S.K. Kulp, Minocycline, a putative neuroprotectant, co-administered with doxorubicin-cyclophosphamide chemotherapy in a xenograft model of triple-negative breast cancer, Exp. Toxicol. Pathol. 68 (2016) 505–515. doi:10.1016/j.etp.2016.08.001.
[182] F. Ahmed, R.I. Pakunlu, A. Brannan, F. Bates, T. Minko, D.E. Discher, Biodegradable polymersomes loaded with both paclitaxel and doxorubicin permeate and shrink tumors, inducing apoptosis in proportion to accumulated drug, J. Control. Release. 116 (2006) 150–158. doi:10.1016/j.jconrel.2006.07.012.
[183] S. Soundararajan, W. Chen, E.K. Spicer, N. Courtenay-Luck, D.J. Fernandes, The nucleolin targeting aptamer AS1411 destabilizes Bcl-2 messenger RNA in human breast cancer cells, Cancer Res. 68 (2008) 2358–2365. doi:10.1158/0008-5472.CAN-07-5723.
[184] E.M. Reyes-Reyes, Y. Teng, P.J. Bates, A new paradigm for aptamer therapeutic AS1411 action: Uptake by macropinocytosis and its stimulation by a nucleolin-dependent mechanism, Cancer Res. 70 (2010) 8617–8629. doi:10.1158/0008-5472.CAN-10-0920.
[185] M.A. Evans, P.J. Huang, Y. Iwamoto, K.N. Ibsen, E.M. Chan, Y. Hitomi, P.C. Ford, S. Mitragotri, Macrophage-mediated delivery of light activated nitric oxide prodrugs with spatial, temporal and concentration control, Chem. Sci. 9 (2018) 3729–3741. doi:10.1039/c8sc00015h.
[186] T.-C. Chou, The mass-action law based algorithm for cost-effective approach for cancer drug discovery and development., Am. J. Cancer Res. 1 (2011) 925–54. http://www.pubmedcentral.nih.gov/articlerender.fcgi?artid=3196289&tool=pmcentrez&rendertype=abstract.
[187] S. Cleator, W. Heller, R.C. Coombes, Triple-negative breast cancer: therapeutic options, Lancet Oncol. 8 (2007) 235–244. doi:10.1016/S1470-2045(07)70074-8.
[188] D. Peer, J.M. Karp, S. Hong, O.C. Farokhzad, R. Margalit, R. Langer, Nanocarriers as an emerging platform for cancer therapy, Nat. Nanotechnol. 2 (2007) 751–760. doi:10.1038/nnano.2007.387.

[189] S.M. Moghimi, J. Szebeni, Stealth liposomes and long circulating nanoparticles: Critical issues in pharmacokinetics, opsonization and protein-binding properties, Prog. Lipid Res. 42 (2003) 463–478. doi:10.1016/S0163-7827(03)00033-X.
[190] C.L. Waite, C.M. Roth, Nanoscale drug delivery systems for enhanced drug penetration into solid tumors: current progress and opportunities., Crit. Rev. Biomed. Eng. 40 (2012) 21–41. doi:10.1615/CritRevBiomedEng.v40.i1.20.
[191] K. Huang, H. Ma, J. Liu, S. Huo, A. Kumar, T. Wei, X. Zhang, S. Jin, Y. Gan, P.C. Wang, S. He, X. Zhang, X.J. Liang, Size-dependent localization and penetration of ultrasmall gold nanoparticles in cancer cells, multicellular spheroids, and tumors in vivo, ACS Nano. 6 (2012) 4483–4493. doi:10.1021/nn301282m.
[192] J.M. Healy, S.D. Lewis, M. Kurz, R.M. Boomer, K.M. Thompson, C. Wilson, T.G. McCauley, Pharmacokinetics and biodistribution of novel aptamer compositions., Pharm. Res. 21 (2004) 2234–46. http://www.ncbi.nlm.nih.gov/pubmed/15648255.
[193] K. Haruta, N. Otaki, M. Nagamine, T. Kayo, A. Sasaki, S. Hiramoto, M. Takahashi, K. Hota, H. Sato, H. Yamazaki, A Novel PEGylation Method for Improving the Pharmacokinetic Properties of Anti-Interleukin-17A RNA Aptamers, Nucleic Acid Ther. 27 (2017) 36–44. doi:10.1089/nat.2016.0627.
[194] J.G. Bruno, A review of therapeutic aptamer conjugates with emphasis on new approaches., Pharmaceuticals (Basel). 6 (2013) 340–57. doi:10.3390/ph6030340.
[195] R. Boisgard, B. Kuhnast, S. Vonhoff, C. Younes, F. Hinnen, J.-M. Verbavatz, B. Rousseau, J.P. Fürste, B. Wlotzka, F. Dollé, S. Klussmann, B. Tavitian, In vivo biodistribution and pharmacokinetics of 18F-labelled Spiegelmers: a new class of oligonucleotidic radiopharmaceuticals., Eur. J. Nucl. Med. Mol. Imaging. 32 (2005) 470–7. doi:10.1007/s00259-004-1669-8.
[196] C. Wilson, A.D. Keefe, Building oligonucleotide therapeutics using non-natural chemistries, Curr. Opin. Chem. Biol. 10 (2006) 607–614. doi:10.1016/j.cbpa.2006.10.001.
[197] J.F. Lee, G.M. Stovall, A.D. Ellington, Aptamer therapeutics advance, Curr. Opin. Chem. Biol. 10 (2006) 282–289. doi:10.1016/j.cbpa.2006.03.015.
[198] K.-N. Kang, Y.-S. Lee, RNA Aptamers: A Review of Recent Trends and Applications, in: J.-J. Zhong (Ed.), Futur. Trends Biotechnol., Springer Berlin Heidelberg, Berlin, Heidelberg, 2013: pp. 153–169. doi:10.1007/10_2012_136.
[199] E.N. Brody, L. Gold, Aptamers as therapeutic and diagnostic agents, Rev. Mol. Biotechnol. 74 (2000) 5–13. doi:10.1016/S1389-0352(99)00004-5.
[200] R. Rouzier, C.M. Perou, W.F. Symmans, N. Ibrahim, M. Cristofanilli, K. Anderson, K.R. Hess, J. Stec, M. Ayers, P. Wagner, P. Morandi, C. Fan, I. Rabiul, J.S. Ross, G.N. Hortobagyi, L. Pusztai, Breast cancer molecular subtypes respond differently to preoperative chemotherapy, Clin. Cancer Res. 11 (2005) 5678–5685. doi:10.1158/1078-0432.CCR-04-2421.
[201] L.A. Carey, E.C. Dees, L. Sawyer, L. Gatti, D.T. Moore, F. Collichio, D.W. Ollila, C.I. Sartor, M.L. Graham, C.M. Perou, The triple negative paradox: Primary tumor chemosensitivity of breast cancer subtypes, Clin. Cancer Res. 13 (2007) 2329–2334. doi:10.1158/1078-0432.CCR-06-1109.
[202] C.M. Perou, Molecular Stratification of Triple-Negative Breast Cancers, Oncologist. 16 (2011) 61–70. doi:10.1634/theoncologist.2011-S1-61.
[203] C. Oakman, G. Viale, A. Di Leo, Management of triple negative breast cancer, Breast.

19 (2010) 312–321. doi:10.1016/j.breast.2010.03.026.
[204] Z. Elsawaf, H.P. Sinn, J. Rom, J.L. Bermejo, A. Schneeweiss, S. Aulmann, Biological subtypes of triple-negative breast cancer are associated with distinct morphological changes and clinical behaviour, Breast. 22 (2013) 986–992. doi:10.1016/j.breast.2013.05.012.
[205] M. Cheang, S.K. Chia, D. Tu, S. Jiang, L.E. Shepherd, K.I. Pritchard, T.O. Nielsen, Anthracyclines in basal breast cancer: The NCIC-CTG trial MA5 comparing adjuvant CMF to CEF, J. Clin. Oncol. 27 (2009) 519. doi:10.1200/jco.2009.27.15s.519.
[206] T. Byrski, J. Gronwald, T. Huzarski, E. Grzybowska, M. Budryk, M. Stawicka, T. Mierzwa, M. Szwiec, R. Wiśniowski, M. Siolek, S.A. Narod, J. Lubinski, M. Foszczynska-Kloda, P. Serrano-Fernández, M. Chosia, M. Uciński, D. Lange, B. Mika, A. Mackiewicz, A. Karczewska, J. Breborowicz, K. Lamperska, S. Gozdecka-Grodecka, M. Bębenek, D. Sorokin, A. Wojnar, O. Haus, J. Sir, S. Niepsuj, K. Gugała, S. Goździ, J. Sygut, B. Kozak-Klonowska, M. Musiatowicz, R. Posmyk, M. Kordek, O. Morawiec, B. Zambrano, L. Waśko, D. Fudali, D. Surdynka, K. Urbański, J. Mituś, J. Ryś, A. Rozmiarek, I. Dziuba, P. Wandzel, C. Szczylik, A. Kozak, A. Kozłowski, Response to neo-adjuvant chemotherapy in women with BRCA1-positive breast cancers, Breast Cancer Res. Treat. 108 (2008) 289–296. doi:10.1007/s10549-007-9600-1.
[207] J. Hugh, J. Hanson, M.C.U. Cheang, T.O. Nielsen, C.M. Perou, C. Dumontet, J. Reed, M. Krajewska, I. Treilleux, M. Rupin, E. Magherini, J. Mackey, M. Martin, C. Vogel, Breast cancer subtypes and response to docetaxel in node-positive breast cancer: Use of an immunohistochemical definition in the BCIRG 001 trial, J. Clin. Oncol. 27 (2009) 1168–1176. doi:10.1200/JCO.2008.18.1024.
[208] W. Zoli, L. Ricotti, F. Barzanti, M. Dal Susino, G.L. Frassineti, C. Milandri, D. Casadei Giunchi, D. Amadori, Schedule-dependent interaction of doxorubicin, paclitaxel and gemcitabine in human breast cancer cell lines, Int. J. Cancer. 80 (1999) 413–416. doi:10.1002/(SICI)1097-0215(19990129)80:3<413::AID-IJC13>3.0.CO;2-I.
[209] R.H. Shanks, D. a. Rizzieri, J.L. Flowers, O.M. Colvin, D.J. Adams, Preclinical evaluation of gemcitabine combination regimens for application in acute myeloid leukemia, Clin. Cancer Res. 11 (2005) 4225–4233. doi:10.1158/1078-0432.CCR-04-2106.
[210] J.S. Lopez, U. Banerji, Combine and conquer: Challenges for targeted therapy combinations in early phase trials, Nat. Rev. Clin. Oncol. 14 (2017) 57–66. doi:10.1038/nrclinonc.2016.96.
[211] K. Sefah, D. Shangguan, X. Xiong, M.B. O'Donoghue, W. Tan, Development of DNA aptamers using Cell-SELEX., Nat. Protoc. 5 (2010) 1169–85. doi:10.1038/nprot.2010.66.
[212] G. Mayer, M.-S.L. Ahmed, A. Dolf, E. Endl, P. a Knolle, M. Famulok, Fluorescence-activated cell sorting for aptamer SELEX with cell mixtures., Nat. Protoc. 5 (2010) 1993–2004. doi:10.1038/nprot.2010.163.
[213] T. Schütze, B. Wilhelm, N. Greiner, H. Braun, F. Peter, M. Mörl, V. a. Erdmann, H. Lehrach, Z. Konthur, M. Menger, P.F. Arndt, J. Glökler, Probing the SELEX process with next-generation sequencing, PLoS One. 6 (2011) 1–10. doi:10.1371/journal.pone.0029604.
[214] N. Mencin, T. Šmuc, M. Vraničar, J. Mavri, M. Hren, K. Galeša, P. Krkoč, H. Ulrich,

B. Šolar, Optimization of SELEX: comparison of different methods for monitoring the progress of in vitro selection of aptamers., J. Pharm. Biomed. Anal. 91 (2014) 151–9. doi:10.1016/j.jpba.2013.12.031.
[215] K. Zhang, K. Sefah, L. Tang, Z. Zhao, G. Zhu, M. Ye, W. Sun, S. Goodison, W. Tan, A novel aptamer developed for breast cancer cell internalization, ChemMedChem. 7 (2012) 79–84. doi:10.1002/cmdc.201100457.
[216] W. Alshaer, H. Hillaireau, J. Vergnaud, S. Mura, C. Deloménie, F. Sauvage, S. Ismail, E. Fattal, Aptamer-guided siRNA-loaded nanomedicines for systemic gene silencing in CD-44 expressing murine triple-negative breast cancer model, J. Control. Release. 271 (2018) 98–106. doi:10.1016/j.jconrel.2017.12.022.
[217] S. Luo, S. Wang, N. Luo, F. Chen, C. Hu, K. Zhang, The application of aptamer 5TR1 in triple negative breast cancer target therapy, J. Cell. Biochem. 119 (2018) 896–908. doi:10.1002/jcb.26254.
[218] Q. Liu, Q. Liao, Y. Zhao, Chemotherapy and tumor microenvironment of pancreatic cancer, Cancer Cell Int. 17 (2017) 1–17. doi:10.1186/s12935-017-0437-3.
[219] O.C. Farokhzad, S. Jon, A. Khademhosseini, T.T. Tran, D. a Lavan, R. Langer, Nanoparticle-Aptamer Bioconjugates : A New Approach for Targeting Prostate Cancer Cells Nanoparticle-Aptamer Bioconjugates : A New Approach for Targeting Prostate Cancer Cells, (2004) 7668–7672. doi:10.1158/0008-5472.CAN-04-2550.
[220] R. Savla, O. Taratula, O. Garbuzenko, T. Minko, Tumor targeted quantum dot-mucin 1 aptamer-doxorubicin conjugate for imaging and treatment of cancer, J. Control. Release. 153 (2011) 16–22. doi:10.1016/j.jconrel.2011.02.015.
[221] S.H. Jalalian, S.M. Taghdisi, N.S. Hamedani, S.A.M. Kalat, P. Lavaee, M. ZandKarimi, N. Ghows, M.R. Jaafari, S. Naghibi, N.M. Danesh, M. Ramezani, K. Abnous, Epirubicin loaded super paramagnetic iron oxide nanoparticle-aptamer bioconjugate for combined colon cancer therapy and imaging in vivo, Eur. J. Pharm. Sci. 50 (2013) 191–197. doi:10.1016/j.ejps.2013.06.015.
[222] G.H. Lyman, Impact of chemotherapy dose intensity on cancer patient outcomes, JNCCN J. Natl. Compr. Cancer Netw. 7 (2009) 99–108. doi:10.6004/jnccn.2009.0009.
[223] L. Zitvogel, L. Apetoh, F. Ghiringhelli, G. Kroemer, Immunological aspects of cancer chemotherapy, Nat. Rev. Immunol. 8 (2008) 59–73. doi:10.1038/nri2216.
[224] L. Bracci, G. Schiavoni, A. Sistigu, F. Belardelli, Immune-based mechanisms of cytotoxic chemotherapy: Implications for the design of novel and rationale-based combined treatments against cancer, Cell Death Differ. 21 (2014) 15–25. doi:10.1038/cdd.2013.67.
[225] N. André, K. Tsai, M. Carré, E. Pasquier, Metronomic Chemotherapy: Direct Targeting of Cancer Cells after all?, Trends in Cancer. 3 (2017) 319–325. doi:10.1016/j.trecan.2017.03.011.
[226] J.S. Brown, R. Sundar, J. Lopez, Combining DNA damaging therapeutics with immunotherapy: More haste, less speed, Br. J. Cancer. 118 (2018) 312–324. doi:10.1038/bjc.2017.376.
[227] E.M. Mastria, L.Y. Cai, M.J. Kan, X. Li, J.L. Schaal, S. Fiering, M.D. Gunn, M.W. Dewhirst, S.K. Nair, A. Chilkoti, Nanoparticle formulation improves doxorubicin efficacy by enhancing host antitumor immunity, J. Control. Release. 269 (2018) 364–373. doi:10.1016/j.jconrel.2017.11.021.
[228] L.A. Emens, G. Middleton, The Interplay of Immunotherapy and Chemotherapy:

Harnessing Potential Synergies, 3 (2015) 436–443. doi:10.1158/2326-6066.CIR-15-0064.The.
[229] W.H. Fridman, F. Pagès, C. Sauts-Fridman, J. Galon, The immune contexture in human tumours: Impact on clinical outcome, Nat. Rev. Cancer. 12 (2012) 298–306. doi:10.1038/nrc3245.